CZECH TECHNICAL UNIVERSITY IN PRAGUE

FACULTY OF BIOMEDICAL ENGINEERING

Department of Biomedical Technology

Doctoral Thesis

Electrocardiographic manifestation of cardiac repolarization dispersion

Ksenia Sedova

Study program: P3921 Biomedical and Clinical Technology

Field of study: 3901V031 Biomedical and Clinical Technology

Supervisor: Assoc. prof. Ing. Milan Tyšler, PhD

Academic adviser: prof. Ing. Peter Kneppo, DrSc.

Kladno 2018

Annotation

Alterations of repolarization heterogeneity in the heart have been established as an arrhythmogenic factor predisposing to malignant cardiac arrhythmias. The assessment of cardiac repolarization heterogeneity on the basis of ECG analysis is of clinical importance for the prognosis of arrhythmias and evaluation of antiarrhythmic therapies.

The purpose of this thesis was to find out the patterns of the development and electrocardiographic manifestation of the repolarization dispersion, including the parameters of repolarization related to the development of ventricular tachyarrhythmias in the ischemia-reperfusion animal model.

The study was scheduled to perform both, experimental research and mathematical modeling. In the experiments on animal hearts *in vivo*, 32 to 88 unipolar electrograms were synchronously recorded from the ventricular myocardium at baseline state and under acute ischemia/reperfusion settings. The electrophysiological characteristics of repolarization heterogeneity in the myocardium, including parameters associated with ventricular fibrillation were obtained. In order to determine the manifestation of the myocardial repolarization parameters in conventional ECG, the mathematical model was applied.

The transmural and apicobasal repolarization gradients were found in the ventricular myocardium *in vivo* but the contribution of the transmural repolarization gradient to the Tpeak-Tend interval was minor to that of the apicobasal one (Arteyeva et al. 2013). Under ischemia/reperfusion settings the global, apicobasal, and borderline dispersions of repolarization increased, what was associated with prolongation of the Tpeak-Tend and QTc interval as well as the T-wave voltage differences between modified upper- and lower-chest precordial leads (T-wave amplitude dispersion) (Sedova et al. 2013, Sedova et al. 2015). The reperfusion ventricular tachyarrhythmias were independently predicted by longer repolarization time in the nonischemic zone reflected in the negative polarity of the terminal phase of the electrocardiographic T wave (Bernikova et al. 2018, in press: J Electrocardiol).

Thus, the present thesis has contributed to improvement of the diagnostic power of ECG methods in the prevention and treatment of malignant arrhythmias. The specific parameters of myocardial repolarization that could serve as predictors of ventricular tachyarrhythmias were determined and electrocardiographic manifestation of these parameters was suggested.

Acknowledgements

I would like to express sincere gratitude to my scientific advisor Associate professor. Ing. Milan Tyšler, Ph.D. for the continuous support of my doctoral study and related research, for his kindness, motivation, and very professional and useful comments. I would like to thank my academic adviser Professor Ing. Peter Kneppo, DrSc. for his insightful advice and encouragement during the time of this research. I am very grateful for the cooperation and support provided by Professor MUDr. Jozef Rosina, Ph.D. and Professor Ing. Karel Roubík, Ph.D.

In addition, I thank the colleagues from the Department of Cardiac Physiology, Institute of Physiology, Komi Science Centre, Ural Branch, Russian Academy of Sciences (Syktyvkar, Russia), doc. Jan Azarov, Ph.D., Olesya Bernikova, M.D., Ph.D., doc. Sergey Kharin, Ph.D., Natalia Arteyeva, Ph.D. for the collaboration, discussions, and support of this research.

Finally, I am deeply thankful to my family and close friends for their inspiration, encouragement and support throughout this research.

Content

State of the art

Malignant ventricular arrhythmias and sudden cardiac death are the often complications of cardiovascular diseases and remain the major clinical problem worldwide (WHO 2017). Acute coronary syndrome as the prevalent form of cardiovascular pathology is associated with high risk of sudden cardiac death caused by ventricular tachycardia and fibrillation (Mehta et al. 2009) because the ischemia-related electrophysiological disturbances including the increased heterogeneity of ventricular repolarization are considered to provide an electrophysiological substrate for lethal arrhythmias (Wit, Janse 2001).

The heterogeneity of repolarization is associated with arrhythmogenesis providing conditions for the unidirectional conduction block (Burton, Cobbe 2001). Moreover, local shortening and lengthening of repolarization can provide triggered activity, provoking the delayed and early afterdepolarization. Although the enhanced dispersion of repolarization has been linked to increased risk of arrhythmia, it is not an assurance of real development of ventricular arrhythmias (Coronel et al. 2009). The contribution of different gradients of repolarization to arrhythmogenesis under ischemic conditions is not clear. In vitro studies have demonstrated that epicardial layers were more sensitive to the ischemic insult that increased the transmural dispersion of repolarization (Kimura et al. 1986, Lukas et al. 1993), whereas no transmural differences in the ischemia effects were observed in vivo (Taggart et al. 2001, Bernikova et al. 2011). Thus, the causes of arrhythmogenesis related to cardiac repolarization heterogeneity are still under investigation.

The assessment of cardiac repolarization heterogeneity on the basis of ECG analysis is of clinical importance as to the prognosis of arrhythmias and evaluation of antiarrhythmic therapies. Specifically, the ECG indices of ventricular repolarization including the QT interval, T wave and Tpeak-Tend durations, the T wave voltage and morphology could reflect the vulnerability of the ventricles to the life-threatening reentrant arrhythmias.

The dispersion of QT interval suggested as a marker for the dispersion of repolarization, though initially seemed promising as an arrhythmia predictor (Priori et al. 1994, Zabel et al. 1998) has not been validated theoretically (Malik et al. 2000) or clinically (Brendorp et al. 2001).

More recently, the Tpeak–Tend interval has been proposed as an index of repolarization dispersion (Yan et al. 1998, Xia et al. 2005, Smetana et al. 2011, Porthan et al. 2013). However, the electrophysiological basis for the Tpeak–Tend remains under discussion. Specifically, it

appears unsolved whether the transmural (Antzelevitch et al. 2007, Patel et al. 2009) or apicobasal (Xia et al. 2005, Opthof et al. 2007) and global (Opthof et al. 2009, Meijborg et al. 2014) dispersion of repolarization contributes more to the T wave genesis and Tpeak–Tend duration. Furthermore, some studies did not demonstrate the significant transmural gradient of action potential durations in the intact heart ventricles (Voss et al. 2009) and considered contribution of transepicardial (i.e., apicobasal, interventricular and anteroposterior) gradients being superior to that of the transmural gradient to development of the total dispersion of repolarization, associated with the generation of the T wave (Xue et al. 2010, Vaykshnorayte et al. 2011, Janse et al. 2012, Meijborg et al. 2014) and the arrhythmia risk (Panikkath et al. 2011, Hetland et al. 2014). The findings of experimental (Guerard at al. 2014) and clinical (Pak et al. 2004) studies consider apicobasal dispersion of repolarization as a major contributor to the triggering of ventricular arrhythmias, and hence more important than transmural dispersion of repolarization.

Thus, the expression of the dispersion of repolarization in the ECG remains unclear. In order to determine the meaning of the electrocardiographic repolarization indices, the measurements of local durations and ends of repolarization are needed to be performed simultaneously with the recording of body surface electrocardiograms. The changes of myocardial repolarization parameters can be obtained by the use of experimental models of cardiovascular diseases such as the acute coronary syndrome. On the part of clinical importance, experimental animal models of cardiovascular diseases are thought to be essential tools for finding new diagnostic approaches and therapeutic strategies (Tsang et al 2016). Thus, local myocardial ischemia/reperfusion due to the transient ligation of left descending coronary artery was applied in this study as the main approach (provocative maneuver) to change the repolarization parameters in ventricles.

Objective and issues of the study

The objective of the study was to determine the patterns of the development and electrocardiographic manifestation of the repolarization dispersion, including parameters of repolarization related to the initiation and maintenance of life-threatening arrhythmias in the ischemia-reperfusion experimental model.

On the basis of the fundamental knowledge of electrophysiological characteristics of the heart associated with arrhythmogenesis, to suggest a reliable marker for prediction of ventricular arrhythmias contributing to improvement of ECG diagnostic methods (extension of the diagnostic base of medical device).

This objective was divided into four specific issues:

1. to determine the repolarization gradients in heart ventricles (transmural, apicobasal ect.) in the baseline state and their changes during ischemia/reperfusion settings,
2. to investigate the ability of ECG indices (QT, Tpeak-Tend, T amplitude) to reflect myocardial repolarization heterogeneity,
3. to describe the myocardial repolarization parameters associated with the ventricular tachycardia/ventricular fibrillation,
4. to determinate the expression of the myocardial repolarization parameters involved in prediction of ventricular arrhythmias in the ECG indices.

The study/thesis is designed to answer the following questions:

- Is the dispersion of repolarization reflected in the above mentioned ECG indices?
- Does (what parameters of) the dispersion of repolarization influence the risk of arrhythmia?
- Could ECG indices of repolarization be used in prediction of ventricular arrhythmias?

Methods

The experimental studies were performed in adult animals (mongrel cats, chinchilla rabbits) of either sex in accordance with the Guide for the Care and Use of Laboratory Animals, 8th Edition published by the National Academies Press (US) 2011. All animal experiments were conducted in the laboratory of our partner - Laboratory of Cardiac Physiology of the Institute of Physiology (Syktyvkar, Russia) and the experimental protocol was approved by the local institutional ethical committee.

***In situ* experimental setup**

Animals were anesthetized with a combination of tiletamin/zolazepame (ZOLETIL® 100, Virbac S.A., Carros, France, 15 mg/kg, i.m.), and xilasin (XYLA, Interchemie, Castenray, Netherlands, 1 mg/kg, i.m.). The animals were intubated and ventilated artificially. The arterial blood gases and pH were monitored periodically and, when necessary, were corrected by adjusting respiratory frequency. The arterial blood pressure was monitored and measured with the Prucka Mac-Lab 2000 system (GE Medical Systems, Germany) in the course of experiments by a catheter (internal diameter 0.6 mm) inserted into aorta via the left carotid artery and attached to the pressure transducer SP844 (50 V·V–1·(cm Hg)–1; MEMSCAP, France). The heart was exposed via midline sternotomy. To prevent cooling, the surface of the heart was moistened intermittently with warm saline.

Electrophysiological recordings

The custom-made electrodes were used to simultaneously record 32 to 88 unipolar electrograms from epicardial, midmyocardial, and endocardial layers in spontaneously beating hearts (Arteyeva et al. 2013, Sedova et al. 2013). Myocardial unipolar electrograms measured relatively to the Wilson's central terminal along with electrocardiograms from limb and precordial leads were recorded by a custom-designed 144-channel computerized mapping system with a bandwidth of 0.05–1,000 Hz at a sampling rate of 4,000 Hz.

In each myocardial lead, the activation time (AT) and the repolarization time (RT) were determined as dV/dt_{min} during the QRS complex and dV/dt_{max} during the T wave, respectively (Coronel et al, 2006). AT and RT were measured relatively to the QRS onset in the limb lead I. The values were determined automatically and corrected manually if necessary. The activation-recovery interval (ARI) serving as a measure of local repolarization duration was calculated as

difference between the RT and AT. ARIs were corrected for the heart rate using the Basset's formula. The total dispersion of repolarization, obtained for either ARIs or RTs, was determined as the difference between the maximal and minimal value from all myocardial leads. The transmural, apicobasal, interventricular repolarization gradients were quantified as differences in the ARIs (RTs) between the appropriate ventricular regions. Under the settings of myocardial ischemia/reperfusion, the borderline repolarization gradient was assessed as the difference between the averages of ARIs (RTs) of the ischemic and nonischemic regions.

Stainless steel needle electrodes were inserted subcutaneously to record ECGs in the standard bipolar limb leads and six modified precordial leads (J1-J6). Taking into account the further midsternal access to the heart, leads J1-J3 were shifted from the usual level upwards to the jugular notch and leads J4-J6 downwards to the inferior costal margin. The positions of J2 and J5 were on the midline, J1 and J6 on the right anterior axillary line, and J3 and J4 on the left anterior axillary line (Sedova et al. 2015). A shortening of action potentials in the ventricles apex due to occlusion of the left descending coronary artery was expected to result in an increase of the apicobasal difference in action potential durations. These changes were expected to be documented by the recording of ECGs in the modified precordial leads system with the leads J1-J3 reflecting potentials of the ventricular base and the leads J4-J6 reflecting potentials of the ventricular apex.

The QRS, QT and Tpeak-Tend intervals were measured in the ECG limb lead II and the QT interval was corrected to the heart rate by the formula QTc=QT-0,175*(RR-300) (Carlsson et al. 1993). The T wave amplitudes were measured in the modified precordial leads. Two averaged values were calculated for the "basal" (J1-J3) and "apical" (J4-J6) leads, respectively, and the difference between these values ("apical" minus "basal") was defined as the longitudinal T wave amplitude dispersion.

Ischemia-reperfusion modeling

In order to induce acute local myocardial ischemia/reperfusion settings, the transient ligation with polycaproamide ligature (3-0) was performed in the left anterior descending coronary artery. The exposure of 30 minute coronary occlusion was followed by 30 minutes of reperfusion produced by the loosening of the ligature.

The elevation of the ST segment in the recorded epicardial electrograms served as the evidence of acute ischemia. After the experiment, 1.5 ml of 0.5% Evans blue dye (Sigma-

Aldrich GmbH, Germany) was injected via the carotid artery catheter. The leads in the non-contrasted zone coincided with the leads, where the elevation of the ST segment was observed during coronary occlusion. The perfused regions were designated as a nonischemic zone. The measure of ischemic (noncontrasted) zone in each animal was performed after experiment with the calibrated paper. The area adjacent to the ischemic zone which was identified as perfused region by Evans blue staining (in other words, being nonischemic), but still demonstrated electrophysiological changes was referred to as a "border" zone (Sedova et al. 2013).

Statistics

All the data are presented as medians and interquartile intervals. Statistical examination was performed with The Primer of Biostatistics 4.01 (McGraw Hill 1998) and SPSS 11.5 using the Wilcoxon test for paired comparisons and the Mann-Whitney test to compare two groups of animals. The Fridman test was applied for multiple comparisons followed by the Newman–Keuls or Dunnet tests when appropriate. The differences were considered significant at $p<0.05$. Multiple regression analysis was used to determine which of independent variables (e.g., different dispersions of repolarization) were significantly associated with the dependent variable (e.g., arrhythmia occurrence).

Simulations

Computer simulations were performed in cooperation with N. Arteyeva, Ph.D. (Department of Cardiac Physiology, Institute of Physiology, Komi Science Center, Ural Branch, Russian Academy of Sciences, Syktyvkar, Russia). Simulations were carried out in the framework of a discrete computer model of the heart ventricles, the so-called cellular automaton, adopted to the feline/rabbit heart ventricular and torso geometry. The model was developed using the experimentally measured anatomical and electrophysiological parameters of the rabbit/feline heart. The inputs of the models were (1) locations of activation foci, (2) activation velocity, (3) amplitude and (4) duration of action potentials (AP). The outputs of the model were the (1) AT sequence, (3) RT sequence and (3) body surface ECGs (Arteyeva et al, 2013, Bernikova et al, 2017).

Results

Myocardial repolarization heterogeneity and Tpeak-Tend interval

Experimental measurements of myocardial electrical potentials were performed to demonstrated significant transmural and apicobasal heterogeneity in ARIs and RTs in the intact rabbit heart. The epicardial local repolarization durations in the left ventricle were shorter than in the right ventricle ($p<0.05$). In the left ventricle, the ARIs at the base and in the free wall were longer than at the apex ($p<0.05$). The values of the end of repolarization corresponded to the distribution of ARIs and were shorter at the left ventricular apex than at the right ventricular base ($p<0.05$). Statistically significant ($p<0.05$) transmural gradient of ARIs was found in the apical part of the left ventricle and in the apical part of the interventricular septum. In the basal portion of the left ventricle and interventricular septum, as well as in the apical and basal portion of the right ventricle, the transmural gradient was not statistically significant. The transmural profiles of the end of repolarization times were uniform in the studied myocardial regions. There were no statistically significant transmural differences between repolarization times in all areas of the myocardium.

Using a mathematical model of the rabbit heart, the correlation between the repolarization gradients (transmural, apicobasal, interventricular) in ventricles and the Tpeak-Tend interval was investigated. The close proximity of Tpeak and Tend instants to the earliest and the latest global ventricular RT was found and values of global dispersion of repolarization and duration of the Tpeak-Tend interval were therefore similar. The global dispersion of repolarization resulted from the apicobasal and transmural repolarization gradients as well as from the difference between apical and basal ATs.

In conclusion, the presence of the transmural difference in repolarization durations in the apical portion of the ventricular myocardium in conjunction with the apicobasal and interventricular repolarization gradients were found in the intact rabbit heart. The simulations showed that the Tpeak-Tend interval reflected the global dispersion of repolarization (for more details, see Arteyeva et al. 2013).

Arteyeva NV, Goshka SL, Sedova KA, Bernikova OG, Azarov JE. What does the T peak-T end interval reflect? An experimental and model study. J Electrocardiol 2013. 46(4): 296.e1–e8. JCR IF 2013 - 1.363

Available online at www.sciencedirect.com

SciVerse ScienceDirect

Journal of Electrocardiology 46 (2013) 296.e1 – 296.e8

JOURNAL OF Electrocardiology

www.jecgonline.com

What does the T_{peak}-T_{end} interval reflect? An experimental and model study☆,☆☆

Natalia V. Arteyeva, PhD,[a] Sergey L. Goshka, MD, PhD,[a] Ksenia A. Sedova, PhD,[a, b, d] Olesya G. Bernikova, MD, PhD,[a, c] Jan E. Azarov, PhD[a, b,*]

[a]*Laboratory of Cardiac Physiology, Institute of Physiology, Komi Science Center, Ural Branch, Russian Academy of Sciences, 50, Pervomayskaya st, Syktyvkar, Russia*

[b]*Department of Physiology, Komi Branch of Kirov State Medical Academy, 11, Babushkin st, Syktyvkar, Russia*

[c]*First Department of Internal Diseases, Komi Branch of Kirov State Medical Academy, 11, Babushkin st, Syktyvkar, Russia*

[d]*Czech Technical University, Faculty of Biomedical Engineering, Nám Sítná 3105, Kladno, Czech Republic*

Abstract

Background: It is unclear whether the T_{peak}-T_{end} interval is an index of the transmural or the total dispersion of repolarization.

Methods: We examined the T_{peak}-T_{end} interval using a computer model of the rabbit heart ventricles based on experimentally measured transmural, apicobasal, and interventricular gradients of action potential duration.

Results: Experimentally measured activation-recovery intervals increased from apex to base, from the left ventricle to the right ventricle, and in the apical portion of the left ventricle from epicardium to endocardium and from the right side of septum to the left side. The simulated T_{peak} corresponded to the earliest end of repolarization, whereas the T_{end} corresponded to the latest end of repolarization. The different components of the global repolarization dispersion were discerned by simulation.

Conclusions: The T_{peak}-T_{end} interval corresponds to the global dispersion of repolarization with distinct contributions of the apicobasal and transmural action potential duration gradients and apicobasal difference in activation times.

Keywords: APD gradient; ARI dispersion of repolarization; Repolarization; Simulation; Total dispersion; T_{peak}-T_{end}; Transmural dispersion

Introduction

A mechanism for the genesis and the utility of the T_{peak}-T_{end} interval still remains a matter of controversy.[1–4] Although it is generally recognized that the T_{peak}-T_{end} interval could hardly be exclusively attributed to the sole repolarization gradient, there are 2 viewpoints concerning T_{peak}-T_{end} interval genesis based on different sets of experimental data.

The first set of measurements performed in isolated preparations revealed an apparent transmural action potential duration (APD) gradient in the heart ventricles producing the voltage gradient responsible for the T-wave inscription on pseudoelectrocardiogram (pseudo-ECG).[5] It was assumed that although the apicobasal gradient also may make a contribution, the transmural voltage gradient plays a predominant role in the genesis of the T wave. Consequently, the T_{peak}-T_{end} interval in precordial ECGs was suggested to provide an index of transmural dispersion of repolarization with full repolarization of the epicardium to coincide with the peak of the T wave and that of the M cells to coincide with the end of the T wave.[5]

On the other hand, no clinically significant transmural APD gradients were observed in situ[6,7]; or at least its contribution to the T-wave genesis was negligible.[8] Accordingly, the alternative viewpoint speculates that the T_{peak}-T_{end} duration depends on the global dispersion of repolarization,[9] basically on the apicobasal repolarization gradient. It was also shown that both the epicardium and endocardium of the 2 ventricles contribute significantly to the total dispersion of

☆ The study was supported by the Ural Branch of the Russian Academy of Sciences (Project No. 12-I-4-2059) and the Program of Presidium of Russian Academy of Sciences (Project No. 12-C-4-1009).

☆☆ Conflict of interests: none.

* Corresponding author. Laboratory of Cardiac Physiology, Institute of Physiology, Komi Science Center, Ural Division, Russian Academy of Sciences, Pervomayskaya st, 50, Syktyvkar, Russia, 167982.

E-mail address: j.azarov@gmail.com

0022-0736/$ – see front matter © 2013 Elsevier Inc. All rights reserved.
http://dx.doi.org/10.1016/j.jelectrocard.2013.02.001

repolarization.[10] Thus, the interventricular APD gradient, in addition to the apicobasal and transmural gradients, also contributed to the development of the T wave.

The experimental studies suggest a correlation between the duration of the T_{peak}-T_{end} interval on ECG and the value of transmural, apicobasal, interventricular, or total dispersion of repolarization measured from a set of ventricular electrodes. The greater the number of leads is used, the more accurate relationship obtained would be. However, there are numerous technical and methodological issues limiting the increase of recording sites. As a result, wide ventricular areas remain a "blank spot," thereby impeding the enhancement of the study quality. The ambiguity with the exact determination of the T_{peak}-T_{end} interval duration adds to the complexity of the experimental investigation.

The aim of the present work was to determine the correlation between the different components of dispersion of repolarization in the heart ventricles and the peak and the end of the T wave by means of a mathematical model of the rabbit heart ventricles, including 3 realistic repolarization gradients, namely, transmural, apicobasal, and interventricular gradients.

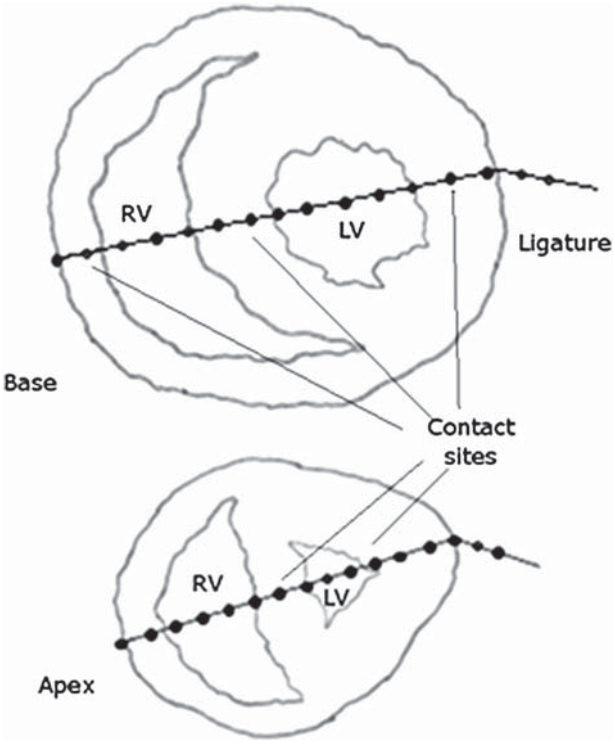

Fig. 1. Schematic presentation of the plunge electrodes placed in the basal and apical portions of the ventricles.

Materials and methods

Experimental preparation

Experimental measurements of activation-recovery intervals (ARIs) were done to obtain realistic APD gradients for the rabbit heart. The investigation conforms to the *Guide for the Care and Use of Laboratory Animals*, *Eighth Edition*, published by the National Academies Press (US; 2011). Ten adult rabbits of both sexes were anesthetized with a Zoletil (Virbac S.A., France)-xylazine (Interchemie werken "De Adelaar" BV, The Netherlands) combination (15 and 1 mg/kg [intramuscular], respectively) and ventilated artificially. The heart was exposed through a midsternal thoracotomy. The arterial blood gases and pH, limb lead ECGs, and arterial blood pressure were monitored throughout the experiment. To prevent cooling, the surface of the heart was moistened continuously with warm saline (38 °C).

For the recording of epicardial ventricular potentials, a sock with 64 electrodes was used with an interelectrode spacing of approximately 5 mm. To obtain the transmural profile of repolarization durations, 2 custom-made flexible plunge electrodes were inserted into the apical and basal thirds of the ventricles. The plunge electrodes were drawn perpendicularly through the right ventricular (RV) free wall, RV cavity, interventricular septum, left ventricular (LV) cavity, and LV free wall (Fig. 1). The outermost RV electrode was fixed at the RV epicardial surface with a knot made on the ligature just adjacent to the lead site to ensure that the electrode position remained in place. Each flexible plunge electrode had 16 lead terminals fixed on the 0.8-mm nylon ligature with 1-mm interelectrode spacing within the myocardial wall thickness.

Two separate sets of 64 unipolar epicardial and 32 intramural electrograms were recorded in reference to the Wilson central terminal in spontaneously beating hearts by means of a custom-designed system (16 bits; bandwidth, 0.05-1000 Hz; sampling rate, 4000 Hz). Potentials were first obtained from the epicardial sock. Afterward, the sock was removed; and the plunge electrodes were immediately inserted. After plunge electrode placement, the heart was allowed to stabilize for 30 minutes before recording of electrograms. Subsequently, the electric signals from the cavities and outside the heart were discarded. This was done by the electrophysiological analysis and careful postmortem inspection of lead positions.

In each lead, the activation time (AT), the end of repolarization time (RT), and ARI were determined as the minimum of the first time derivative during the QRS complex, the maximum time derivative during the ST-T complex, and the time difference between the former and the latter, respectively.[11] The values were determined automatically and corrected manually if necessary. For each parameter—AT, ARI, and RT—the data obtained from the adjacent leads of the epicardial sock were clustered and averaged to give 1 apical, 1 lateral (middle portion), and 1 basal value for the LV and 1 lateral (apical portion) and 1 basal value for the RV. Statistical examination was performed using statistical packages Primer of Biostatistics 4.01 (McGraw Hill, 1998) using the Wilcoxon test for paired comparisons and Friedman test followed by the Newman-Keuls test for multiple comparisons. The differences were considered significant at $P < .05$. Descriptive statistical data are given as median (25th percentile-75th percentile).

Simulations

Simulations were carried out in the framework of a discrete computer model of the heart ventricles, the so-called

cellular automaton. The model was a hexagonal pattern consisting of ≈ 100,000 cells with intercellular space of 0.25 mm. The details of model construction and modeling activation were described earlier.[12] In the present study, the model was adapted to the rabbit heart ventricular and torso geometry. The input of the model was (1) the location of activation foci and (2) the morphology of action potentials and the distribution of APD throughout the ventricles. The output of the model was the (1) activation sequence, (2) end of repolarization sequence, and (3) body surface ECGs. The initial foci of activation in the model were set in the interventricular septum, on the border of its middle and lower portions, and in the subendocardium of the LV apex. In the subendocardial layers of the model, the activation velocity was thrice higher than in the rest of the model, imitating the conduction system.

Action potentials of simplified morphology were proportionally lengthened or shortened depending on the duration values (Fig. 2). The distribution of APDs in the model was calculated on the basis of APD values in the nodal points (Fig. 3). The nodal points were the epi- and endocardial model cells with the assigned AT and APD values. The settings were done in a manner ensuring the correspondence of the assigned values to the representative experimental measurements. The APDs for the nodal points where no measurements were performed were determined by the linear interpolation on the basis of the known values. The RT value for a nodal point was calculated as the sum of the assigned AT and APD. The distribution of the nodal points in the model allowed for the simulations of transmural, apicobasal, left-to-right, or posterior-anterior APD gradients.

The body surface potentials were calculated as:

$$V_{\text{obs}} = -K * \sum_{i=1}^{N} \mathbf{Grad}_i * \mathbf{R}/\mathrm{R}^3,$$

where V_{obs} is the potential value in the observation point, located on the body surface; **K** is the volume conductor property factor; **R** is the vector, directed from the *i*th model cell into the observation point; $\mathbf{Grad}_i$ is the gradient of the action potential value in the *i*th model cell; and *N* is the total number of model cells.

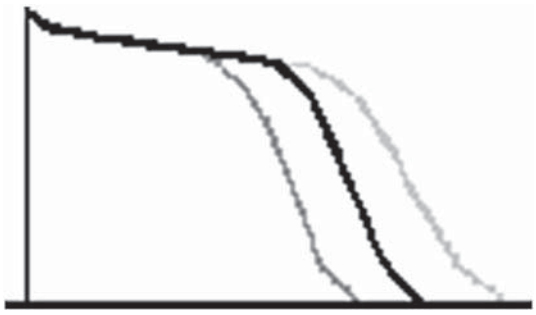

Fig. 2. The simplified action potential morphology used in the model. Action potentials were proportionally lengthened or shortened depending on the duration value.

The value of $\mathbf{Grad}_i$ in each time moment was calculated as:

$$\mathbf{Grad}_i = \sum_{k=1}^{12} \mathbf{Rk} * (p_i - p_k),$$

where **Rk** is the vector, directed from the *i*th model cell to 1 of 12 neighboring model cells; p_{i} is the potential value in the *i*th model cell; p_{k} is the potential value in one of 12 neighboring model cells in the given time moment; potential values in each model cell varied in the range of 100 mV according to the given AP morphology. Besides, the resultant repolarization vector was calculated as a sum of action potential gradients in all model cells.

The ECGs were calculated taking into account the realistic geometry of the torso and heart of the rabbit. The anatomical axis of the heart ventricles was oriented 30° ventrally and to the left from the vertical axis. The peak of the simulated T wave was defined as the *maximal potential value*, and the end of the simulated T wave was defined as the *last nonzero potential value*.

Results

Experimental data

The data on the epicardial activation and end of repolarization sequences corresponded to those previously reported by our group.[13,14] Briefly, the animals were in sinus rhythm on ECG with a heart rate of 248 (226; 293) beats per minute. The activation wave broke through on the epicardium in the apical thirds of the LV and RV, traveling to the rest of ventricles and finally to the base.

The experimentally measured ARI and RT values are listed in Tables 1 and 2. The end of repolarization sequence proceeded from the LV apex to the RV base. The epicardial distributions of repolarization durations were similar in the present and previous studies, with the ARIs (surrogate for APDs) increasing from the apex to the base and from the LV to the RV, although the durations of ARIs were shorter in the present study as compared with the above cited investigations, presumably because of the use of sodium thiopental as an anesthetic agent in the previous study.

Specifically, on the ventricular surface (Table 1), ARIs were the shortest at the LV apex (as compared with the other 4 areas; $P < .05$) and the longest at the RV base and lateral surface (as compared to 3 LV areas; $P < .05$). In the LV, ARIs were longer on the base and free wall than on the apex ($P < .05$). The RT distribution demonstrated regional differences similar to the ARI differences (Table 1). The ARIs tended to be shorter on the epicardium than on the endocardium and shorter on the right side of the interventricular septum than on the left side, with the statistically significant ($P < .05$) transmural—including transseptal—ARI gradients being observed in the apical portion of the ventricular myocardium (Table 2).

Simulations

On the basis of the measured activation and repolarization variables in the representative experiment, further

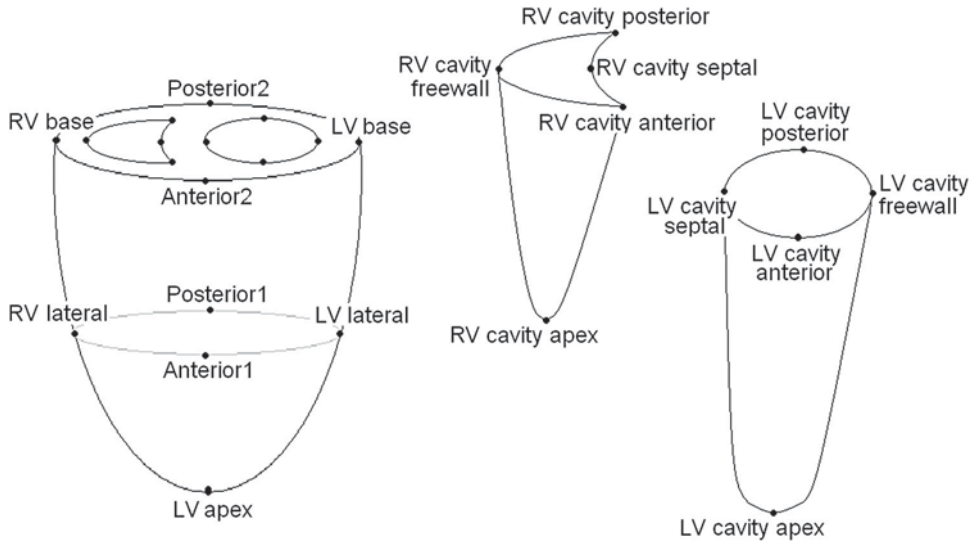

Fig. 3. The location of the nodal points for the simulation of the APD distribution. For detailed description, see Table 1.

simulations were developed. The values set for the nodal points of the model are listed in Table 3.

Activation sequence

The simulated activation sequence (Fig. 4A) corresponded to our experimental data. Activation spreads from the apex to the base of the ventricles and from endo- to epicardium. The interventricular septum activates from the left to the right. The last areas to be activated were the subepicardium of the RV base and the subendocardium of the right side of the septal base.

APD distribution

The APD distribution (Fig. 4B) was simulated on the basis of the measured ARIs in the nodal points (Table 3). The transmural APD gradients varied slightly along the apicobasal axis and were eventually set at 8 to 12 milliseconds for the RV, 10 to 15 milliseconds for the LV, and 11 to 13 milliseconds for the interventricular septum, with the APD values on the left side of the septum being longer than those on the right one. According to the measured data, the apicobasal APD gradient was set nearly twice as large, notably, at 24 milliseconds for the LV epicardium, 29 milliseconds for the RV epicardium and LV free wall endocardium, and 31 milliseconds for the RV free wall endocardium. Interventricular (left-to-right) APD gradient was 5 to 10 milliseconds, and it was no anterior-posterior APD gradient. As no M-cell–like behavior was observed in the experiments, the transmural APD profiles in the model were linear with the progressive APD increase from the epicardium to the endocardium.

Repolarization sequence and ECGs

The dominating direction of repolarization sequence in the model (Fig. 4C) was from the apex to the base of the ventricles and from the epi- to the endocardium according to the measured data. The earliest repolarization in the model occurred on the epicardium of the apex (150 milliseconds) corresponding to the T_{peak} in the aVF lead. The T_{peak} was 3 milliseconds earlier in V_1 and 4 milliseconds later in V_6 as compared to aVF, respectively. The T_{peak} in aVF corresponded to the moment of the maximal magnitude of the resultant repolarization vector (Fig. 5). The latest repolarization occurred on the endocardium of the RV base (208 milliseconds) corresponding to the T_{end} on all ECGs. Thus, the T_{peak}-T_{end} interval (58 milliseconds) exactly coincided with the total dispersion of repolarization.

Mathematical formulation

In the case of normal activation sequence (when the apex is depolarized earlier than the base) and normal repolarization sequence (from the apex to the base and from the epicardium to the endocardium as was demonstrated in the experimental measurements), let the epicardial point 1 be the region of the earliest repolarization, the point 2 be the region of the latest repolarization, and the point 3 be the closest epicardial place to the point 2 (Fig. 6). Fig. 6 displays

Table 1
The experimentally measured ARIs and RTs on the rabbit ventricular epicardium.

	RV base	LV base	RV lateral	LV lateral	LV apex
ARI, ms	117*†‡ (105-120)	99* (90-103)	118*†‡ (105-127)	95* (91-100)	87 (81-92)
RT, ms	127*†‡ (117-140)	105* (99-109)	122*†‡ (116-135)	97 (90-103)	93 (86-100)

The data are presented as median (25%-75%).
* $P<.05$ vs the LV apex.
† $P<.05$ vs the LV lateral.
‡ $P<.05$ vs the LV base.

Table 2
The experimentally measured transmural gradients of the ARIs and RTs in the rabbit ventricular free walls and the interventricular septum.

		RV free wall		Septum		LV free wall	
		Epi	Endo	RV endo	LV endo	Endo	Epi
ARI	Base	112 (89-130)	113 (92-134)	109 (86-118)	112 (109-116)	118 (106-129)	114 (100-124)
	Apex	111 (82-126)	116 (94-121)	112* (107-121)	122 (111-140)	132 (110-137)	111* (102-129)
RT	Base	114 (83-139)	114 (103-134)	120 (97-140)	119 (115-129)	132 (116-150)	133 (119-143)
	Apex	119 (97-134)	124 (116-133)	121 (117-129)	131 (118-141)	131 (120-146)	134 (117-145)

The data are presented as median (25%-75%). Endo indicates endocardium; Epi, epicardium.
* $P<.05$ vs opposite LV endo.

2 possible cases when the latest repolarization occurred in the RV free wall (as it was observed in our experiment) or in the posterolateral area of the LV.

Then

$$T_{end}-T_{peak} = RT_2-RT_1, \text{where}$$

RT_1 and RT_2 are the end of repolarization times at the points 1 and 2, respectively.

As

$$RT = AT + APD,$$

Then

$$T_{end}-T_{peak} = (AT_2 + APD_2)-(AT_1 + APD_1), \text{where}$$

AT_1 and APD_1 are the AT and APD at the point 1, respectively, and AT_2 and APD_2 are the AT and APD at the point 2, respectively.

This expression can be rewritten as

$$T_{end}-T_{peak} = (AT_2-AT_1) + (APD_2-APD_1)$$

or

$$T_{end}-T_{peak} = \Delta AT + (APD_2-APD_1), \text{where}$$

ΔAT is the difference in ATs between the regions of the earliest and the latest repolarization.

On the other hand,

$$APD_2 = APD_3 + TMG, \text{and } APD_3 = APD_1 + ABG, \text{where}$$

TMG is the transmural APD gradient and ABG is the apicobasal (epicardial) APD gradient.

Hence,

$$T_{end}-T_{peak} = \Delta AT + (APD_1 + ABG + TMG-APD_1),$$

or

$$T_{end}-T_{peak} = \Delta AT + ABG + TMG \quad (1)$$

Thus, we demonstrated that the duration of the T_{peak}-T_{end} interval is a sum of 3 components, that is, the transmural APD gradient, the apicobasal (epicardial) APD gradient, and the difference in ATs between the apex and the base of the ventricles.

For the representative values listed in Table 4, the difference in ATs between the regions of the earliest and the latest repolarization is 19 milliseconds (27 − 8 milliseconds). The epicardial apicobasal APD gradient is equal to 29 milliseconds (179 − 150 milliseconds). The transmural APD gradient in the base of the RV free wall is 12 milliseconds (Table 1).

Table 3
The settings of the ATs, APDs, and RTs for the nodal points of the model on the basis of the measured values in the representative experiment.

Nodal point	Description	AT, ms	APD, ms	RT, ms
RV base	Epicardium of the RV free wall base	28	170	198
RV lateral	Epicardium of the RV lateral free wall	20	161	181
LV base	Epicardium of the LV free wall base	29	165	194
LV lateral	Epicardium of the LV lateral free wall	22	151	173
LV apex	Epicardium of the LV apex	11	142	153
Posterior 1	Epicardium of the posterior middle of the ventricles	22	156	178
Posterior 2	Epicardium of the posterior base of the ventricles	27	167	194
Anterior 1	Epicardium of the anterior middle of the ventricles	19	156	175
Anterior 2	Epicardium of the anterior base of the ventricles	29	167	196
RV cavity free wall	Endocardium of the RV free wall base	27	181	208
RV cavity septal	Right endocardium of the septal base	29	167	196
RV cavity posterior*	Endocardium of the RV posterior base	27	171	198
RV cavity anterior*	Endocardium of the RV anterior base	27	171	198
RV cavity apex*	Endocardium of the RV apex	10	152	162
LV cavity free wall	Endocardium of the LV free wall base	24	180	204
LV cavity septal	Left endocardium of the septal base	21	179	200
LV cavity posterior*	Endocardium of the LV posterior base	22	180	202
LV cavity anterior*	Endocardium of the LV anterior base	22	180	202
LV cavity apex*	Endocardium of the LV apex	1	152	153

The locations of the nodal points are shown on Fig. 3. The asterisks denote the interpolated values, whereas the rest of the data correspond to the experimentally measured values in the representative experiment (sinus rhythm; cycle length, 301 milliseconds).

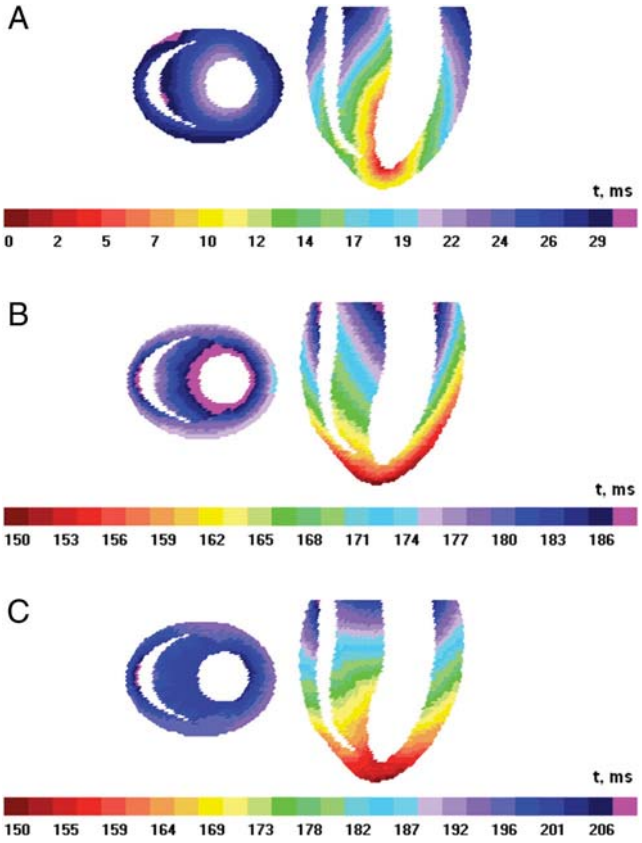

Fig. 4. The results of simulations. A, The simulated activation sequence. B, The simulated APD distribution. C, The simulated end of repolarization sequence. The time from the beginning of activation in the model is shown on scales.

The sum of these 3 components is 60 milliseconds, which is very close to the T_{peak}-T_{end} interval (58 milliseconds) in the aVF lead. Thus, the derived formula is actual.

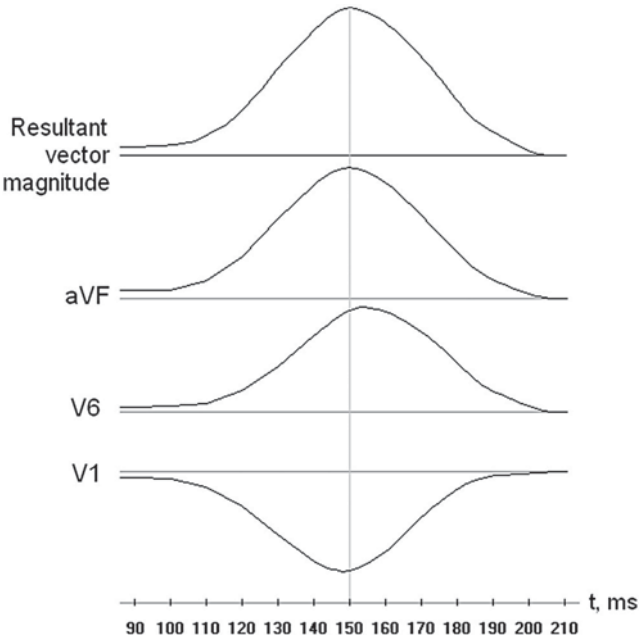

Fig. 5. The T wave in the simulated precordial and limb leads and the magnitude of the resultant repolarization vector. The time from the beginning of activation in the model is shown.

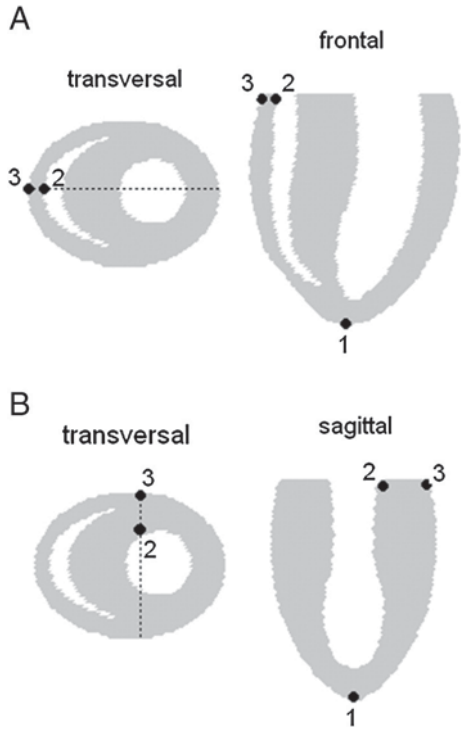

Fig. 6. Schematic illustration to the formula (1). A, The region of the latest repolarization is located within the free ventricular wall. B, The region of the latest repolarization is located in the posterolateral septum. 1, The site of the earliest repolarization. 2, The site of the latest repolarization. 3, Epicardial site close to the site 2. The hatches on the transversal projections indicate the planes of the frontal/sagittal projection.

Discussion

The major simulation findings

Our model coupled with the experimental measurements demonstrates the close proximity of the T_{peak} instant to the earliest global ventricular RT as well as that of the T_{end} instant to the latest global ventricular RT. This resulted in the similarity of values of global dispersion of repolarization and duration of the T_{peak}-T_{end} interval, thereby supporting the previous experimental observations.[9] Furthermore, simulations allowed the analysis of the contribution of activation sequence and different APD gradients to the global dispersion of repolarization and the T_{peak}-T_{end} interval.

For the verification of the suggested equation for the T_{peak}-T_{end} interval duration, the T_{peak} and T_{end} values were taken from the aVF lead. In this lead, T_{peak} was coincident with the time instant of the resultant vector maximal amplitude. The ends of the T wave were the same for all simulated leads because even the small fraction of the last

Table 4
Activation times, APDs, and RTs in the zones of the earliest and the latest repolarization (simulated data).

	AT, ms	APD, ms	RT, ms
The zone of the earliest epicardial RT[a]	8	142	150
The zone of the latest epicardial RT	29	170	199
The zone of the global latest RT	27	181	208

[a] Coincides with the global earliest RT.

repolarizing myocardium caused a nonzero voltage in all ECGs in a noise-free simulation. In the V_1 through V_6 leads, the moment of the T_{peak} varied by ±3 to 4 milliseconds in relation to the aVF T_{peak}. This may be explained by the effects of both the local electrical heterogeneity in the myocardium (eg, transmural) and the different projections of a resultant T-wave vector on the precordial leads due to their proximity to the heart. These interlead variations were rather small in relation to the T_{peak}-T_{end} duration and possibly would be barely detected in the clinical setting. Thus, the accuracy of the suggested equation for the T_{peak}-T_{end} interval was not affected significantly even in the presence of the difference in the T_{peak}-T_{end} interval in precordial leads. However, it may be important to measure the peak of the T wave from distant ECG leads, such as aVF, which are less predisposed to local distortions but reflect the resultant vector and global dispersion of repolarization.

The generation of the electrocardiographic T wave is generally related to the differences in RTs between ventricular regions. The provided formulations demonstrated how the global RT gradient responsible for the duration of the T_{peak}-T_{end} interval could be substituted with the relatively independent measures, namely, specific AT and APD gradients. We showed that the duration of the T_{peak}-T_{end} interval was the sum of 3 components: the transmural APD gradient, the apicobasal (epicardial) APD gradient, and the difference in AT between the apex and base of the ventricles. When the T wave is generated only by a segment of the ventricular wall (eg, the wedge preparation), the apicobasal APD gradient is small, as well as the difference in ATs between the upper and the lower edges of the segment. In this case, the peak of the T wave would correspond to the complete repolarization of the epicardium; and the T_{peak}-T_{end} interval would be actually an index of transmural dispersion of repolarization, as it was found in wedge preparations.[5]

The findings of the present simulations suggested that the peak of the T wave in the limb and precordial leads corresponded to the earliest end of repolarization. An explanation for this could be that, after the first area had fully repolarized, the number of electrical generators in the heart decreased; and the T-wave voltage began to decay. Apparently, the end of the T wave coincided to the latest end of repolarization. Thus, the T_{peak}-T_{end} interval corresponded to the global dispersion of repolarization, which is in accordance with the experimental findings in vivo.[7,9] However, the cited investigations did not demonstrate the significant transmural gradient. The present study, on the other hand, showed the presence of the transmural gradient in the in vivo setting and underscored that (1) the transmural APD gradient made a distinct contribution to the T_{peak}-T_{end} interval but that (2) this contribution is inferior to that of the apicobasal APD gradient and apicobasal AT difference.

Experimental data and validation of the model

The heart position and orientation were set in the model to comply with the intact rabbit heart-torso relationship that is undoubtedly different from the human and requires careful application of the study results. However, the changes in heart-torso relationships hardly modified the major findings of the present investigation.

The results of simulations of the T-wave generation in the body surface ECGs depend necessarily on the repolarization gradients set in the model. There is controversy concerning the direction of the apicobasal gradient and a mere existence of the transmural gradient of repolarization timing in the in situ heart. To ensure the reliable setting of the APD values, we experimentally measured the epicardial and intramyocardial ARIs and demonstrated the presence of the apicobasal, interventricular, and transmural ARI gradients, which were subsequently used for the simulations.

The data on the epicardial ARI and RT distribution corresponded to those previously reported by our group.[13,14] The similar apex-to-base repolarization sequence has been consistently demonstrated in small mammals,[15–17] whereas, in large animals, either the apex-to-base[18] or base-to-apex[19] repolarization patterns were observed. The present study demonstrated the transmural repolarization duration gradients in the in situ rabbit heart. Furthermore, we found the transseptal gradient of ARIs, which is, to our knowledge, the first report from an in situ mammalian heart study. The statistically significant transmural difference in repolarization durations was documented only in the apical portion of the ventricles. However, at simulation, the transmural including transseptal repolarization gradients were set not only for the apical but also for the basal portion of the ventricles, where the gradients were not statistically significant even though they were observed in the majority of the animals. This was done for the sake of clarity to provide rather uniform transmural difference along the wall and to reinforce the role of the transmural gradient in case that the latter was not documented because of low statistical power. Another reason for the inclusion of the basal transseptal gradient was to approximate the model to the data obtained from the arterially perfused septal preparations.[20]

The present study suggested an explanation for the relationship between the T_{peak}-T_{end} interval and ventricular activation sequence and repolarization gradients in normal conditions with the upright T wave in the precordial and limb leads. This imposes limitations for the interpretation of the present results, as the activation process and repolarization pattern could be dramatically affected in the abnormal heart and the contribution of the different components to the T_{peak}-T_{end} interval duration could be changed. Another challenge for the investigation of ECG expression of ventricular repolarization is the cases with the complex morphology of the T wave (eg, biphasic). These problems were outside the scope of the present study.

Clinical implication

The T_{peak}-T_{end} interval has been at present suggested as a marker for the prediction of ventricular dispersion of repolarization and the development of the functional arrhythmic substrate,[3] which may substitute for, at least in part, compromised[21,22] QT dispersion as an arrhythmia predictor. The data of the present study support the suggestion that the T_{peak}-T_{end} interval can be used in clinical conditions when

the changes of the repolarization dispersion on a large scale (eg, along ventricular walls) are expected, such as in heart failure, pacing, extrasystoles, and cardiomyopathy. On the other hand, the increase of transmural dispersion of repolarization (which is usually concerned with such settings as myocardial ischemia) would be expressed in the T_{peak}-T_{end} interval if the increase of transmural dispersion resulted in the augmentation of the global dispersion of repolarization. Presumably, such conditions can be readily met when myocardial ischemia is superimposed on the otherwise affected myocardium as was shown recently.[23]

Conclusion

The present study experimentally demonstrated the presence of the transmural difference in repolarization durations in the apical portion of the ventricular myocardium in conjunction with the apicobasal and interventricular repolarization gradients. The simulations show that the T_{peak}-T_{end} interval reflected the global dispersion of repolarization resulting from the apicobasal and transmural repolarization gradients and the difference in ATs between the apex and the base of the ventricles.

References

1. Patel C, Burke JF, Patel H, et al. Is there a significant transmural gradient in repolarization time in the intact heart? Cellular basis of the T wave: a century of controversy. Circ Arrhythm Electrophysiol 2009;2:80.
2. Opthof T, Coronel R, Janse MJ. Is there a significant transmural gradient in repolarization time in the intact dog? Circ Arrhythmia Electrophysiol 2009;2:89.
3. Panikkath R, Reinier K, Uy-Evanado A, et al. Prolonged T_{peak}-to-T_{end} interval on the resting ECG is associated with increased risk of sudden cardiac death. Circ Arrhythm Electrophysiol 2011;4:441.
4. Smetana P, Schmidt A, Zabel M, et al. Assessment of repolarization heterogeneity for prediction of mortality in cardiovascular disease: peak to the end of the T wave interval and nondipolar repolarization components. J Electrocardiol 2011;44:301.
5. Yan GX, Antzelevitch C. Cellular basis for the normal T wave and the electrocardiographic manifestations of the long-QT syndrome. Circulation 1998;98:1928.
6. Taggart P, Sutton PM, Opthof T, et al. Transmural repolarization in the left ventricle in humans during normoxia and ischaemia. Cardiovasc Res 2001;50:454.
7. Opthof T, Coronel R, Wilms-Schopman FJ, et al. Dispersion of repolarization in canine ventricle and the electrocardiographic T wave: Tp-e interval does not reflect transmural dispersion. Heart Rhythm 2007;4:341.
8. Vaykshnorayte MA, Azarov JE, Tsvetkova AS, Vityazev VA, Ovechkin AO, Shmakov DN. The contribution of ventricular apicobasal and transmural repolarization patterns to the development of the T wave body surface potentials in frogs (*Rana temporaria*) and pike (*Esox lucius*). Comp Biochem Physiol A Mol Integr Physiol 2011;159:39.
9. Xia Y, Liang Y, Kongstad O, Holm M, Olsson B, Yuan S. T_{peak}-T_{end} interval as an index of global dispersion of ventricular repolarization: evaluations using monophasic action potential mapping of the epi- and endocardium in swine. J Interv Card Electrophysiol 2005;14:79.
10. Kongstad O, Xia Y, Liang Y, et al. Epicardial and endocardial dispersion of ventricular repolarization. A study of monophasic action potential mapping in healthy pigs. Scand Cardiovasc J 2005;39:342.
11. Coronel R, de Bakker JM, Wilms-Schopman FJ, et al. Monophasic action potentials and activation recovery intervals as measures of ventricular action potential duration: experimental evidence to resolve some controversies. Heart Rhythm 2006;3:1043.
12. Arteyeva NV, Antonova NA, Roshchevskaya IM, Shmakov DN, Roshchevsky MP. 3-D anisotropic computer model of canine heart ventricles' activation. p. 51. In: Preda I, editor. Electrocardiology'98. Singapore-New Jersey-London-Hong Kong: World Sci; 1999.
13. Azarov JE, Shmakov DN, Vityazev VA, et al. Ventricular repolarization pattern under heart cooling in the rabbit. Acta Physiol (Oxf) 2008;193:129.
14. Azarov JE, Shmakov DN, Vityazev VA, Roshchevskaya IM, Roshchevsky MP. Activation and repolarization patterns in the ventricular epicardium under sinus rhythm in frog and rabbit hearts. Comp Biochem Physiol A Mol Integr Physiol 2007;146:310.
15. Watanabe T, Delbridge LM, Bustamante JO, McDonald TF. Heterogeneity of the action potential in isolated rat ventricular myocytes and tissue. Circ Res 1983;52:280.
16. Kanai A, Salama G. Optical mapping reveals that repolarization spreads anisotropically and is guided by fiber orientation in guinea pig hearts. Circ Res 1995;77:784.
17. Poelzing S, Veeraraghavan R. Heterogeneous ventricular chamber response to hypokalemia and inward rectifier potassium channel blockade underlies bifurcated T wave in guinea pig. Am J Physiol Heart Circ Physiol 2007;292:H3043.
18. Szentadrassy N, Banyasz T, Biro T, et al. Apico-basal inhomogeneity in distribution of ion channels in canine and human ventricular myocardium. Cardiovasc Res 2005;65:851.
19. Bauer A, Becker R, Karle C, et al. Effects of the I(Kr)-blocking agent dofetilide and of the I(Ks)-blocking agent chromanol 293b on regional disparity of left ventricular repolarization in the intact canine heart. J Cardiovasc Pharmacol 2002;39:460.
20. Sicouri S, Glass A, Ferreiro M, Antzelevitch C. Transseptal dispersion of repolarization and its role in the development of torsade de pointes arrhythmias. J Cardiovasc Electrophysiol 2010;21:441.
21. Zabel M, Klingenheben T, Franz MR, Hohnloser SH. Assessment of QT dispersion for prediction of mortality or arrhythmic events after myocardial infarction: results of a prospective long-term follow-up study. Circulation 1998;97:2543.
22. Brendorp B, Elming H, Jun L, et al. QT dispersion has no prognostic information for patients with advanced congestive heart failure and reduced left ventricular systolic function. Circulation 2001;103:831.
23. Kozhevnikov D, Caref EB, El-Sherif N. Mechanisms of enhanced arrhythmogenicity of regional ischemia in the hypertrophied heart. Heart Rhythm 2009;6:528.

Ventricular repolarization gradients in experimental model of ischemia/reperfusion

Alterations of ventricular repolarization were studied in an open-chest feline model of coronary artery occlusion-reperfusion. Before ischemia, the transmural gradients of the RTs and ARIs were found in the right ventricular base and apex, left ventricular base, middle, and apex (Fig. 1). ARIs in the endocardium of the base and the apex of the left and right ventricles were greater than those in the epicardium ($p<0.05$). In the middle of the left ventricle, epicardial ARIs were shorter than midmyocardial and endocardial ARIs ($p<0.05$). ARIs increased from the apex to the base of the heart resulting in the development of the apicobasal gradient of ARIs. The apicobasal differences of ARIs were significant for the epicardial and midmyocardial layers (Tabl. 1, $p<0.05$).

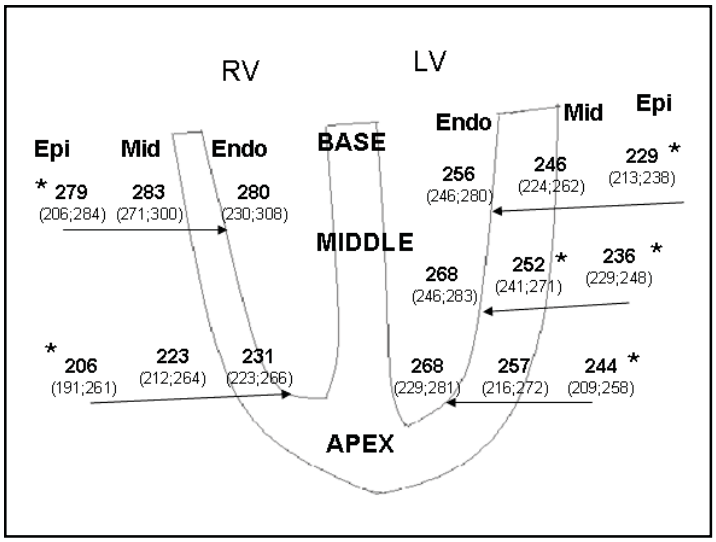

Figure 1. Transmural profiles of activation-recovery intervals (ARIs) in base and apex of the left (LV) and right (RV) ventricles and in the middle of the LV in feline heart.
Values are medians and interquartile intervals (25%; 75%), n = 18; *$p<0.05$ vs endocardium.

Table 1. Apicobasal distribution of activation-recovery intervals (ARIs, ms) in the ventricular myocardium of a cat

ARI, ms	Base	Apex
Epi	240 (213;265)	217 (207;247)*
Mid	248 (229;2778)	232 (221;266)*
Endo	259 (253;280)	252 (237;275)

Values are medians and interquartile intervals (25%; 75%), n = 18; *$p<0.05$ vs Base.
Epi, epicardium; Mid, midmyocadium; Endo, endocardium.

Under the ischemic exposure, the ARIs shortened uniformly in the epicardial, midmiocardial, and endocardial layers of the affected area ($p<0.05$), whereas ARIs in the non-ischemic area remained unaltered. The increase of the borderline gradient and total dispersion of ARIs was observed as a consequence of local shortening of ARIs in the in the middle and apex part of the left ventricle. During the reperfusion, ARIs in the nonischemic zone remained unchanged, while ARIs in the ischemic region lengthened ($p<0.05$). The borderline ARIs gradient and the total ARI dispersion were restored to baseline values after the 30 minutes of reperfusion.

Since oxidative stress during ischemia/reperfusion settings could be a key determinant of action potential duration shortening in an ischemic context, the synthetic echinochrome was applied as antioxidant to influence the ischemia-induced repolarization changes. Animals treated with echinochrome demonstrated least shortening of ARIs compared with control animals. As result, during ischemia the borderline gradient and total dispersion of ARIs were less in the group given echinochrome in comparison with controls but there were no significant quantitative differences in occurrence of ventricular arrhythmias between the groups.

In conclusion, under ischemic conditions, the global, apicobasal, and borderline dispersions of repolarization increased, whereas the transmural gradients did not change. Antioxidant agent echinochrome reduced ischemia-related augmentation of repolarization dispersion, but did not decrease vulnerability to ventricular tachyarrhythmias (for more details, see Sedova et al. 2013).

Sedova KA, Bernikova OG, Goshka SL, Pokhilo ND, Atopkina LN, Shmakov DN, Kharin SN. Effects of an antioxidant agent on alterations of ventricular repolarization in a coronary artery occlusion-reperfusion experimental model. Experimental & Clinical Cardiology 2013. 19(1). JCR IF 2013 - 0.758

Effects of an antioxidant agent on alterations of ventricular repolarization in a coronary artery occlusion-reperfusion experimental model

Ksenia A Sedova PhD[1,2], Olesya G Bernikova MD PhD[1,3], Sergey L Goshka MD PhD[1], Nataly D Pokhilo Ph[4], Lubov N Atopkina Ph[4], Dmitry N Shmakov PhD[1], Sergey N Kharin PhD[1,5]

KA Sedova, OG Bernikova, SL Goshka, et al. Effects of an antioxidant agent on alterations of ventricular repolarization in a coronary artery occlusion-reperfusion experimental model. Exp Clin Cardiol 2013.

BACKGROUND AND OBJECTIVE: Antioxidant agents can prevent oxidative stress and, therefore, cardiac arrhythmias. Electrophysiological mechanisms underlying antiarrhythmic action of antioxidants are not well understood. Echinochrome is an antioxidant and iron-chelating agent of natural origin. Effects of synthetic echinochrome on ischemia- and reperfusion-induced alterations of ventricular repolarization were studied in a coronary artery occlusion-reperfusion model.

METHODS: Cats underwent a brief coronary occlusion-reperfusion sequence (30 min/30 min). To map repolarization, activation-recovery intervals (ARIs) were measured using 30 to 41 left ventricular unipolar extracellular electrograms. Echinochrome was administered intravenously at a dose of 1 mg/kg 5 min before occlusion and/or 5 min before reperfusion.

RESULTS: Echinochrome raised the central aortic pressure and did not affect ARIs in nonischemic myocardium. When echinochrome was administered before reperfusion, restoration of ventricular repolarization during reperfusion was delayed. When echinochrome was administered before both occlusion and reperfusion, the ischemia-induced shortening of ARIs was reduced, and restoration of ARIs during reperfusion was normalized. Ventricular arrhythmias were observed in all of the animals both during occlusion and during reperfusion.

CONCLUSIONS: Echinochrome does not affect repolarization in nonischemic myocardium. The preventive cardioprotective effect of echinochrome is that it reduces ischemia-induced shortening of repolarization duration, diminishes reperfusion-induced increasing of repolarization heterogeneity and raises arterial pressure.

Key Words: *Antioxidant; Cardiac electrophysiology; Experimental model; Ischemia; Reperfusion; Repolarization*

Ischemia- and reperfusion-induced ventricular arrhythmias are caused by alterations of ventricular repolarization because of the influence of reactive oxygen species on ion channels (1). Antioxidants can prevent oxidative stress and, therefore, cardiac arrhythmias. However, electrophysiological mechanisms underlying antiarrhythmic action of antioxidants are not well understood. A combination of an antioxidant and an iron-binding agent is a greater protection against susceptibility to oxidative stress-induced ventricular arrhythmias than the antioxidant alone (2).

Echinochrome (6-ethyl-2,3,5,7,8-pentahydroxy-1,4-naphthoquinone) is an antioxidant and iron-chelating agent of natural origin (3-5). Its cardioprotective and antiarrhythmic effects has been shown (6). Some known physiological effects of echinochrome do not appear to be attributable to its antioxidant and iron-chelating properties. These are normalization of electromechanical coupling in myocardium (7), a cardioprotective effect under calcium disbalance in myocardium (8), and hyperpolarizing action on neurons (9). An effective synthesis of echinochrome was described (10). However, it remains unknown how echinochrome affects cardiac repolarization.

The objective of the present study was an investigation of effects of an antioxidant echinochrome on ischemia- and reperfusion-induced alterations of ventricular repolarization during a brief coronary occlusion-reperfusion sequence in situ. In addition, effects of echinochrome on the central aortic pressure were analyzed. We report our results from using synthetic echinochrome in an open-chest feline model.

METHODS

The work was carried out in accordance with the *Guide for the Care and Use of Laboratory Animals, 8th Edition* published by the National Academies Press (United States) in 2011. The study protocol was approved by the local institutional ethical committee.

Animal preparation

Experiments were performed on 16 adult mongrel cats of both sexes, weighing 2.5 kg to 4.5 kg. Animals were anesthetized with Zoletil 100 (Virbac, France) using a dose of 15 mg/kg intramuscularly and xylazine (Xyla, Interchemie, Holland) using a dose of 1 mg/kg intramuscularly.

A tracheostomy was performed, and an endotracheal tube was positioned to allow mechanical ventilation. Catheters (internal diameter 1 mm) were inserted into the femoral vein for administration of drugs and saline and for withdrawal of blood samples, and into the aorta (through the left carotid artery) to measure central aortic pressure. Steel needle electrodes were inserted subcutaneously to record the standard bipolar limb lead electrocardiograms. A midsternal thoracotomy was performed, and the heart was suspended in a pericardial cradle. The left anterior descending coronary artery was isolated distally (Figure 1), and a silk suture was placed around it to act as a ligature and induce occlusion.

Six flexible multipolar electrodes were inserted by means of a suture needle into the left ventricular wall (Figure 1) to record extracellular electrograms. Each electrode contained eight unipolar recording sites separated by 1 mm. Electrodes were fabricated with isolated copper wires (70 μm diameter), each fastened off with a knot on a vicryl thread (0.8 mm diameter).

Heparin (250 IU/kg) was administered intravenously to prevent coronary artery thrombosis during occlusion. Every 10 min during occlusion, blood samples were withdrawn from the femoral vein to measure the activated partial thromboplastin time. Blood clots did not

[1]*Laboratory of Cardiac Physiology, Institute of Physiology of the Komi Science Centre of the Ural Branch of the Russian Academy of Sciences, Syktyvkar, Russia;* [2]*Czech Technical University, Faculty of Biomedical Engineering, Nám Sítná 3105, Kladno, Czech Republic;* [3]*First Department of Internal Diseases, Komi Branch of Kirov State Medical Academy, Syktyvkar;* [4]*G.B. Elyakov Pacific Institute of Bioorganic Chemistry, Far Eastern Branch, Russian Academy of Sciences, Vladivostok;* [5]*Department of Physiology, Komi Branch of Kirov State Medical Academy, Syktyvkar, Russia*

Correspondence: Dr Sergey Kharin, Institute of Physiology of the Komi Science Centre of the Ural Branch of the Russian Academy of Sciences, 50 Pervomayskaya Street, Syktyvkar, 167982, Komi Republic, Russia. Telephone 7-8212-240085, fax 7-8212-240085, e-mail s.kharin@mail.ru

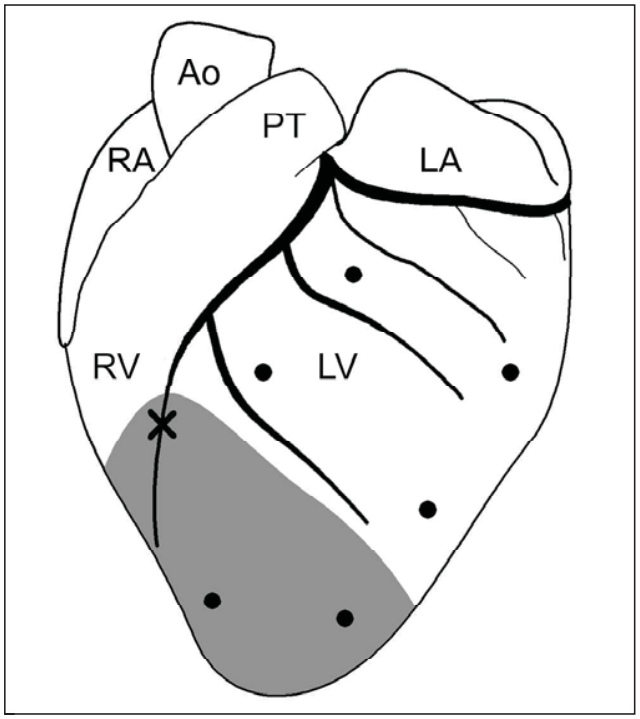

Figure 1) *A scheme of the localization of transmural electrodes (black circles) and occlusion site (cross) in feline hearts. Ao Aorta; LA Left atrium; LV Left ventricle; PT Pulmonary trunk; RA Right atrium (the left atrial appendage is uplifted); RV Right ventricle. The ischemic region is shown by the grey colour*

develop in any of the blood samples, testifying to the adequacy of heparinization and the absence of coronary artery thrombosis.

During the experiment, the core temperature was monitored and maintained constant at 35°C to 37°C. Warm (37°C) saline was applied intermittently to the heart to moisten the epicardium and prevent surface cooling.

On completion of the experiment, the animal was euthanized by extirpation of the heart under general anesthesia.

Animal groups

Three groups of animals were studied. Group E1 (five animals) was given synthetic echinochrome in a dose of 1 mg/kg 5 min before reperfusion (at 25 min of occlusion), and group E2 (five animals) was given synthetic echinochrome in a dose of 1 mg/kg 5 min before occlusion and 5 min before reperfusion. The dosage of echinochrome was chosen on the basis of its ability to protect from myocardial ischemia-reperfusion injury (11,12). Synthetic echinochrome was provided by the G.B. Elyakov Pacific Institute of Bioorganic Chemistry of the Far Eastern Branch of the Russian Academy of Sciences (Vladivostok, Russia). Echinochrome was administered intravenously (through the femoral vein catheter) for 1 min as a 0.2% solution in a 0.1% sodium bicarbonate solution (10 mg of echinochrome was dissolved in 5 mL of a 0.1% sodium bicarbonate solution using ultrasound bath). Group C (six animals) was given an equivalent volume of saline.

Recordings

The electrocardiogram (leads I, II and III) and central aortic pressure (transducer SP844, 50 µV/V/cmHg, MEMSCAP, France) were continuously monitored on a physiological recorder (Prucka Mac-Lab 2000, GE Medical Systems GmbH, Germany). Forty-eight unipolar electrograms and standard bipolar limb lead electrocardiograms were acquired using a custom-designed computerized multiplexed data acquisition system, allowing simultaneous recording of up to 128 signals with a bandwidth of 0.05 Hz to 1000 Hz at a sampling rate of

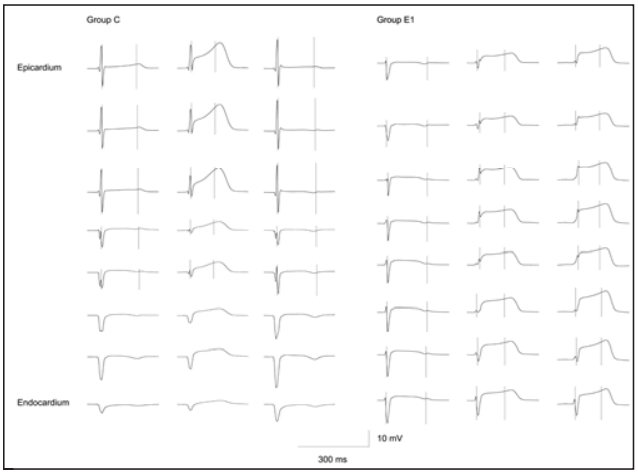

Figure 2) *Ventricular electrograms in cats. Original tracings of unipolar electrograms from a flexible electrode inserted along the epicardial-endocardial axis into the apical left ventricular wall (the ischemic region) at the baseline state (left), 30 min of occlusion (middle) and 30 min of reperfusion (right) in the control (group C) and echinochrome-administered (group E1) cats. Local activation and repolarization times are indicated by upright markers. The tracings without markers were excluded from the analysis because these were unipolar electrograms from recording sites located in the left ventricular cavity*

4000 Hz and an accuracy of 12 bits). Examples of the original graphs of electrograms are shown in Figure 2.

After baseline (preocclusion) electrocardiograms, electrograms and central aortic pressure were recorded under sinus rhythm, coronary occlusion was performed. At the end of the 30 min occlusion, the ligature was released to allow reperfusion for 30 min. Electrocardiograms, electrograms and central aortic pressure were recorded under sinus rhythm at the following time points: 5 min and 30 min of occlusion and 5 min and 30 min of reperfusion.

At the end of the 30 min reperfusion, the left anterior descending coronary artery was religated at the same site, and 1.5 mL of 0.5% Evans blue dye (Reanal, Hungary) was injected into the carotid artery catheter to delineate the in vivo area at risk (Figure 3) and to verify that two of six electrodes were located in this area. Elevation of the ST segment was observed in electrograms recorded in the ischemic region during occlusion (Figure 2). The heart was then cut to determine recording sites located in the left ventricular cavity. Electrograms from these recording sites were excluded from further analysis.

Measurements

Thirty to 41 electrograms were analyzed in each experimental animal. Activation-recovery intervals (ARIs), corrected for heart rate by Bazett's formula, were used for the evaluation of repolarization durations. ARI was defined as the interval between the time of the minimum first derivative of the QRS complex (local activation time) and the maximum first derivative of the T wave (local repolarization time) of unipolar electrograms (13). The computer-assisted measurements of local activation and repolarization times were reviewed and corrected by the experimenter if required. The total ARI dispersion was calculated as the difference between the shortest and the longest corrected ARIs. The boundary gradient was defined as the difference between the averaged corrected ARIs of ischemic and nonischemic regions.

Analysis of ventricular arrhythmias

An arrhythmia score was given as follows: 0, no arrhythmias; 1, monomorphic ventricular extrasystoles <30/min; 2, single or coupled monomorphic ventricular extrasystoles >30/min; 3, polymorphic ventricular extrasystoles; 4, coupled polymorphic ventricular extrasystoles; 5, unstable ventricular tachycardia (<30 s); 6, stable ventricular

TABLE 1
Activation-recovery intervals (ARIs), boundary gradient and total dispersion of ARIs during coronary artery occlusion-reperfusion in cats

		Group E1, n=5		Group C, n=6		Group E2, n=5	
Time point		Nonischemic region	Ischemic region	Nonischemic region	Ischemic region	Nonischemic region	Ischemic region
ARIs							
Baseline		234±51	239±29	232±29	221±33	245±35	229±38
Occlusion	5 min	220±60	157±34*†	224±24	175±31*†	238±33	194±32*†‡§
	30 min	215±60	136±46*†¶	238±28	163±32*†¶	240±32	180±27*†‡§¶
Reperfusion	5 min	222±45	177±62*†**	234±27	192±58†**	242±29	171±31*†**
	30 min	220±41	175±61*†‡**	240±26	238±46*¶**	249±30	221±36‡§¶**
Boundary gradient of ARIs							
Baseline		12±8		11±12		6±6	
Occlusion	5 min	51±26*		56±15*		35±20‡	
	30 min	62±9*		74±25*		54±27*	
Reperfusion	5 min	59±9*		57±36*		72±30*	
	30 min	68±18*‡		24±20**		54±26*‡	
Total dispersion of ARIs							
Baseline		73±38		66±12		78±23	
Occlusion	5 min	101±22		111±20*		85±10‡	
	30 min	123±10*		126±32*		112±20*	
Reperfusion	5 min	115±14		113±47*		120±18*	
	30 min	137±26*‡		87±41**		97±8*‡§	

*Data are presented in ms as the mean ± SD. Group C Control; Group E1 Given synthetic echinochrome in a dose of 1 mg/kg 5 min before reperfusion (at 25 min of occlusion); Group E2 Given synthetic echinochrome in a dose of 1 mg/kg 5 min before occlusion and 5 min before reperfusion. *P<0.05 occlusion and reperfusion versus baseline; †P<0.05 ischemic versus nonischemic region in the same period; ‡P<0.05 Group E1 or group E2 versus group C; §P<0.05 Group E2 versus group E1; ¶P<0.05 30 min of occlusion/reperfusion versus 5 min of occlusion/reperfusion for the corresponding region; **P<0.05 reperfusion versus 30 min of occlusion for the corresponding region*

tachycardia (>30 s); and 7, ventricular fibrillation. Arrhythmias were assessed at 5 min intervals throughout occlusion and reperfusion. For each interval, arrhythmias of the greatest grade were taken into account. Scores for each animal were summed for occlusion and reperfusion. The mean arrhythmia score for each group was then calculated for occlusion and reperfusion.

Statistical analysis

All data are presented as the mean ± SD. Comparisons between groups were carried out using the Mann-Whitney test. Analyses of differences in arrhythmia incidence between groups were carried out using the χ^2 test. Comparisons between time points were carried out by the Wilcoxon test. A value of P<0.05 was considered to be statistically significant.

RESULTS

At baseline, there was no difference in ARIs among the animal groups (Table 1). In each group, there was no difference in ARIs between the regions affected and unaffected by the subsequent ischemia (Table 1). Preocclusion infusion of echinochrome (group E2) did not affect repolarization during the following 5 min.

During coronary occlusion, ARIs in the nonischemic region remained unchanged, while ARIs in the ischemic region shortened progressively in all the groups (Table 1). This resulted in a significant increase in the boundary gradient and total dispersion of ARIs (Table 1). Group E2 showed the least shortening of ARIs in the ischemic region compared with two other groups (Table 1). Pre-reperfusion infusion of echinochrome (group E1) did not affect repolarization during the last 5 min of occlusion. There were no differences in the total ARI dispersion and the boundary ARI gradient between the groups at 30 min of occlusion (Table 1).

During reperfusion, ARIs in the nonischemic region remained unchanged, while ARIs in the ischemic region lengthened in all the animal groups (Table 1). At 30 min of reperfusion, ARIs in the

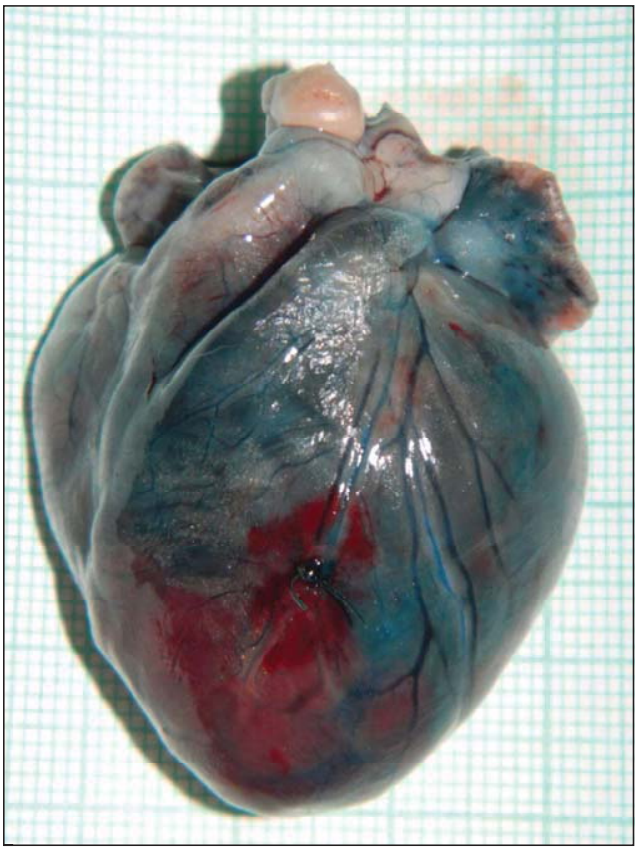

Figure 3) *Assessment of area at risk in feline hearts (perfusion with Evans blue). The nonperfused (ischemic) region is not dyed*

TABLE 2
Comparison of the animal groups in relation to types of ventricular arrhythmias during coronary artery occlusion-reperfusion

	Occlusion			Reperfusion		
Type of arrhythmias	Group C (n=6)	Group E1 (n=5)	Group E2 (n=5)	Group C (n=6)	Group E1 (n=5)	Group E2 (n=5)
No arrhythmias	0	1	0	1	2	0
Monomorphic ventricular extrasystoles (<30/min)	5	4	5	2	0	2
Single or coupled monomorphic ventricular extrasystoles (>30/min)	2	1	2	2	1	1
Polymorphic ventricular extrasystoles	0	1	2	0	0	0
Coupled polymorphic ventricular extrasystoles	1	1	0	0	0	1
Unstable ventricular tachycardia (<30 s)	1	1	0	2	2	1
Stable ventricular tachycardia (>30 s)	0	0	0	1	1	0
Ventricular fibrillation	0	0	0	0	0	1

Data presented as n. Group C Control; Group E1 Given synthetic echinochrome in a dose of 1 mg/kg 5 min before reperfusion (at 25 min of occlusion); Group E2 Given synthetic echinochrome in a dose of 1 mg/kg 5 min before occlusion and 5 min before reperfusion

TABLE 3
Comparison of the animal groups in relation to the occurrence of ventricular arrhythmias during coronary artery occlusion–reperfusion

	Ventricular extrasystoles				Ventricular tachycardia/fibrillation			
	Occlusion		Reperfusion		Occlusion		Reperfusion	
Group	0–15 min	16–30 min	0–5 min	6–30 min	0–15 min	16–30 min	0–5 min	6–30 min
Group C (n=6)	5	4	2	2	0	0	3	0
Group E1 (n=5)	4	2	1	0	0	1	2	0
Group E2 (n=5)	3	5	4	1	0	0	2	0

Data presented as n. Group C Control; Group E1 Given synthetic echinochrome in a dose of 1 mg/kg 5 min before reperfusion (at 25 min of occlusion); Group E2 Given synthetic echinochrome in a dose of 1 mg/kg 5 min before occlusion and 5 min before reperfusion

TABLE 4
Comparison of the experimental groups in relation to arrhythmia scores* in a feline model of coronary artery occlusion-reperfusion

Period	Group C (n=6)	Group E1 (n=5)	Group E2 (n=5)
Occlusion	4.7±2.9	6.6±7.1	4.4±1.7
Reperfusion	4.2±2.6	3.6±4.6	4.2±4.1

*Group C Control; Group E1 Given synthetic echinochrome in a dose of 1 mg/kg 5 min before reperfusion (at 25 min of occlusion); Group E2 Given synthetic echinochrome in a dose of 1 mg/kg 5 min before occlusion and 5 min before reperfusion. *0, no arrhythmias; 1, monomorphic ventricular extrasystoles <30/min; 2, single or coupled monomorphic ventricular extrasystoles >30/min; 3, polymorphic ventricular extrasystoles; 4, coupled polymorphic ventricular extrasystoles; 5, unstable ventricular tachycardia (<30 s); 6, stable ventricular tachycardia (>30 s); and 7, ventricular fibrillation*

ischemic region were slightly greater than those at baseline in group C and were not different from those at baseline in group E2, but were significantly less than those at baseline in group E1. ARIs in the ischemic region at 30 min of reperfusion in group E1 were significantly shorter than those in group C and group E2 (Table 1). The boundary ARI gradient and the total ARI dispersion were not restored to the baseline values by the 30 min reperfusion in the echinochrome-administered groups, in contrast with group C (Table 1). However, the total ARI dispersion at 30 min of reperfusion was significantly closer to the baseline value in group E2 as compared with group E1 (Table 1).

Heart rate in group E1 remained unchanged during the occlusion-reperfusion period: 176±18 beats/min, 182±21 beats/min and 180±18 beats/min at baseline, 30 min of occlusion and 30 min of reperfusion, respectively. In group C, heart rate at baseline, 30 min of occlusion and 30 min of reperfusion was 155±17 beats/min, 163±18 beats/min and 154±12 beats/min (P<0.05 versus occlusion), respectively. In group E2, heart rate at baseline, 30 min of occlusion and 30 min of reperfusion was 140±17 beats/min, 147±19 beats/min, and 161±14 beats/min (P<0.05 versus baseline), respectively. There were the following differences in heart rate: between group C and group E1 at 30 min of reperfusion (P<0.05); and between group E1 and group E2 at baseline (P<0.05) and at 30 min of occlusion (P<0.05).

All the animal groups showed ventricular arrhythmias both during occlusion and reperfusion (Table 2). Arrhythmias were observed in almost all the animals both during occlusion and during reperfusion. There were no ventricular arrhythmias during occlusion in only one cat in group E1 and no reperfusion-induced ventricular arrhythmias in two cats in group E2 and one cat in group C. There were no significant differences in the incidence of ventricular extrasystoles and ventricular tachycardia among the animal groups during occlusion (Table 3). In all the groups, reperfusion-induced ventricular tachycardia (and spontaneously reversible fibrillation lasted for 35 s in one cat in group E2) developed mainly within the initial 5 min of reperfusion, while reperfusion-induced ventricular extrasystoles were observed throughout reperfusion (Table 3). There was no significant difference in arrhythmia scores among the animal groups (Table 4).

Arterial pressure did not differ among the animal groups at baseline (Table 5). In group C, the systolic, diastolic and mean pressures tended to decrease during occlusion and tended to rise to baseline values during reperfusion, and there were no significant changes in the pulse pressure. Group E1 showed the similar dynamics of arterial pressure during occlusion. Pre-reperfusion infusion of echinochrome (group E1) resulted in the rapid rise in the systolic, diastolic and mean pressures. Then, during reperfusion, the systolic, diastolic and mean pressures slightly fell and did not differ from the baseline values. The pulse pressure in group E1 remained unchanged during occlusion and reperfusion. In group E2, the rapid rise in the systolic, diastolic and mean pressures occurred after each infusion of echinochrome with the further decrease to baseline values; the significant increase in the pulse pressure was only after the second (pre-reperfusion) infusion of echinochrome.

DISCUSSION

Electrophysiological mechanisms underlying antiarrhythmic action of antioxidants are not well understood. As has been reported previously, a combination of an antioxidant and an iron-binding agent is a greater protection against susceptibility to oxidative stress-induced ventricular arrhythmias than the antioxidant alone (2). The purpose of the

TABLE 5
The effect of echinochrome on arterial pressure (mmHg) during coronary artery occlusion-reperfusion in cats

			Occlusion			Reperfusion	
Group	**Baseline**	**Baseline + E**	**5 min**	**25 min**	**30 min + E**	**5 min**	**30 min**
Systolic pressure							
Group C	103±14	–	96±11	91±9	–	96±15	104±18
Group E1	94±15	–	88±9	82±16	101±18*	92±16†‡	93±9†
Group E2	97±21	110±20*	93±14‡	95±10	106±14*	107±32†	90±7†‡
Diastolic pressure							
Group C	79±16	–	72±12	68±10	–	75±12	75±17
Group E1	74±12	–	67±13	64±17	79±18*	72±15‡	70±14
Group E2	76±21	86±19*	75±14	75±8	82±10*	77±16	71±7‡
Mean pressure							
Group C	87±15	–	80±12	77±9	–	82±13	85±16
Group E1	80±13	–	74±16	70±16	86±18*	79±15‡	77±12
Group E2	83±21	94±20*	81±15‡	81±9	90±11*	89±24	78±7‡
Pulse pressure							
Group C	24±2	–	23±5	27±5	–	21±4	28±8
Group E1	22±6	–	23±8	18±6	22±4	20±5	23±6
Group E2	21±1	24±4	18±2	20±3	24±5*	30±15*	20±3

*Data presented as mean ± SD. E Echinochrome; Group C Control, n=6; Group E1 Given synthetic echinochrome in a dose of 1 mg/kg 5 min before reperfusion (at 25 min of occlusion), n=5; Group E2 Given synthetic echinochrome in a dose of 1 mg/kg 5 min before occlusion and 5 min before reperfusion, n=5. *P<0.05 versus the state before administration of echinochrome; †P<0.05 versus occlusion at 25 min; ‡P<0.05 versus the state with infusion of echinochrome (at 30 min of occlusion)*

present study was to investigate effects of echinochrome on ischemia- and reperfusion-induced alterations of ventricular repolarization in an open-chest feline model of a brief coronary occlusion-reperfusion sequence. Synthetic echinochrome was used as an antioxidant and an iron-binding agent (3-5). Previously, evidence for cardioprotective effects of echinochrome from myocardial ischemia-reperfusion injury has been reported in acute canine and chronic rabbit models of coronary artery occlusion-reperfusion (11,12). Clinical investigations confirm that treatment with echinochrome prevents infarct expansion induced by reperfusion (14).

The major findings of the present study are as follows: echinochrome does not affect repolarization of nonischemic myocardium; echinochrome reduces ischemia-induced shortening of repolarization; and the positive effect of echinochrome on arterial pressure appears quickly.

There was no effect of echinochrome on ARIs in the nonischemic region, and the preocclusion infusion of echinochrome reduced the ischemia-induced shortening of ARIs. One might assume that echinochrome inhibits ionic current through the ATP-regulated potassium channels (K_{ATP} channels); however, appropriate research is required to confirm this assumption.

Ventricular repolarization in the control cats was restored to the baseline state by the 30 min reperfusion. In contrast, restoration of ventricular repolarization was delayed within the 30 min reperfusion in cats treated with the pre-reperfusion infusion of echinochrome. This delay testified that a normalization of ionic currents was decelerated. This might be attributable to the activation both of potassium (other than the K_{ATP} current) and calcium currents by echinochrome (9) and to the dependence of potassium currents on intracellular calcium (15).

Increased ventricular repolarization heterogeneity can provide the potential substrate for ventricular arrhythmias. An index of repolarization heterogeneity is spatial dispersion of repolarization (16,17). In the study reported here, all the animal groups showed both occlusion and reperfusion ventricular arrhythmias. This was in consistent agreement with the increased total ARI dispersion at occlusion and reperfusion in all the animal groups. However, the twofold increased total ARI dispersion at 30 min of reperfusion in the echinochrome-administered cats (group E1) testified maintenance of a greater remaining risk of ventricular arrhythmias compared with two other groups. In spite of this fact, there was no difference in reperfusion-induced arrhythmia incidence and scores between the animal groups. Our observations were in consistent agreement with no effect of echinochrome on the incidence of cardiac rhythm disorders reported for dogs by other researchers (12). However, the decreased number, frequency, duration and severity of reperfusion arrhythmic episodes have been observed by application of echinochrome before myocardial reperfusion in patients (7,14). The discrepancies between clinical and experimental study results may be due to species differences. It is possible that there is a certain threshold of the antiarrhythmic activity of antioxidant agents, whereas the probability of reperfusion-induced arrhythmias in dogs and cats is less than in humans because of differences in the coronary collateral circulation. Residual flow to ischemic myocardium during coronary artery occlusion in dogs and cats is significantly greater than that in humans (18,19). As a result, reperfusion-induced oxidative stress and, therefore, a probability of reperfusion-induced arrhythmias appear to be less.

Infusion of echinochrome resulted in the rise in arterial pressure. This rise could be attributable to an increase in cardiac output and/or vascular resistance. The assumption that an increase in stroke volume (the inotropic effect) could occur after echinochrome administration, was in consistent agreement with other findings. Increasing ventricular contractility could be associated with a normalization of the pump function of the heart, because echinochrome activates the calcium current (9) and promotes stabilization of intracellular calcium content (8,20) through maintenance of the activity of cardiomyocyte membrane receptors and ryanodine receptors of the sarcoplasmic reticulum (20). The echinochrome-induced increase in arterial pressure reported for our study were in consistent agreement with the positive inotropic effect of echinochrome on isolated human right atrial strips (7). However, an increase in vascular resistance could not be excluded because echinochrome could affect calcium homeostasis in vascular muscle cells as it occurs in cardiac myocytes.

The present study has limitations. Lipid peroxidation products were not measured. Therefore, we had no data on whether the infusions of echinochrome caused decreasing generation of reactive oxygen species within the myocardium. However, it was shown previously that echinochrome, being a very lipophilic compound (5) with a high free radical scavenging activity (3-5), decreases lipid peroxidation (21,22). Also, no histological examination was performed, and we do not have data on infarct size. However, the dosage used causes a significant reduction of infarct size in experimental animals (11,12).

Neither cardiac output nor vascular resistance was measured. Both these parameters are needed to suggest the mechanism of the rise in arterial pressure after infusion of echinochrome.

In summary, echinochrome does not affect repolarization in non-ischemic myocardium, but reduces ischemia-induced shortening of repolarization and diminishes reperfusion-induced increasing of repolarization heterogeneity. Infusion of echinochrome has a rapid positive effect on arterial pressure.

ACKNOWLEDGEMENTS: This work was supported by the Ural Branch of the Russian Academy of Sciences (Projects No. 12-C-4-1009 and 13-4-SP-359).

REFERENCES

1. Carmeliet E. Cardiac ionic currents and acute ischemia: From channels to arrhythmias. Physiol Rev 1999;79:917-1017.
2. Karahaliou A, Katsouras C, Koulouras V, et al. Ventricular arrhythmias and antioxidative medication: Experimental study. Hellenic J Cardiol 2008;49:320-8.
3. Lebedev AV, Levitskaya EL, Tikhonova EV, Ivanova MV. Antioxidant properties, autooxidation, and mutagenic activity of echinochrome a compared with its etherified derivative. Biochemistry (Moscow) 2001;66:885-93.
4. Lebedev AV, Ivanova MV, Levitsky DO. Echinochrome, a naturally occurring iron chelator and free radical scavenger in artificial and natural membrane systems. Life Sci 2005;76:863-75.
5. Lebedev AV, Ivanova MV, Levitsky DO. Iron chelators and free radical scavengers in naturally occurring polyhydroxylated 1,4-naphthoquinones. Hemoglobin 2008;32:165-79.
6. Mishchenko NP, Fedoreev SA, Bagirova VL. Histochrome: A new original domestic drug. Pharm Chem J 2003;37:48-52.
7. Afanasiev SA, Vechersky YuYu, Ponomarenko IV, Shipulin VM. Effect of an antioxidant histochrome on electrical stability of the myocardium of patients with ischemic heart disease in the early post-occlusion period of aortocoronary bypass surgery. Kardiologiia 2000;40:30-3.
8. Vinokurov AA, Alabovskiĭ VV, Shul'zhenko VS, Ivanova MV, Lebedev AV. Effect of antioxidant histochrome preparation on the contractile function and metabolism of the isolated rat heart under conditions of "calcium paradox", ischemia, and reperfusion. Vopr Med Khim 2001;47:483-90.
9. Mischenko NP, Fedoreev SA, Zapara TA, Ratushnyak AS. Effects of histochrom and emoxypin on biophysical properties of electroexcitable cells. Bull Exp Biol Med 2009;147:196-200.
10. Anufriev VPh, Novikov VL, Maximov OB, et al. Synthesis of some hydroxynaphthazarins and their cardioprotective effects under ischemia-reperfusion in vivo. Bioorg Med Chem Lett 1998;8:587-92.
11. Shvilkin AV, Afonskaia NI, Cherpachenko NM, et al. Evaluating the protective effect of polyhydroxy-1,4-naphthoquinones in a model of experimental myocardial occlusion-reperfusion. Kardiologiia 1991;31:81-2.
12. Shvilkin AV, Serebriakov LI, Tskitishvili OV, et al. Effect of echinochrome on experimental myocardial reperfusion injury. Kardiologiia 1991;31:79-81.
13. Millar CK, Kralios FA, Lux RL. Correlation between refractory periods and activation-recovery intervals from electrograms: Effects of rate and adrenergic interventions. Circulation 1985;72:1372-9.
14. Buĭmov GA, Maksimov IV, Perchatkin VA, et al. Effect of the bioantioxidant histochrome on myocardial injury in reperfusion therapy on patients with myocardial infarction. Ter Arkh 2002;74:12-6.
15. Piao L, Li J, McLerie M, Lopatin AN. Cardiac IK1 underlies early action potential shortening during hypoxia in the mouse heart. J Mol Cell Cardiol 2007;43:27-38.
16. Antzelevitch C. Role of spatial dispersion of repolarization in inherited and acquired sudden cardiac death syndromes. Am J Physiol Heart Circ Physiol 2007;293:H2024-38.
17. Killeen MJ, Sabir IN, Grace AA, Huang CL-H. Dispersions of repolarization and ventricular arrhythmogenesis: Lessons from animal models. Prog Biophys Mol Biol 2008;98:219-29.
18. Harken AH, Simson MB, Haselgrove J, Wetstein L, Harden WR 3rd, Barlow CH. Early ischemia after complete coronary ligation in the rabbit, dog, pig, and monkey. Am J Physiol 1981;241:H202-10.
19. Maxwell MP, Hearse DJ, Yellon DM. Species variation in the coronary collateral circulation during regional myocardial ischemia: A critical determinant of the rate of evolution and extent of myocardial infarction. Cardiovasc Res 1987;21:737-46.
20. Belostotskaya GB, Darashina IV, Golovanova TA, Khrustaleva RS, Tsyrlin VA. The estimation of freshly isolated rat cardiomyocytes functional state under oxidative stress. Regional Circ Microcirc 2008;7:85-92.
21. Markov VA, Buymov GA, Maximov IV, et al. Effect of a novel water soluble bioantioxidant histochrome on reperfusion injury after thrombolysis in patients with acute myocardial infarction. Kardiologiia 1999;39:20-3.
22. Afanas'ev SA, Lasukova TV, Cherniavskiĭ AM, Vecherskiĭ IuIu, Ponomarenko IV. The effect of histochrome on the lipid peroxidation indices during the surgical treatment of patients with ischemic heart disease of different functional classes. Eksp Klin Farmakol 1999;62:32-4.

Electrocardiographic markers of ventricular repolarization heterogeneity

The analysis of ECG parameters of cardiac repolarization in the standard bipolar limb leads revealed significant prolongation of the QTc and Tpeak-Tend intervals during 30-minute coronary occlusion in cats. The QTc interval was prolonged after the 15th and 30th minute of coronary occlusion as compared with the baseline ($p<0.05$). The significant prolongation of the Tpeak-Tend interval was observed after the 30th minute of coronary occlusion compared with the baseline ($p<0.05$). ECGs recorded from the precordial leads demonstrated changes of the T wave amplitude. At baseline, the negative T wave was observed in the "basal" leads J1–J3 and the positive T wave was observed in the "apical" leads J4–J6 presenting the longitudinal dispersion of the T wave amplitude. The amplitude of the T wave in the leads J1–J3 increased (the T wave became more negative) after 15 and 30 minutes of coronary occlusion ($p<0.05$), at the same time the amplitude of the T wave in leads J4–J6 also increased (the T wave became more positive) in response to acute ischemia ($p<0.05$). Thus, the longitudinal T wave amplitude dispersion increased significantly after 15 and 30 minutes of coronary occlusion.

In conclusion, the dynamics of the repolarization dispersion changes during acute ischemia could be assessed by the measurements of the longitudinal T wave amplitude dispersion, Tpeak-Tend and QTc intervals from the body surface ECGs (for more details, see Sedova et al. 2015).

Sedova K, Bernikova O, Azarov J, Shmakov D, Vityazev V, Kharin S. Effects of echinochrome on ventricular repolarization in acute ischemia. J Electrocardiol 2015. 48(2): 181-186. JCR IF 2015 - 1.290

Available online at www.sciencedirect.com

ScienceDirect

Journal of Electrocardiology 48 (2015) 181 – 186

JOURNAL OF Electrocardiology

www.jecgonline.com

Effects of echinochrome on ventricular repolarization in acute ischemia☆,☆☆

Ksenia Sedova, PhD,[a, b,*] Olesya Bernikova, MD, PhD,[a] Jan Azarov, PhD,[a, c, d] Dmitry Shmakov, PhD,[a] Vladimir Vityazev, PhD,[a] Sergey Kharin, PhD[a, c]

[a] *Laboratory of Cardiac Physiology, Institute of Physiology, Komi Science Centre, Ural Branch, Russian Academy of Sciences, 50, Pervomayskaya St, Syktyvkar, Russian Federation*

[b] *Department of Biomedical Technology, Czech Technical University in Prague, Nam Sitna 3105, Kladno, Czech Republic*

[c] *Department of Physiology, Medical Institute of Syktyvkar State University, 11, Babushkin St, Syktyvkar, Russian Federation*

[d] *Department of Physiology, Komi Branch of Kirov State Medical Academy, 11, Babushkin St, Syktyvkar, Russian Federation*

Abstract

Background: Myocardial ischemic electrophysiological alterations are associated with the generation of reactive oxygen species. However, electrophysiological effects of antioxidants are unclear. Our objective was to determine the effects of the antioxidant echinochrome on ventricular repolarization in a feline model of 30-min ischemia.

Methods and results: Activation–recovery intervals were measured from 64 ventricular electrograms recorded before and during the LAD ligation in untreated animals (controls, n = 5) and animals given echinochrome (1 mg/kg, n = 5 and 2 mg/kg, n = 7). In controls, ischemia resulted in the increase of repolarization dispersion, QTc and Tpeak–Tend intervals and precordial T wave amplitude dispersion. Echinochrome attenuated the ischemic increase of repolarization dispersion. The increased dose of echinochrome abolished the ischemic ECG repolarization changes but did not modify the incidence of ventricular arrhythmias.

Conclusion: Echinochrome modified ischemic alterations of repolarization dispersion that were associated with the changes of the body surface T wave amplitude dispersion and Tpeak–Tend interval.

Keywords: Ischemia; Repolarization; Antioxidant; Animal model

Introduction

Acute cardiac ischemia causes electrophysiological alterations that may lead to fatal arrhythmias. Among these alterations is the increase in the content of reactive oxygen species (ROS), which produce a wide spectrum of proarrhythmic effects [1]. Antioxidants may reduce the susceptibility to cardiac arrhythmias by the prevention of oxidative stress [2]. A pigment of sea urchins echinochrome A (2,3,5,7,8-pentahydroxy-6-ethyl-1,4-naphthoquinone), an antioxidant agent characterized by iron chelation and free-radical scavenging abilities [3], has been reported to render cardioprotective effects in ischemia/reperfusion models [4], but its electrophysiological effects, that may underlie a potential antiarrhythmic action, are not well understood.

The assessment of cardiac repolarization on the basis of ECG analysis during acute coronary syndrome is of clinical importance as to the prognosis of arrhythmias and evaluation of antiarrhythmic therapies. Specifically, the ECG indices of ventricular repolarization including the QT interval, T wave and Tpeak–Tend durations, the T wave voltage and morphology could reflect the vulnerability of the ventricles to the life-threatening reentrant arrhythmias. The total dispersion of repolarization, which is associated with both the arrhythmic susceptibility and the generation of the T wave, is determined by several so-called ventricular repolarization gradients with the contribution of transepicardial (i.e., apicobasal, interventricular and anteroposterior) gradients being superior to that of the transmural gradient [5–9].

The action potential duration predominantly shortens in the ischemic conditions thereby modifying dispersion of repolarization [10]. We hypothesized that echinochrome as an antioxidant agent could influence the ventricular repolarization-associated

☆ The authors declare no conflicts of interests.

☆☆ The study was supported by the Ural Branch of the Russian Academy of Sciences (Projects No. 12-C-4-1009, 13-4-SP-359 and 13-4-032-KSC). The sponsor has not been involved in study design, the collection, analysis and interpretation of data, in the writing of the report and in the decision to submit the article for publication.

* Corresponding author at: Department of Biomedical Technology, Czech Technical University in Prague, Nam Sitna 3105, Kladno, Czech Republic, 27201.

E-mail address: sedova.ks@gmail.com

http://dx.doi.org/10.1016/j.jelectrocard.2015.01.003

manifestations of myocardial ischemia. The objective of the present study was to measure the effects of echinochrome on repolarization durations and dispersion and to test if these effects were associated with the changes of the body surface ECG parameters in an open-chest feline model of 30-min ischemia.

Material and methods

The study was carried out in accordance with the Guide for the Care and Use of Laboratory Animals, 8th Edition published by the National Academies Press (US) 2011, and the experimental protocol was approved by the local institutional ethical committee. The experiments were performed in a total of 17 adult mongrel cats of both sexes, weighing 2.5 to 4.5 kg. Animals were anesthetized with zoletil (ZOLETIL® 100, Virbac S.A., Carros, France; 15 mg/kg, i.m.) and xylazine (XYLA, Interchemie, Castenray, Holland; 1 mg/kg, i.m.). Then, the animals were intubated and artificially ventilated. Catheters (internal diameter 1 mm) were inserted into the femoral vein for the administration of drugs and saline. Stainless steel needle electrodes were inserted subcutaneously to record ECGs in the standard bipolar limb leads and six modified precordial leads (J1–J6). Taking into account the further midsternal access to the heart, these leads were shifted from the usual level upwards to the jugular notch (J1–J3) and downwards to the inferior costal margin (J4–J6). The positions of J2 and J5 were in the midline, J1 and J6 in the right anterior axillary line, and J3 and J4 in the left anterior axillary line (Fig. 1). A shortening of action potentials in the apical part of the heart ventricles due to occlusion of the left descending coronary artery was expected to result in an increase of the apicobasal difference in action potential durations and these changes were expected to be documented by the recording of ECGs in the modified precordial leads system with the leads J1–J3 reflecting potentials of the ventricular base and the leads J4–J6 reflecting potentials of the ventricular apex.

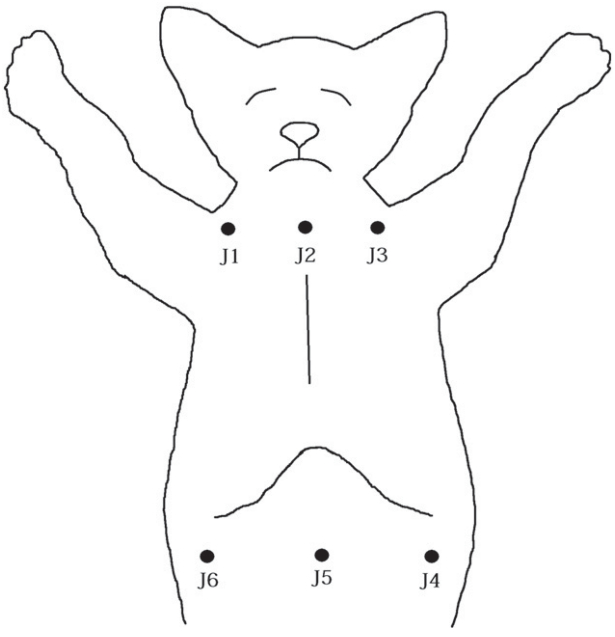

Fig. 1. Schematic presentation of the distribution of precordial leads.

The heart was exposed through a midsternal approach and was suspended in a pericardial cradle. In order to induce coronary occlusion, a polycaproamide ligature (No. 3-0) was placed around the left anterior descending coronary artery (LAD). During the experiment, the core temperature was monitored and maintained constant at 35–37 °C. Warm (37 °C) saline was applied intermittently to the heart to moisten the epicardium and prevent surface cooling. A 64-electrode epicardial sock was placed on the heart ventricles to record unipolar electrograms. The signals were isolated, amplified, multiplexed, and recorded by a custom-designed 144-channel computerized mapping system with a bandwidth of 0.05–1000 Hz at a sampling rate of 4000 Hz. The data were obtained at baseline and 5, 15, and 30 min of coronary occlusion with the incision being sutured before the recordings.

The ischemic area and the leads enclosed within this area were determined by two methods. The elevation of the ST segment on the recorded epicardial electrograms served as the evidence of acute ischemia. After the experiment the 1.5 ml of 0,5% Evans blue dye (Reanal, Hungary) was injected via the carotid artery catheter. The leads in the noncontrasted zone coincided with the leads, where the elevation of the ST segment was observed during coronary occlusion. The perfused regions were designated as a nonischemic zone (Supplementary 1).

The animals were divided into three groups. Two groups were given echinochrome in the doses of 1 mg/kg and 2 mg/kg (n = 5 and n = 7 respectively) being administered as a 0.2% solution in a 0.1% sodium bicarbonate solution 5 min before coronary occlusion. Five cats served as the controls and underwent LAD ligation, but did not receive antioxidant treatment. Instead, an equivalent volume of saline was infused to the control animals before coronary occlusion.

The analysis of the recorded epicardial electrograms included the measurement of activation–recovery intervals (ARIs), which were used for the evaluation of local repolarization duration. Each ARI was defined as the interval between the activation time and the end of the repolarization time, determined as dV/dt min during the QRS complex and dV/dt max during the ST-T complex respectively [11]. The dV/dt max moment was determined automatically, inspected by the observer, and corrected manually if necessary. The dispersion of repolarization was calculated as the difference between the longest ARI in the nonischemic area and the shortest ARI in the ischemic zone.

The QRS, QT and Tpeak–Tend intervals were measured in the limb lead II ECG and the QT interval was corrected to heart rate by the formula QTc = QT − 0,175*(RR-300) [12]. The T wave amplitudes were measured in the modified precordial leads. Two averaged values were calculated for the “basal” (J1–J3) and “apical” (J4–J6) leads, respectively, and the difference between these values (“apical” minus “basal”) was defined as the longitudinal T wave amplitude dispersion.

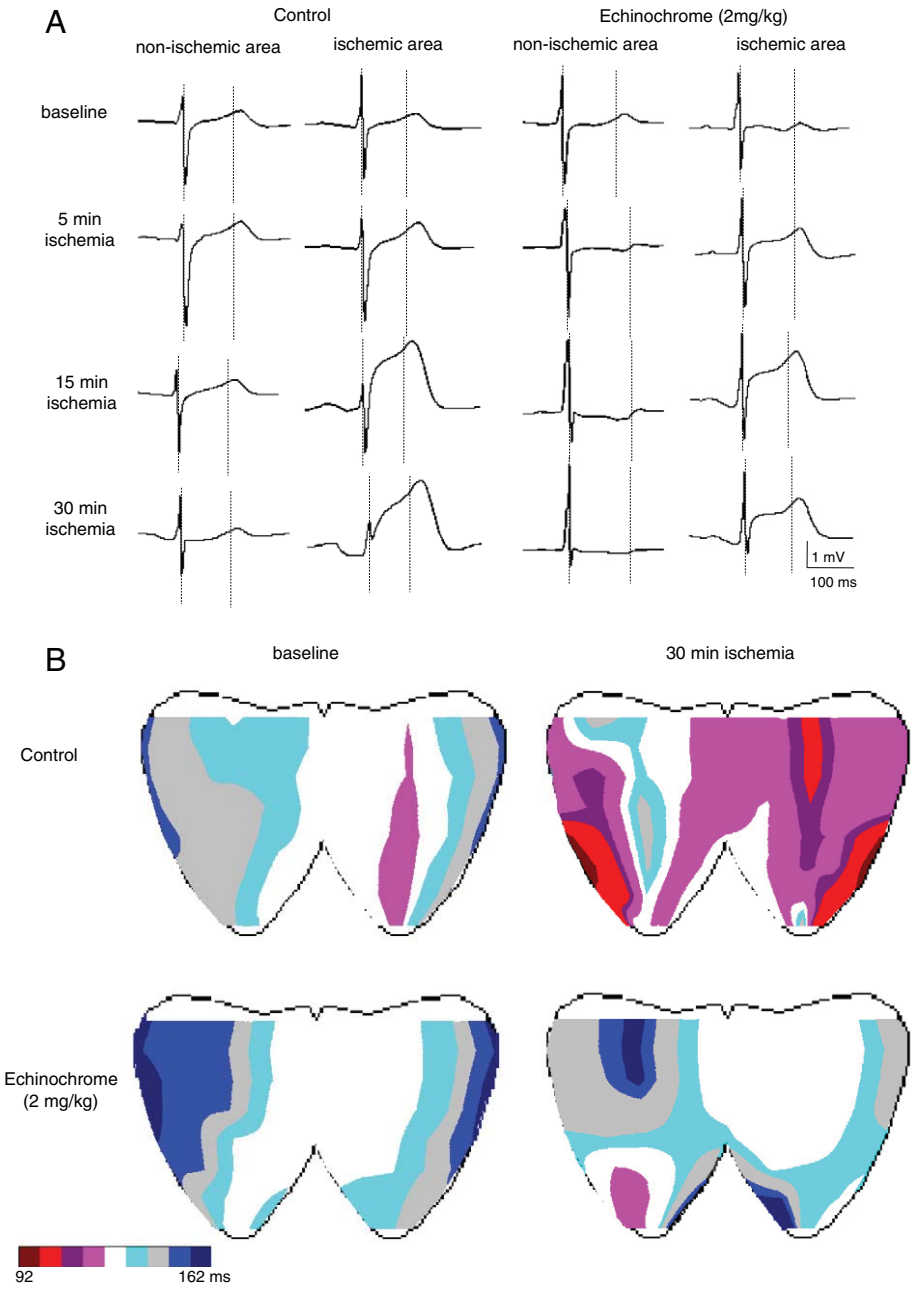

Fig. 2. A. Ventricular epicardial electrograms led from the ischemic (left ventricular apex) and nonischemic (left ventricular base) areas in control and echinochrome-treated (2 mg/kg) cats. Dashed lines designate the local activation and end of repolarization time instants. B. Representative isochronal maps of ventricular epicardial activation–recovery intervals at the baseline state and at 30 min of coronary occlusion in the control and 2 mg/kg echinochrome groups. The left and right sides of each map correspond to the anterior and posterior epicardial aspects, respectively. Arrows point at ischemic areas. See the less degree of ischemic shortening of activation–recovery intervals in echinochrome-treated animal.

The assessment of ventricular arrhythmias was performed before and during coronary occlusion. The score of arrhythmia was given for each 5 min period during coronary occlusion as follows: 0, no arrhythmias; 1, monomorphic ventricular extrasystoles <30/min; 3, single or coupled monomorphic ventricular extrasystoles >30/min; 3, polymorphic ventricular extrasystoles >30/min; 4, coupled polymorphic ventricular extrasystoles >30/min; 5, unstable ventricular tachycardia (<30 s); 6, stable ventricular tachycardia (>30 s); 7, ventricular fibrillation. For each interval, arrhythmias of the greatest grade were taken into account. The mean arrhythmia score was calculated for each group at baseline and at 5, 15 and 30 min of coronary occlusion.

The data are expressed as median (25% percentile; 75% percentile). Statistical examination was carried out by the Friedman test followed by the Newman–Keuls test for paired comparisons. Comparisons between groups were carried out by the Mann–Whitney test. The chi-squared test

Table 1
Ischemia-induced ARI shortening during coronary occlusion.

Periods	Control (n = 5)	Echinochrome 1 mg/kg (n = 5)	Echinochrome 2 mg/kg (n = 7)
Baseline (ARI, ms)	146 (130; 171)	104 (80; 114)	128 (106; 135)
Changes at:			
5 min ischemia	27 (24; 32)	18 (12; 31)	8 (3; 25)
15 min ischemia	43 (36; 61)	17 (15; 53)	11 (9; 24) #
30 min ischemia	42 (36; 59)	24 (17; 33)	13 (9; 31) #*

Intensity of ischemic injury is expressed as the shortening of ARIs from baseline. Data are presented as median (25% percentile; 75% percentile), ms.
# $p < 0.05$ versus control group.
* $p < 0.05$ versus 1 mg/kg dose.

assessed the difference in ventricular arrhythmias between the control and echinochrome groups. The differences at $p < 0.05$ were considered significant.

Results

Ventricular repolarization

There were no differences in the baseline distribution of ARIs between the groups, and the administration of echinochrome prior to coronary occlusion did not change ARIs and their distribution on the ventricular epicardium. Coronary occlusion resulted in the shortening of ARIs in the ischemic area ($p < 0.05$), whereas ARIs in the nonischemic area remained unaltered during ischemic exposure as expected (Fig. 2). The extent of ischemic ARI shortening was less in the animals treated with 2 mg/kg echinochrome at 15 min and 30 min of coronary occlusion in comparison with the control group ($p < 0.05$). Infusion of echinochrome in a dose of 2 mg/kg demonstrated the more pronounced effect to decrease the ischemia-induced ARIs shortening at 30 min ischemia as compared with the lower dose ($p < 0.05$, Table 1).

A significant increase of the ARI dispersion ($p < 0.05$) was observed in control and treated animals as a consequence of the local shortening of ARIs in the apical zone of the ventricles during ischemia. The extent of the increase of the ARI dispersion in the group given 2 mg/kg echinochrome was significantly less in comparison with the control and 1 mg/kg echinochrome groups (Table 2).

Table. 2
Ischemia-induced increase of the ARI dispersion during coronary occlusion.

Changes of ARI dispersion (ms) at periods	Control (n = 5)	Echinochrome 1 mg/kg (n = 5)	Echinochrome 2 mg/kg (n = 7)
5 min ischemia	21 (12; 29)	20 (4; 23)	12 (8; 13)#
15 min ischemia	21 (17; 33)	30 (14; 34)	13 (6; 17)#
30 min ischemia	17 (17; 27)	32 (30; 32)	13 (5; 18)#,*

Intensity of ischemic injury is expressed as the increase of the ARI dispersion from baseline. Data are presented as median (25% percentile; 75% percentile), ms.
# $p < 0.05$ versus control group.
* $p < 0.05$ versus 1 mg/kg dose.

ECG

ECG parameters were analyzed in the control animals (n = 5) and the animals treated with 2 mg/kg of echinochrome (n = 7). As the animals treated with 1 mg/kg of echinochrome did not differ from controls in the ischemia-induced changes of ARI duration and dispersion, these animals were omitted from the analysis for the sake of clarity.

The analysis of ECG parameters of cardiac repolarization in the standard bipolar limb leads revealed the significant prolongation of the QTc and Tpeak–Tend intervals during coronary occlusion in the control group but not in the groups treated with echinochrome. On the other hand, ischemia resulted in the significant prolongation of the QRS complex in the animals given echinochrome (Table 3). ECGs recorded from the precordial leads demonstrated changes of the T wave amplitude. At baseline, we observed the negative T wave in the "basal" leads J1–J3 and the positive T wave in the "apical" leads J4–J6, presenting the longitudinal dispersion of the T wave amplitude in both groups. During coronary occlusion, the amplitude of the T wave in the leads J4–J6 was increased (the T wave became more positive) in both groups of animals ($p < 0.05$), whereas the T wave in the leads J1–J3 increased (the T wave became more negative) only in the control group ($p < 0.05$). Thus, the longitudinal T wave amplitude dispersion was increased significantly at 15 and 30 min of coronary occlusion in the control animals, but not in the treated group (Table 3).

There was no difference in the incidence of ischemia-induced ventricular arrhythmias between the animal groups (Table 4).

Discussion

Ischemia is known to shorten myocardial action potential durations [10]. The present study demonstrated the correspondent shortening of ARIs, surrogates for the action potential durations. These alterations resulted in the increase of the dispersion of repolarization since the ARIs in the ischemic area shortened and those in the normal myocardium remained unaltered. Echinochrome led to the attenuation of the *extent* of the abovementioned changes. Accordingly, the untreated animals demonstrated the ischemia-related increase in the QTc and Tpeak–Tend intervals as well as the longitudinal T wave amplitude dispersion in the precordial leads. On the other hand, the animals given echinochrome had no changes of these ECG parameters suggested for the estimation of repolarization dispersion. In spite of the favorable repolarization changes, echinochrome led to the paradoxical QRS prolongation during ischemia. However, the observed electrophysiological effect of echinochrome did not lead to the change in arrhythmia susceptibility.

The most consistent physiological effect of echinochrome is reported to be an antioxidative activity [3] and, as such, it is implied that echinochrome compensated for some ROS-mediated action potential duration shortening in an ischemic context. It has been suggested that an increase in the sarcolemmal $I_{K(ATP)}$ current resulted from the collapse of the mitochondrial $\Delta\Psi m$ mediated by superoxide anions produced during ischemia and reperfusion flowing through the

Table 3
Temporal and amplitude ECG parameters during ischemia in the control and echinochrome (2 mg/kg) groups.

	Baseline	5 min ischemia	15 min ischemia	30 min ischemia
	Intervals, ms (standard limb lead II)			
Control (n = 5)				
RR	405 (348; 434)	388 (348; 435)	348 (309; 435)	348 (300; 445)
QRS	42 (38; 46)	40 (40; 50)	44 (39; 47)	46 (41; 48)
QTc	171 (165; 179)	173 (166; 180)	178 (173; 189)*	175 (172; 183)*
Tpeak–Tend	37 (34; 40)	38 (35; 40)	37 (36; 40)	39 (37; 40)*
Echinochrome (2 mg/kg, n = 7)				
RR	396 (372; 448)	381 (355; 454)	385 (362; 433)	368 (310; 441)
QRS	36 (35; 40)	42 (37; 44)	42 (39; 46)*	41 (38; 44)
QTc	178 (170; 185)	186 (174; 194)	183 (174; 195)	173 (170; 181)
Tpeak–Tend	39 (35; 44)	40 (38; 42)	40 (38; 41)	38 (36:40)
Mean T wave voltage, mV (modified precordial leads)				
Control (n = 5)				
J1–J3, “basal”	−0.11 (−0.13; −0.09)	−0.12 (−0.13; −0.10)	−0.14 (−0.15; −0.12)*	−0.15 (−0.15; −0.12)*
J4–J6, “apical”	0.11 (0.10; 0.17)	0.14 (0.11; 0.18)	0.17 (0.14; 0.21)*	0.17 (0.16; 0.21)*
Dispersion	0.20 (0.20; 0.28)	0.25 (0.20; 0.30)	0.31 (0.26; 0.35)*	0.33 (0.28; 0.35)*
Echinochrome (2 mg/kg, n = 7)				
J1–J3, “basal”	−0,12 (−0.13; −0.11)	−0,13 (−0.14; −0.12)	−0,14 (−0.14; −0.13)	−0,14 (−0.14; −0.12)
J4–J6, “apical”	0,11 (0.10; 0.12)	0,11 (0.10; 0.13)	0,14 (0.13; 0.15)	0,13 (0.11; 0.14)*
Dispersion	0,24 (0.22; 0.25)	0,25 (0.24; 0.27)	0,28 (0.27; 0.30)	0,27 (0.23; 0.28)

Data are presented as median (25% percentile; 75% percentile).
* $p < 0.05$ versus baseline state.

internal membrane anion channels [2]. Due to abundance of the K(ATP) channels in cardiomyocytes, the increase in this current could lead to the significant shortening of action potential duration [13], which could be documented by ARI abbreviation. Since echinochrome is characterized by antioxidative properties, it could diminish superoxide anion production and, consequently, attenuate ARI changes in ischemia as it was observed in the present study.

The myocardial dispersion of repolarization has long been recognized as one of arrhythmogenic electrophysiological prerequisites [14] and, therefore, a reliable noninvasive index reflecting the dispersion of repolarization is strongly desired. The present study demonstrated that the ischemia-induced increase of repolarization inhomogeneity was associated with the increase of the QTc and Tpeak–Tend intervals in the limb leads in untreated animals. It is noteworthy, that the attenuation of repolarization changes by echinochrome abolished the correspondent ECG alterations. The mechanism of these effects could be related to the prolongation of the final portion of the T wave due to the increase of the apicobasal gradient of repolarization, which in turn was caused by the significant repolarization shortening in the ischemic apical region of the left ventricle. The contribution of the transmural gradient in these phenomena was likely negligible. On one hand, experimental and simulation studies [8,15] demonstrated that its influence on the Tpeak–Tend duration was inferior to that of the apicobasal gradient. On the other hand, our previous study in the framework of the same experimental model of myocardial ischemia showed that the electrophysiological changes were uniform in subepicardial, intramural and subendocardial layers of the ischemic zone [16] and, consequently, no changes of the transmural gradient were expected. The QT interval was also reported to prolong in patients with acute ischemia caused by coronary occlusion during angioplasty [17] and, at least in part, this prolongation could be ascribed to the early dilation of the left ventricle [18].

Table 4
The mean arrhythmia scores during 30-min ischemia.

	Control (n = 5)	Ech 1 mg/kg (n = 5)	Ech 2 mg/kg (n = 7)
Baseline	0	0	0
Echinochrome	–	0	0.14
5 min ischemia	0.14	0	0.14
15 min ischemia	1	1	0.14
30 min ischemia	0.71	1	0.57

For calculation procedures see “Methods.” No differences in the arrhythmia incidence were found between the studied groups.

However, the clinical use of the QT and Tpeak–Tend intervals as predictors of fatal ventricular arrhythmias has been, in the least, conflicting [19–22]. One likely reason for the clinically unsatisfactory predictive values of these indices is the technical difficulty in the measurements of the T wave offset. From this viewpoint, the T wave voltage determinations could present a promising approach for the evaluation of the dispersion of repolarization. Here, we found that the longitudinal T wave amplitude dispersion changes were related to the changes of the epicardial dispersion of repolarization at ischemic exposure and the attenuation of the epicardial repolarization alterations by echinochrome abolished the changes of the T wave amplitude dispersion. Therefore, the measurements of the difference between the T wave voltages in the “basal” and “apical” precordial leads might present a useful tool for the evaluation of myocardial dispersion of repolarization. However, it is noteworthy that the recording of the body surface leads with

the open thorax modifies the resulting ECGs. This presents a limitation for the interpretation of the present findings.

It may have been expected that the echinochrome-induced reduction of the dispersion of repolarization associated with the correspondent ECG changes would lead to the lower incidence of reentrant arrhythmias. However, the clear electrophysiological and electrocardiographic effects of echinochrome did not result in an antiarrhythmic action, at least in the framework of the present experimental model. This negative result of the study could be due to the fact that the echinochrome related change of the dispersion of repolarization did not reach a definite (though unknown) threshold in face of unexpected and disadvantageous QRS prolongation associated with echinochrome. This observation is also consistent on one hand with the data of Coronel et al. [23] who pointed out that the dispersion of repolarization could not solely predict reentrant arrhythmias, and on the other hand, with the findings suggesting that the benefit of clinical use of antioxidant agents remains equivocal [24,25].

Conclusions

The study demonstrated the ability of the antioxidant echinochrome to decrease the ischemia-induced alterations of ventricular repolarization in a dose-dependent manner in a feline model of coronary occlusion. The dynamics of the repolarization dispersion changes could be assessed by the measurements of the longitudinal T wave amplitude dispersion, Tpeak–Tend and QTc intervals from the body surface ECGs. However, the attenuation by echinochrome of the ischemia-induced alterations of dispersion of repolarization did not result in the lowering of the incidence of ventricular arrhythmias during the ischemic episode.

Supplementary data to this article can be found online at http://dx.doi.org/10.1016/j.jelectrocard.2015.01.003.

Acknowledgments

This study was supported by the Ural Branch of the Russian Academy of Sciences (Projects Nos. 12-C-4-1009, 13-4-SP-359 and 13-4-032-KSC). Synthetic echinochrome was provided by the G. B. Elyakov Pacific Institute of Bioorganic Chemistry of the Far Eastern Branch of the Russian Academy of Sciences (Vladivostok, Russian Federation).

References

[1] Jeong EM, Liu M, Sturdy M, Gao G, Varghese ST, Sovari AA, et al. Metabolic stress, reactive oxygen species, and arrhythmia. J Mol Cell Cardiol 2012;52(2):454–63.
[2] Brown DA, Aon MA, Frasier CR, Sloan RC, Maloney AH, Anderson EJ, et al. Cardiac arrhythmias induced by glutathione oxidation can be inhibited by preventing mitochondrial depolarization. J Mol Cell Cardiol 2010;48(4):673–9.
[3] Lebedev AV, Ivanova MV, Levitsky DO. Echinochrome, a naturally occurring iron chelator and free radical scavenger in artificial and natural membrane systems. Life Sci 2005;76:863–75.
[4] Shvilkin AV, Serebriakov LI, Tskitishvili OV, Sadretdinov SM, Kol'tsova EA, Maksimov OB, et al. Effect of echinochrom on experimental myocardial reperfusion injury. Kardiologiia 1991;31(11):79–81.
[5] Xue J, Chen Y, Han X, Gao W. Electrocardiographic morphology changes with different type of repolarization dispersions. J Electrocardiol 2010;43(6):553–9.
[6] Vaykshnorayte MA, Azarov JE, Tsvetkova AS, Vityazev VA, Ovechkin AO, Shmakov DN. The contribution of ventricular apicobasal and transmural repolarization patterns to the development of the T wave body surface potentials in frogs (*Rana temporaria*) and pike (*Esox lucius*). Comp Biochem Physiol A Mol Integr Physiol 2011;159(1):39–45.
[7] Janse MJ, Coronel R, Opthof T, Sosunov EA, Anyukhovsky EP, Rosen MR. Repolarization gradients in the intact heart: Transmural or apico-basal? Prog Biophys Mol Biol 2012;109:6–15.
[8] Arteyeva NV, Goshka SL, Sedova KA, Bernikova OG, Azarov JE. What does the T(peak)-T(end) interval reflect? An experimental and model study. J Electrocardiol 2013;46(4):296.e1–8.
[9] Meijborg VM, Conrath CE, Opthof T, Belterman CN, de Bakker JM, Coronel R. Electrocardiographic T wave and its relation with ventricular repolarization along major anatomical axes. Circ Arrhythm Electrophysiol 2014;7(3):524–31.
[10] Carmeliet E. Cardiac ionic currents and acute ischemia: From channels to arrhythmias. Physiol Rev 1999;79:917–1017.
[11] Millar CK, Kralios FA, Lux RL. Correlation between refractory periods and activation-recovery intervals from electrograms: Effects of rate and adrenergic interventions. Circulation 1985;72:1372–9.
[12] Carlsson L, Abrahamsson C, Andersson B, Duker G, Schiller-Linhardt G. Proarrhythmic effects of the class III agent almokalant: Importance of infusion rate, QT dispersion, and early after depolarizations. Cardiovasc Res 1993;27:2186–93.
[13] Akar FG, O'Rourke B. Mitochondria are sources of metabolic sink and arrhythmias. Pharmacol Ther 2011;131(3):287–94.
[14] Han J, Moe GK. Nonuniform recovery of excitability in ventricular muscle. Circ Res 1964;14:44–60.
[15] Xia Y, Liang Y, Kongstad O, Holm M, Olsson B, Yuan S. Tpeak-Tend interval as an index of global dispersion of ventricular repolarization: Evaluations using monophasic action potential mapping of the epi- and endocardium in swine. J Interv Card Electrophysiol 2005;14:79–87.
[16] Bernikova OG, Sedova KA, Azarov YE, Shmakov DN. Ventricular myocardial repolarization in acute coronary occlusion and reperfusion in cats. Dokl Biol Sci 2011;437:69–71.
[17] Elming H, Brendorp B, Kober L, Sahebzadah N, Torp-Petersen C. QTc interval in the assessment of cardiac risk. Card Electrophysiol Rev 2002;6:289–94.
[18] Kenigsberg D, Khanal S, Kowalski M, Krishnan S. Prolongation of the QTc interval is seen uniformly during early transmural ischemia. J Am Coll Cardiol 2007;49:1299–305.
[19] Panikkath R, Reinier K, Uy-Evanado A, Teodorescu C, Hattenhauer J, Mariani R, et al. Prolonged Tpeak-to-Tend interval on the resting ECG is associated with increased risk of sudden cardiac death. Circ Arrhythm Electrophysiol 2011;4:441–71.
[20] Hetland M, Haugaa KH, Sarvari SI, Erikssen G, Kongsgaard E, Edvardsen T. A novel ECG-index for prediction of ventricular arrhythmias in patients after myocardial infarction. Ann Noninvasive Electrocardiol 2014;19:330–7.
[21] Smetana P, Schmidt A, Zabel M, Hnatkova K, Franz M, Huber K, et al. Assessment of repolarization heterogeneity for prediction of mortality in cardiovascular disease: Peak to the end of the T wave interval and nondipolar repolarization components. J Electrocardiol 2011;44:301–8.
[22] Porthan K, Viitasalo M, Toivonen L, Havulinna AS, Jula A, Tikkanen JT, et al. Predictive value of electrocardiographic T-wave morphology parameters and T-wave peak to T-wave end interval for sudden cardiac death in the general population. Circ Arrhythm Electrophysiol 2013;6(4):690–6.
[23] Coronel R, Wilms-Schopman FJ, Opthof T, Janse MJ. Dispersion of repolarization and arrhythmogenesis. Heart Rhythm 2009;6(4):537–43.
[24] Tamargo J, Caballero R, Gómez R, Delpón E. Cardiac electrophysiological effects of nitric oxide. Cardiovasc Res 2010;87(4):593–600.
[25] Rodrigo R, Prieto JC, Castillo R. Cardioprotection against ischaemia/reperfusion by vitamins C and E plus n-3 fatty acids: Molecular mechanisms and potential clinical applications. Clin Sci (Lond) 2013;124(1):1–15.

Assessment of repolarization heterogeneity for prediction of ventricular tachyarrhythmias

The objective of the next step of the study was to investigate the role of repolarization heterogeneity in arrhythmia occurrence under ischemia/reperfusion settings.

The following tasks were stated:

- to find out which parameters of the myocardial repolarization predict the VT/VF,
- to determine the ECG expression of these parameters.

Intramyocardial electrograms were recorded in 24 cats during 30-minute coronary occlusion and subsequent reperfusion to find out specific parameters of myocardial repolarization contributing as predictors of VT/VF at reperfusion and to determine the ECG expression of these specific parameters.

At reperfusion onset, 10 cats demonstrated ventricular tachyarrhythmias (4 VF and 6 VT episodes). This VT/VF group showed the longer of ARIs in nonischemic zone [183 (177;202) vs 154 (140;170) ms in susceptible and resistant animals, respectively, $p<0.05$]. This observation has been explained by the changes in the area adjacent to the ischemic zone which was identified as nonischemic by Evans blue staining but still demonstrated electrophysiological changes. This region is referred to as the "border" zone. As a result, the animals with reperfusion-induced VT/VF demonstrated the prolonged RTs in nonischemic area. It should be noted that heart rate was slower at baseline state and during ischemia/reperfusion exposure in fibrillating cats in comparison to nonfibrillating.

The differences between the VT/VF and no VT/VF groups were evaluated using following electrophysiological parameters at 1 min of reperfusion: RTs, ATs, global and transmural dispersion of repolarization, RR. The groups demonstrated differences in RR interval, RTs of nonischemic zone and RTs of ischemic zone. Transmural and global RT dispersion, AT delay did not differ between the groups at 1 minute of reperfusion. Only the nonischemic RTs were significant predictors of VT/VF in a multivariate logistic regression model. ROC curve analysis showed significant association between VT/VF occurrence and nonischemic RTs (AUC 0.854, $P = 0.004$). The nonischemic RTs greater than a cutoff value of 173 ms predict VT/VF with sensitivity 0.900, specificity 0.786, positive predictive value 0.750 and negative predictive value 0.909.

The next step of the analysis was to investigate how the long nonischemic RTs which are primarily essential for the arrhythmic events could be expressed in ECG. Simulations were carried out in the framework of a computer model of the feline heart ventricles. The critical point of the model was that the APD changes in the border zone were simulated in two ways: 1) as a progressive transition between normal and ischemic APD values and 2) with the APD prolongation in the border zone. These two patterns of APD changes corresponded to the data obtained in the arrhythmia-resistant and susceptible animals. The body surface potentials were then computed for these two settings. The prolongation of APD in the border zone resulted in prolonged, biphasic T wave with the negative terminal potential in the leads mostly proximal to the heart. In the case of the progressive APD shortening in the border zone of ischemia the T wave was monophasic.

In conclusion, reperfusion ventricular tachyarrhythmias were predicted by prolonged repolarization times in the border/nonischemic area, which was expressed in precordial terminal T wave inversion as demonstrated by computer simulations (for more details, see Bernikova et al, 2017).

Bernikova OG, Sedova KA, Arteyeva NV, Ovechkin AO, Kharin SN, Shmakov DN, Azarov JE. Repolarization in perfused myocardium predicts reperfusion ventricular tachyarrhythmias. J Electrocardiol. In press. JCR IF 2016 – 1.514

Journal of Electrocardiology xxx (2017) xxx–xxx

Contents lists available at ScienceDirect

Journal of Electrocardiology

journal homepage: www.jecgonline.com

Repolarization in perfused myocardium predicts reperfusion ventricular tachyarrhythmias

Olesya G. Bernikova, MD, PhD [a,b,*], Ksenia A. Sedova, PhD [a,d], Natalia V. Arteyeva, PhD [a], Aleksey O. Ovechkin, MD, PhD [a,b], Sergey N. Kharin, PhD [a,c], Dmitry N. Shmakov, PhD [a], Jan E. Azarov, PhD [a,c]

[a] Laboratory of Cardiac Physiology, Institute of Physiology, Komi Science Center, Ural Branch, Russian Academy of Sciences, Pervomayskaya st., 50, Syktyvkar, Russia
[b] Department of Therapy, Medical Institute of Pitirim Sorokin Syktyvkar State University, Oktyabrskiy pr., 55, Syktyvkar, Russia
[c] Department of Physiology, Medical Institute of Pitirim Sorokin Syktyvkar State University, Oktyabrskiy pr., 55, Syktyvkar, Russia
[d] Department of Biomedical Technology, Faculty of Biomedical Engineering, Czech Technical University in Prague, Nam. Sítná 3105, Kladno, Czech Republic

ARTICLE INFO

Available online xxxx
Keywords:
Arrhythmias
ECG
Ischemia-reperfusion
Repolarization
Simulation

ABSTRACT

Background: Aim of the study was to find out which myocardial repolarization parameters predict reperfusion ventricular tachycardia and fibrillation (VT/VF) and determine how these parameters express in ECG.
Methods: Coronary occlusion and reperfusion (30/30 min) was induced in 24 cats. Local activation and end of repolarization times (RT) were measured in 88 intramyocardial leads. Computer simulations of precordial electrograms were performed.
Results: Reperfusion VT/VF developed in 10 animals. Arrhythmia-susceptible animals had longer RTs in perfused areas [183(177;202) vs 154(140;170) ms in susceptible and resistant animals, respectively, $P < 0.05$]. In logistic regression analysis, VT/VFs were associated with prolonged RTs in the perfused area (OR 1.068; 95% CI 1.012–1.128; $P = 0.017$). Simulations demonstrated that prolonged repolarization in the perfused/border zone caused precordial terminal T-wave inversion.
Conclusions: The reperfusion VT/VFs were independently predicted by the longer RT in the perfused zone, which was reflected in the terminal negative phase of the electrocardiographic T-wave.

Introduction

Life-threatening arrhythmias arising in the setting of acute coronary syndrome during either ischemic or reperfusion phases potentially lead to the sudden cardiac death and constitute a major medical and public problem. A distinct subset of ventricular arrhythmias including ventricular fibrillation (VF) and ventricular tachycardia (VT) is related to reperfusion. The presence of reperfusion therapy related VT/VF has been shown to confer an independent mortality risk factor [1]. Development of prognostic criteria for fatal ventricular arrhythmias in the ischemia/reperfusion conditions remains a major research challenge.

VT/VF development requires a coexistence of a specific functional myocardial substrate and a triggering mechanism. Activation slowing which can be documented as QRS widening is recognized as a definite proarrhythmic factor which constitutes the arrhythmogenic substrate by a reentrant circuit. Alterations of repolarization contribute to both the substrate and triggering, e.g., shortening and lengthening of repolarization predispose to delayed and early afterdepolarization, respectively, serving as the trigger, and dispersion of repolarization/refractoriness defined as a time difference between the earliest and the latest end of repolarization times provides conditions for unidirectional conduction block [2]. However, the role of the repolarization alterations in arrhythmic susceptibility is not clear as compared to activation. Increasing the dispersion of repolarization does not necessarily result in the development of ventricular arrhythmias [3]. This notion is also supported by the fact that different indices suggested for the estimation of the dispersion of repolarization such as QT dispersion [4] or Tpeak-Tend interval [5,6] often give unsatisfactory or conflicting results when utilized clinically. Changes of myocardial repolarization in ischemic conditions are complex. Action potential duration (APD) undergoes a sequential evolution from initial transient prolongation [7] to further prominent shortening [8]. In vitro studies have demonstrated that repolarization parameters in subepicardial layers were more sensitive to the ischemic insult leading to increase of transmural dispersion of repolarization [9,10], whereas no transmural differences in the ischemia effects on repolarization were observed in vivo [11,12].

The aim of the study was to find out specific parameters of myocardial repolarization contributing as predictors of VT/VF at reperfusion and to determine the ECG expression of these specific parameters.

* Corresponding author at: Laboratory of Cardiac Physiology, Institute of Physiology, Komi Science Center, Ural Branch, Russian Academy of Sciences, Pervomayskaya st., 50, Syktyvkar 167982, Russia.
E-mail address: bernikovaog@gmail.com (O.G. Bernikova).

https://doi.org/10.1016/j.jelectrocard.2017.12.003
0022-0736/

Methods

Experimental setup

The experiments were performed in 24 healthy adult mongrel cats weighing from 2,5 to 4,5 kg. The investigation was carried out in accordance with the *Guide for the Care and Use of Laboratory Animals, 8th Edition* published by the National Academies Press (US) 2011 and was approved by the institutional ethical committee. Animals were anesthetized with zoletil (ZOLETIL® 100, Virbac S.A., Carros, France, 15 mg/kg, i.m.) and xylazine (XYLA, Interchemie, Castenray, Netherlands, 1 mg/kg, i.m.). The animals were intubated and ventilated artificially. The thorax was opened by a midsternal incision. To prevent cooling, the surface of the heart was moistened intermittently with warm saline. A catheter (internal diameter 0.6 mm) was introduced into aorta via the left carotid artery and attached to a pressure transducer SP844 (50 V V–1·(cm Hg)–1; MEMSCAP, France). The arterial blood pressure was monitored and measured with the Prucka Mac-Lab 2000 system (GE Medical Systems, Germany) in the course of experiments.

Twelve flexible custom-made plunge multipolar electrodes were inserted perpendicularly by means of a suture needle into the anterior and lateral left ventricular (LV) wall at the basal, middle and apical levels and into the base and the apex of the right ventricular (RV) wall. Each of the LV and RV electrodes bore equidistantly separated eight or four unipolar leads, respectively. Electrodes were fabricated with isolated 70-μm copper wires, fixed with a knot on a 0.8-mm vicryl thread. After the electrode placement, the heart was allowed to stabilize for 30 min. Then the transient ligation with a polycaproamide ligature (No 3-0) was done at the border of the lower and middle third of the left anterior descending coronary artery (LAD). 30 min coronary occlusion was followed by 30 min of reperfusion produced by the loosening of the ligature. The data were sampled at baseline, at 1 and 30 min after LAD ligation, and at 1 min of reperfusion.

Electrophysiology recordings

88 unipolar electrograms were simultaneously recorded from subepicardial, midmyocardial, and subendocardial layers in spontaneously beating hearts by means of a custom-designed system (16 bits; bandwidth 0.05 to 1000 Hz; sampling rate 4000 Hz). In each lead, an activation time (AT), end of repolarization time (RT), and activation-recovery interval (ARI) were determined as a minimum of the first time derivative of potential during QRS complex, a maximum time derivative during T-wave, and the time difference between the former and the latter, respectively [13]. A transmural RT dispersion was quantified as a difference between the maximal and minimal RT values from epicardial (Epi), intramural (Inm) and endocardial (Endo) in each lead. A global RT dispersion was calculated as a difference between the maximal and minimal RT values from all leads. The corrected ARIc was calculated by the equation ARIc = ARI-0.175 × (RR-300) [14].

At the end of each experiment, Evans blue dye (Sigma-Aldrich GmbH, Germany) was injected into the aorta after LAD reocclusion in

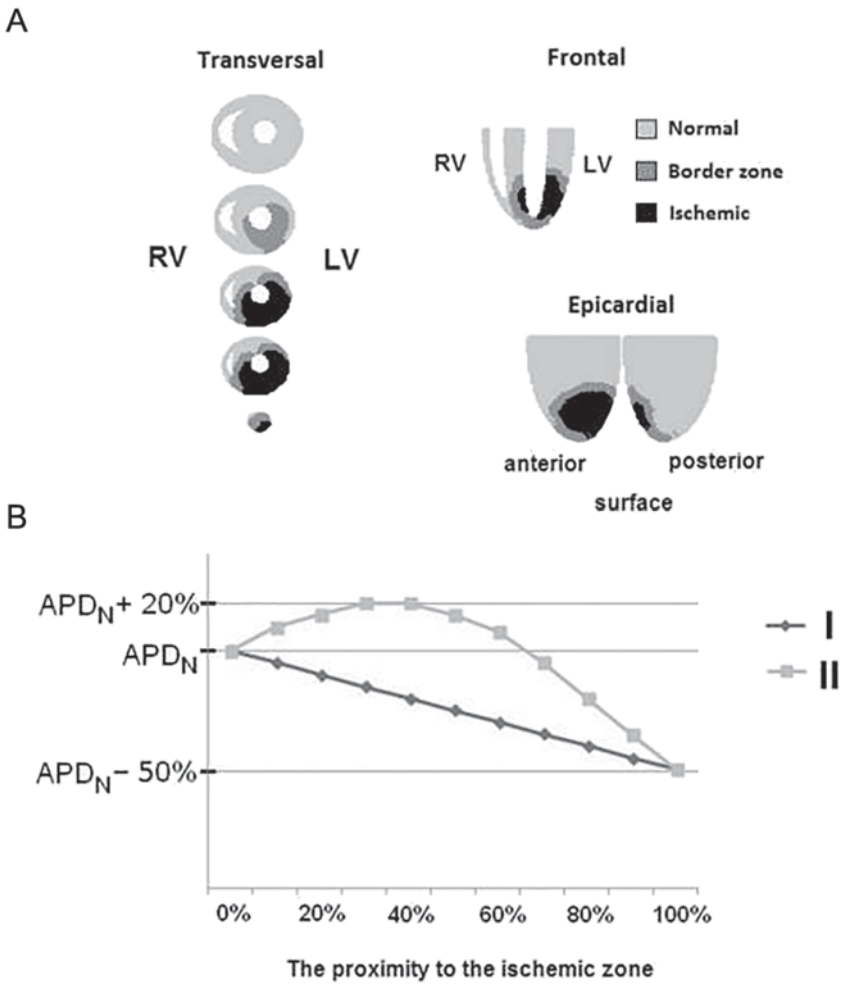

Fig. 1. A-The ischemic and border zones corresponded to the LAD occlusion. B-The different (I, II) simulated APD changes in the border zone depending on the proximity to the ischemic zone (0% – the region of normal perfusion, 100% – the region of ischemia). APDN – the APD value in the model cell, corresponding to the normal APD distribution in the model. I – the shortening of APD in the border zone, II – the prolongation of APD in the border zone.

Please cite this article as: Bernikova OG, et al, Repolarization in perfused myocardium predicts reperfusion ventricular tachyarrhythmias, Journal of Electrocardiology (2017), https://doi.org/10.1016/j.jelectrocard.2017.12.003

the same place for the determination of perfused (blue-colored) and nonperfused, or ischemic, (non-dyed) areas of ventricular myocardium. The extent of ischemic damage was assessed as a percentage ratio of the area of the noncontrasted zone to the area of the anterior surface of the heart determined on the calibrated paper and expressed in squared millimeters. The border zone was identified as a perfused (stained by Evans

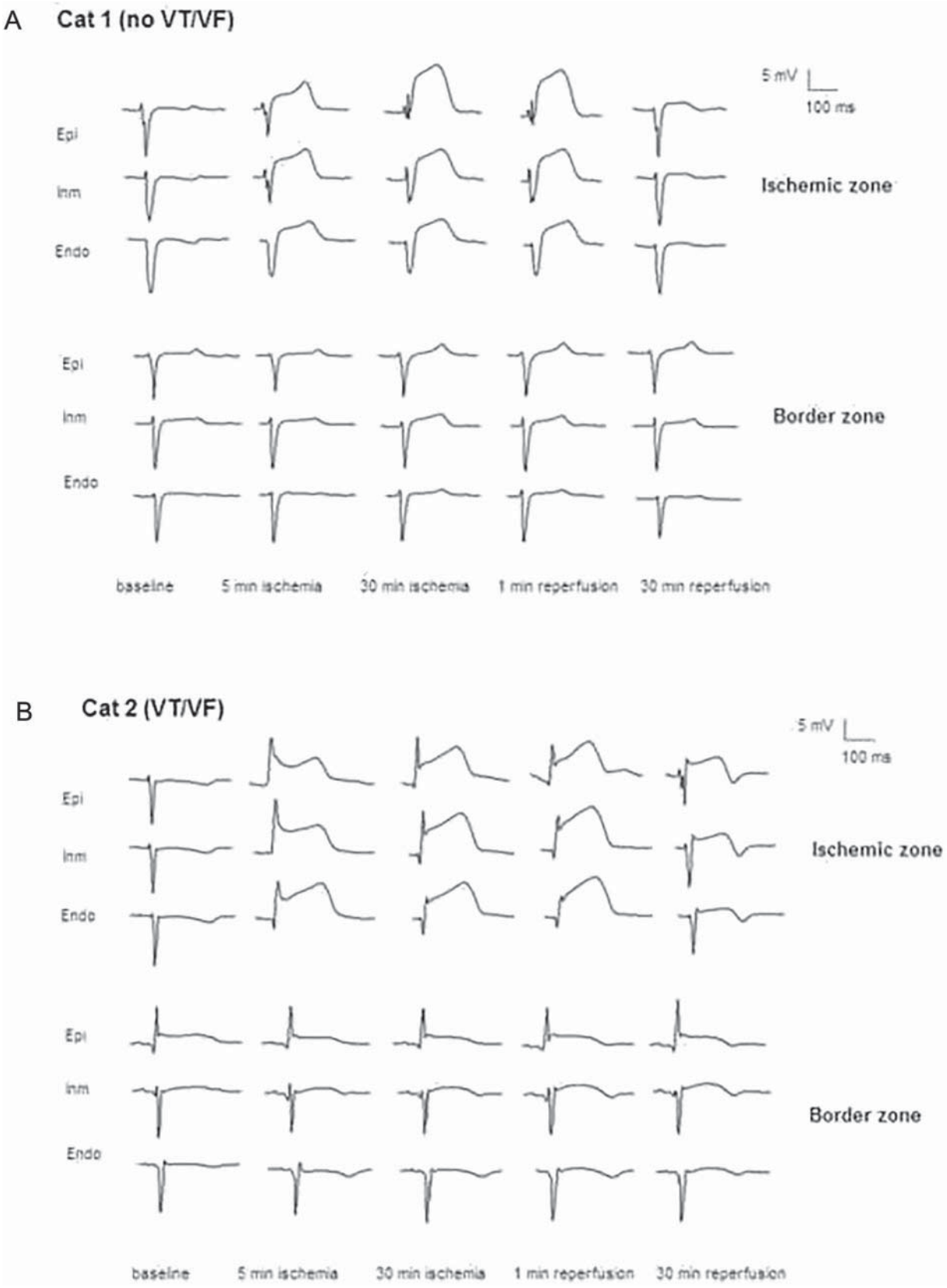

Fig. 2. The electrograms registered in the course of the LAD occlusion and reperfusion of no VT/VF group (A) and VT/VF group (B). The electrograms were recorded from the subepicardial (epi), intramural (inm) and subendocardial (endo) ventricular layers in the ischemic and border zones.

Please cite this article as: Bernikova OG, et al, Repolarization in perfused myocardium predicts reperfusion ventricular tachyarrhythmias, Journal of Electrocardiology (2017), https://doi.org/10.1016/j.jelectrocard.2017.12.003

Table 1
Electrophysiological parameters at baseline and ischemia-reperfusion settings (medians and interquartile ranges, n = 24).

	ATi	RTi	RTp	RR	Global DOR	Transmural DOR
Baseline	17(15;19)	154(135;178)	154(138;170)	382(353;426)	35(27;53)	5(4;10)
Ischemia 1 min	20(18;24)*	122(112;136)*	150(136;175)	383(359;434)	56(46;67)*	6(3;10)
Ischemia 30 min	21(18;26)*	116(101;132)*	157(138;180)	373(335;403)	65(55;75)*	5(3;10)
Reperfusion 1 min	20(17;26)*	125(98;139)*	159(137;169)	367(328;407)	61(53;76)*	5(4;8)
Reperfusion 30 min	18(16;22)	141(116;164)	151(137;165)	373(336;389)	52(40;61)	6(5;9)

ATi (activation time), RTi (repolarization time) of the ischemic zone; RTp (repolarization time) of the perfused zone; DOR-dispersion of repolarization.
* $P < 0.05$ vs baseline.

blue) area adjacent to the ischemic zone, but still demonstrating electrophysiological changes. The remote perfused myocardium with no changes in ventricular electrograms was referred to as a nonischemic zone. The animals were categorized into groups according to presence or absence of the sustained VT/VF within the early reperfusion period that would have required defibrillation shock due to dramatic hemodynamic impairment.

Statistical analysis

Data are expressed as medians and interquartile intervals. Statistical analysis was performed with SPSS package (IBM SPSS Statistics 23). The Mann-Whitney test was used to compare groups of animals presenting with VT/VF (VT/VF-susceptible animals, VT/VF group) and those free of VT/VF (VT/VF-resistant animals, no VT/VF group). Wilcoxon and Friedman tests were applied for paired and multiple comparisons, respectively, within the same groups. The association of myocardial repolarization parameters with VT/VF occurrence was assessed by univariate and multivariate logistic regression analysis (backward elimination method) and receiver operating characteristics (ROC) curve analysis. The differences were considered significant at $P < 0.05$.

Computer simulations

Simulations were carried out in the framework of a discrete computer model of the heart ventricles, a so-called cellular automaton, adapted to the feline heart ventricular and torso geometry. The model was developed on the basis of our previous simulations of the rabbit heart described earlier [15] using the experimentally measured anatomical and electrophysiological parameters of the feline heart. The inputs of the model were locations of activation foci, activation velocity, amplitude and duration of action potentials (AP). The initial foci of activation in the model were set in the interventricular septum, on the border of its middle and apical thirds, and in the subendocardium of the LV apex. In the subendocardial layers of the model, the activation velocity was thrice higher than in the rest of the model, imitating conducting system. The AP configuration was simulated on the basis of the study [9] and the normal APD distribution on the basis of experimental intramural ARI measurements. The outputs of the model were the AT sequence, RT sequence and body surface potentials. The simulated RTs were calculated as a sum of the correspondent ATs and APDs. The body surface potentials were calculated from the ventricular action potential gradients [15]. The location of the precordial leads in the model was analogous to those in humans.

The size and location of the ischemic and border zones in the model (Fig. 1A) corresponded to the experimentally determined ischemic zone under the LAD occlusion. The ischemic zone was simulated by the activation velocity decrease by 50%, APD shortening by 50% and the inhomogeneous decrease of the AP amplitudes, from 50% in the epicardial to 20% in the endocardial layers of the model. The changes of the model parameters mimicking ischemia corresponded to the experimental feline data [9,12]. In the border zone the APDs were changed in two ways according to the experimental data [12]. The first scenario was the progressive transition between the normal and ischemic APD values and the other one included the APD prolongation in the border zone (Fig. 1B). For both ischemic scenarios, AP amplitudes in the border zone were gradually changed from the ischemic to the normal values.

Results

Myocardial repolarization in ischemia/reperfusion settings

Fig. 2 displays alterations of myocardial electrograms during ischemia and reperfusion. Typical elevation of ST-segment was observed in electrograms recorded from Epi, Inm and Endo layers of the ischemic zone, whereas electrograms led from the perfused border zone demonstrated T-wave changes and only moderate ST-segment displacement. The changes of the studied myocardial electrophysiological parameters are listed in Table 1. As expected, RTs progressively decreased and ATs increased during occlusion in the ischemic zone and then progressively restored during reperfusion. In the perfused zone, RTs remained relatively stable, which led to a significant increase of global RT dispersion, with its magnitude being close to a difference between the RTs in the ischemic and perfused zones. As Epi, Inm and Endo RTs in ischemic zone changed uniformly; transmural RT dispersion did not change in the

Table 2
Electrophysiological parameters of the VT/VF group (n = 10) and no VT/VF group (n = 14) at baseline and ischemia-reperfusion settings (medians and interquartile ranges).

VT/VF/ no VT/VF	ATi	RTi	RTp	RR	Global DOR	Transmural DOR
Baseline	17(16;19)	186(175;198)	181 (178;183)	426(402;431)‡	34(27;92)	6(4;9)
	17(14;19)	156(139;175)	155(148;176)	364(329;383)	37(28;49)	5(3;10)
Ischemia 1 min	22(18;26)	150(132;158)*,‡	177(172;198)	430(410;487)‡	61(52;82)	6(2;9)
	20(17;22)	134(116;144)*	161(148;178)	369(341;385)	52(44;62)*	7(3;11)
Ischemia 30 min	27(19;32)*	134(122;150)*	185(170;203)‡	397(378;423)‡	72(66;86)*,‡	5(4;9)
	21(19;23)*	122(104;140)*	159(138;185)	345(313;374)	57(52;72)*	5(2;9)
Reperfusion 1 min	19(17;27)	145(136;169)*,‡	189(177;202)‡	400(388;472)‡	69(58;85)	6(4;8)
	20(17;23)*	127(103;135)*	154(140;170)	332(313;369)	61(52;72)*	5(4;9)
Reperfusion 30 min	17(16;19)	180(160;190)‡	183(160;190)	364(283;409)‡	47(38;74)	6(5;13)
	18(17;23)	137(127;168)	157(144;170)	358(328;386)	53(41;58)*	6(4;8)

ATi (activation time), RTi (repolarization time) of the ischemic zone; RTp (repolarization time) of the perfused zone; DOR-dispersion of repolarization.
* $P < 0.05$ vs baseline.
‡ $P < 0.05$ vs no VT/VF group.

Please cite this article as: Bernikova OG, et al, Repolarization in perfused myocardium predicts reperfusion ventricular tachyarrhythmias, Journal of Electrocardiology (2017), https://doi.org/10.1016/j.jelectrocard.2017.12.003

course of occlusion and reperfusion. Heart rate (RR interval) also remained unchanged.

VT/VF incidence during reperfusion

In 1–5 min after reperfusion onset, 10 cats demonstrated ventricular tachyarrhythmias (4 VF and 6 sustained VT episodes). At baseline state and during ischemia/reperfusion, heart rate was slower (RR interval longer) in the VT/VF-susceptible as compared to VT/VF-resistant animals (Table 2). Both groups demonstrated similar decrease in RTs recorded in the ischemic area, but RTs in the perfused areas differed between the two groups (Table 2). These differences are at least in part explained by opposite changes in the border zone [16] adjacent to the ischemic zone which was identified as perfused region by Evans blue staining, but still demonstrated electrophysiological changes. In this border zone, the VT/VF-resistant cats demonstrated a decrease in rate-corrected ARIs presenting a progressive transition from the ischemic to normal myocardium [129(115;142) ms and 123(113;138) ms at baseline and at 1 min of reperfusion, respectively, P = 0.046]. In contrast, in VT/VF-susceptible animals, the rate-corrected ARIs increased in the border area [136(118;144) ms and 145(137;152) ms at baseline and at 1 min of reperfusion, respectively, P = 0.011]. This effect is consistent with our previous observation [12]. The increase in repolarization duration (ARIs) expressed in development of a terminal T-wave inversion seen in the electrograms led from the border zone in the arrhythmia-susceptible animals (Fig. 2).

Myocardial repolarization predictors of VT/VF

We evaluated the differences between the VT/VF and no VT/VF groups in following electrophysiological parameters at 1 min of reperfusion (a timepoint preceding all VT/VF episodes): RTs, ATs, global and transmural dispersion of repolarization, RR. The groups differed between each other in RR interval, RTs of the perfused zone and RTs of the ischemic zone, whereas the transmural and global RT dispersion, AT delay did not differ between the groups at 1 min of reperfusion (Table 2). There were no statistically significant differences between groups in the size (area) of the ischemic zone. The area of the ischemic zone was 20(15;22)% and 18(14;21)% of the area of the anterior heart surface in VT/VF-susceptible and VT/VF-resistant cats, respectively (P = 0.462).

In a univariate logistic regression analysis RTs in the perfused areas and RR intervals demonstrated significant association with the occurrence of VT/VF during reperfusion. Only RTs in the perfused areas remained significant predictors of VT/VF in a multivariate logistic regression model (Table 3). ROC curve analysis (Fig. 3) showed significant association between VT/VF occurrence and RTs in the perfused areas (AUC 0.854, P = 0.004). The RTs in the perfused areas greater than a cut-off value of 173 ms predict VT/VF with sensitivity 0.900, specificity 0.786, positive predictive value 0.750 and negative predictive value 0.909.

ECG imaging of prolonged repolarization in the perfused zone (computer simulation)

Computer simulation was performed in order to find out ECG markers of the long RTs in the perfused areas which were demonstrated to be a repolarization predictor of reperfusion VT/VF. Normal activation sequence was from apex to base and from *endo-* to epicardium and the latest areas to be activated were subepicardium of the LV base and the right subendocardium of the septal base. In ischemia, activation slowed by 50% in the nonperfused zone, which resulted in a prolongation of the total activation time (by 23%, or 46 ms vs 38 ms), and a shift of the area of the latest activation to the LV lateral subepicardium (Fig. 4A).

According to APD distribution and activation sequence (Fig. 4A), the model had a repolarization sequence from apex to base, from LV to RV and from anterior wall to posterior wall under normal conditions (Fig. 4A). Ischemia altered repolarization in the apical portion of the ventricles. In case of APD shortening in the border zone of ischemia (Fig. 4A, panels Ischemic I), the general pattern of repolarization was not changed; because the ischemic zone with short APDs and early RTs coincided with the zone of the early RTs under the normal conditions. In case of APD prolongation in the border zone of ischemia (Fig. 4A, panels Ischemic II), the area of the latest RTs moved from the base to the apical portion of the ventricles.

The delayed activation in the ischemic zone expressed in a widening and little loss of the QRS voltage (Fig. 4B). The elevation of the ST-segment was observed in all the simulated precordial leads, especially in the leads most proximal to the heart (V2–V4). In case of APD shortening in the border zone of ischemia, T-wave was monophasic (Fig. 4B, panel Ischemic I), whereas lengthening the border APDs resulted in the T-wave prolongation and development of a terminal phase of negative potential in the leads proximal to the heart (V2–V3) (Fig. 4B, panel Ischemic II).

Table 3
Reperfusion VT/VF association with parameters of repolarization observed at 1 min of reperfusion.

Variables	Univariate regression model			Multivariate regression model		
	OR	95% CI	P	OR	95% CI	P
DOR	1.032	0.981–1.085	0.221			
RTi	1.032	0.999–1.065	0.057			
RTp	**1.068**	**1.012–1.128**	**0.017**	**1.068**	**1.012–1.128**	**0.017**
RR	**8.868 E + 10**	**51.971–1.513 E + 20**	**0.020**	17,387,249	0.001–4.391 E + 17	0.173

RTi, RTp – repolarization time of ischemic and perfused zones, respectively; DOR– dispersion of repolarization.
The bold data had a statistical significance (P<0.05).

Discussion

The prevention of life-threatening arrhythmias during the ischemic attack requires the establishment of reliable signs which herald the impending VT/VF. These ECG markers could relate to the processes of

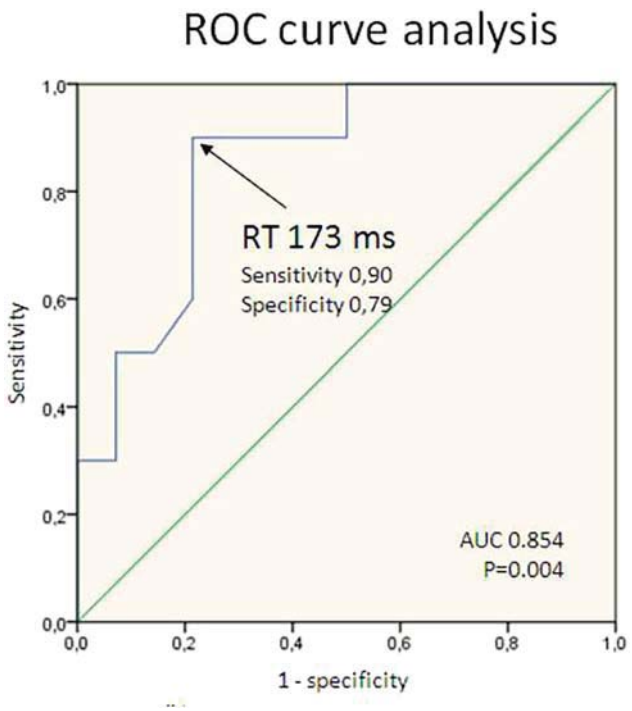

Fig. 3. Receiver operating characteristic curve analysis.

Please cite this article as: Bernikova OG, et al, Repolarization in perfused myocardium predicts reperfusion ventricular tachyarrhythmias, Journal of Electrocardiology (2017), https://doi.org/10.1016/j.jelectrocard.2017.12.003

ventricular depolarization and repolarization. The QRS prolongation and J-wave pattern have been reported to be predictors of VF in acute ischemia [17]. In the present study, we attempted to find out which change of ventricular repolarization was responsible for the proarrhythmic properties.

When different parameters of ventricular repolarization were tested, only long RTs in the perfused areas independently influenced the arrhythmic susceptibility. The prolonged RTs in the perfused zone resulted from the lengthening of repolarization in the border zone. The published data concerning electrophysiological parameters of the border zone are not consistent. Specifically, the border zone has been reported to have a shortened [18] or prolonged refractory period [16]. The latter refractory period prolongation in the border area could provide a substrate for initiation of malignant ventricular tachyarrhythmias [19]. Due to a limited number of intramural electrodes we could not analyze repolarization in the border zone separately from the "true" nonischemic zone, but were necessitated to pool all the electrophysiological data obtained from the perfused regions together. However, our analysis combined with simulations yielded a result that the electrophysiological properties of the perfused/border area can affect arrhythmogenesis in the conditions of acute coronary syndrome. A paradoxical consequence of these findings is that a treatment preventing malignant arrhythmias during anischemic attack should be targeted not to the damaged regions (a therapeutic agent can be hardly delivered to the nonperfused regions), but to the perfused areas which could be much more easily treated during an ischemic episode.

Mechanisms of development of early reperfusion arrhythmias could be associated with appearance of reentry waves due to the heterogeneity of the recovery of excitability in the myocardium [20] and development of trigger activity during reperfusion [21,22]. The increased border zone RTs could influence arrhythmogenesis in two ways. First, since APD dramatically shortened in a"true" ischemic zone, the greater the RT in perfused areas, the greater the RT dispersion. Dispersion of repolarization has long been recognized as a

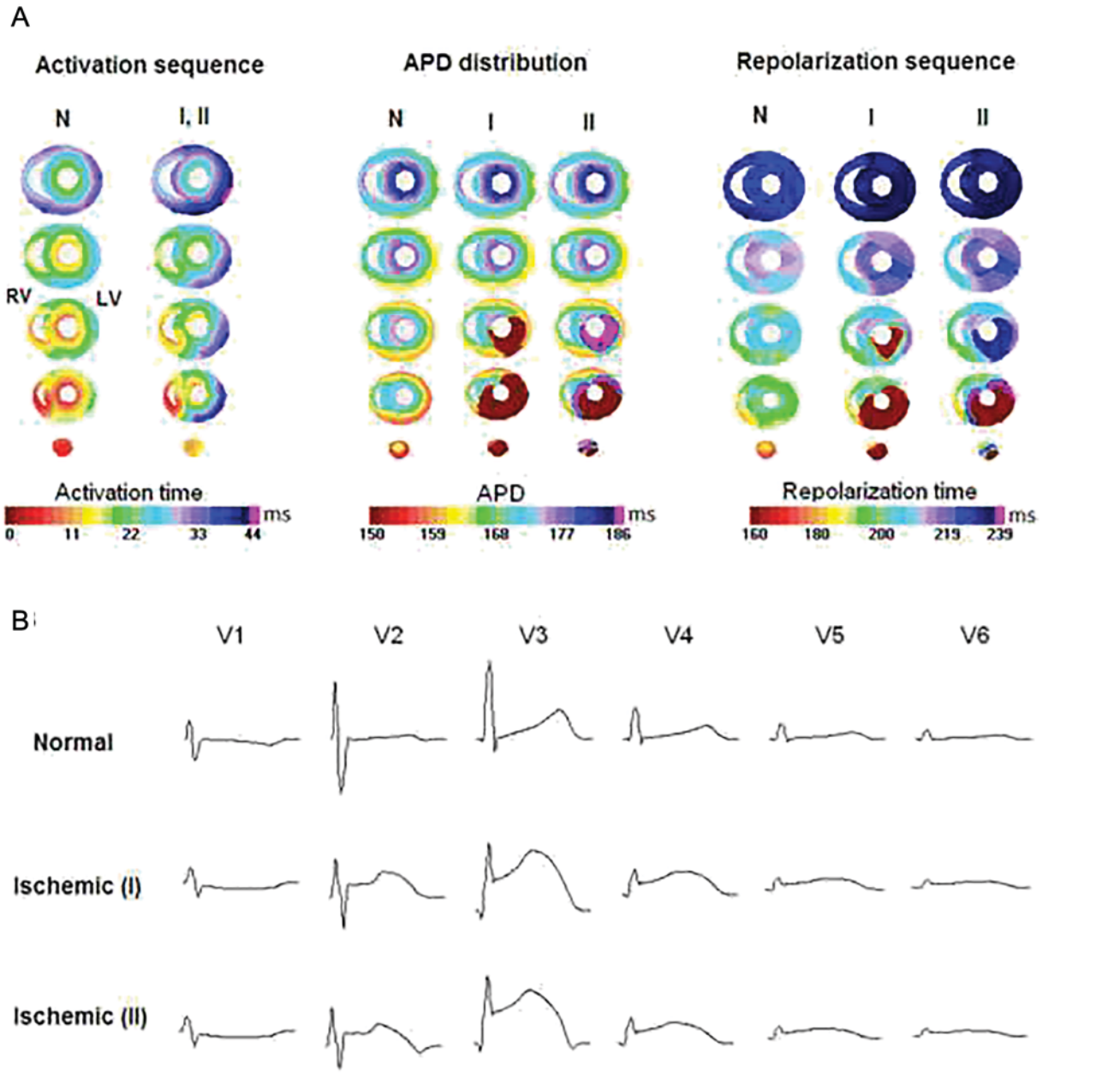

Fig. 4. A–The transversal views of the simulated normal and ischemic activation sequence, APD distribution and RT sequence. The time is given from the onset of activation. The scale depicts time from activation onset. B–The normal and ischemic simulated precordial leads. I – the shortening of APD in the border zone, II – the prolongation of APD in the border zone.

Please cite this article as: Bernikova OG, et al, Repolarization in perfused myocardium predicts reperfusion ventricular tachyarrhythmias, Journal of Electrocardiology (2017), https://doi.org/10.1016/j.jelectrocard.2017.12.003

proarrhythmic factor [3], which underlies the unidirectional conduction block and reentrant substrate. However, RT dispersion did not predict arrhythmias. Another explanation for the role of prolonged border zone RTs in arrhythmic susceptibility could be an increased propensity to early afterdepolarizations triggering activity [21].

The simulations suggested that the APD prolongation in the border zone produced the negative terminal phase of the T-wave in the precordial leads (Fig. 4B). The APD increase in the border zone shifted the area of the latest RTs from the basal part toward the apex. This resulted in the inversion of the general T-vector in the terminal period of repolarization. However, its magnitude during this period was small, and as a consequence, these changes were detectable only in the torso leads closest to the heart. Thus, this alteration in the T-wave morphology could be readily discerned. Experimentally we could not test this suggestion directly as the thorax was opened and precordial ECG recordings were impossible. However, the similar T-wave morphology was seen in animals with VT/VF in the anterior wall myocardial leads (Fig. 2) and was expected to be expressed in precordial leads. These findings suggest that the terminal T-wave inversion indicative of border APD prolongation could serve as a predictor of the fatal ventricular tachyarrhythmias.

Many attempts were undertaken to assess myocardial repolarization (repolarization dispersions) from ECG parameters and to use these parameters as predictors of ventricular arrhythmias. Among these, QT dispersion has been compromised [4], and the clinical utility of the Tpeak-Tend interval remains ambiguous [5,6,23,24]. To some extent, this uncertainty could be due to technical issues concerning the T-wave end determination. Prognostic criteria based on morphological or amplitude ECG indices would be more promising. The presence of terminal T-wave inversion could be useful for the VT/VF prognosis in ischemic attack as it could be clearly seen in ECG tracings. However, experimental conditions impose inevitable limitations on interpretation of the findings and whether this ECG marker could really serve as a VF predictor in clinical settings is subject to further testing.

Conclusions

The longer RTs in the perfused zone at the beginning of reperfusion were found to be an independent predictor of fatal ventricular arrhythmias during the reperfusion period. The simulations showed that the lengthening of action potential durations in the border zone was manifested in the precordial ECG leads by the terminal T-wave inversion which could be further evaluated as a VT/VF predictor in clinical settings.

Acknowledgements

This work was supported by the Ural Branch of the Russian Academy of Sciences (Project 15-3-4-16).

References

[1] Mehta RH, Starr AZ, Lopes RD, Hochman JS, Widimsky P, Pieper KS, et al. APEX AMI Investigators: incidence of and outcomes associated with ventricular tachycardia or fibrillation in patients undergoing primary percutaneous coronary intervention. JAMA 2009;301:1779–89.
[2] Burton FL, Cobbe SM. Dispersion of ventricular repolarization and refractory period. Cardiovasc Res 2001;50:10–23.
[3] Coronel R, Wilms-Schopman FJ, Opthof T, Janse MJ. Dispersion of repolarization and arrhythmogenesis. Heart Rhythm 2009;6:537–43.
[4] Zabel M, Klingenheben T, Franz MR, Hohnloser SH. Assessment of QT dispersion for prediction of mortality or arrhythmic events after myocardial infarction: results of a prospective, long-term follow-up study. Circulation 1998;97:2543–50.
[5] Smetana P, Schmidt A, Zabel M, Hnatkova K, Franz M, Huber K, et al. Assessment of repolarization heterogeneity for prediction of mortality in cardiovascular disease: peak to the end of the T wave interval and nondipolar repolarization components. J Electrocardiol 2011;44:301–8.
[6] Porthan K, Viitasalo M, Toivonen L, Havulinna AS, Jula A, Tikkanen JT, et al. Predictive value of electrocardiographic T-wave morphology parameters and T-wave peak to T-wave end interval for sudden cardiac death in the general population. Circ Arrhythm Electrophysiol 2013;6:690–6.
[7] Verkerk AO, Veldkamp MW, van Ginneken AC, Bouman LN. Biphasic response of action potential duration to metabolic inhibition in rabbit and human ventricular myocytes: role of transient outward current and ATP-regulated potassium current. J Mol Cell Cardiol 1996;28:2443–56.
[8] Carmeliet E. Cardiac ionic currents and acute ischemia: from channels to arrhythmias. Physiol Rev 1999;79:917–1017.
[9] Kimura S, Bassett AL, Kohya T, Kozlovskis PL, Myerburg RJ. Simultaneous recording of action potentials from endocardium and epicardium during ischemia in the isolated cat ventricle: relation of temporal electrophysiologic heterogeneities to arrhythmias. Circulation 1986;74:401–9.
[10] Lukas A, Antzelevitch C. Differences in the electrophysiological response of canine ventricular epicardium and endocardium to ischemia. Circulation 1993;88:2903–15.
[11] Taggart P, Sutton PM, Opthof T, Coronel R, Trimlett R, Pugsley W, et al. Transmural repolarisation in the left ventricle in humans during normoxia and ischemia. Cardiovasc Res 2001;50:454–62.
[12] Bernikova OG, Sedova KA, Azarov YE, Shmakov DN. Ventricular myocardial repolarization in acute coronary occlusion and reperfusion in cats. Dokl Biol Sci 2011;437:69–71.
[13] Coronel R, de Bakker JM, Wilms-Schopman FJ, Opthof T, Linnenbank AC, Belterman CN, et al. Monophasic action potentials and activation recovery intervals as measures of ventricular action potential duration: experimental evidence to resolve some controversies. Heart Rhythm 2006;3(9):1043–50.
[14] Carlsson L, Abrahamsson C, Andersson B, Duker G, Schiller-Linhardt G. Proarrhythmic effects of the class III agent almokalant: importance of infusion rate, QT dispersion, and early afterdepolarizations. Cardiovasc Res 1993;27:2186–93.
[15] Arteyeva NV, Goshka SL, Sedova KA, Bernikova OG, Azarov JE. What does the T(peak)-T(end) interval reflect? An experimental and model study. J Electrocardiol 2013;46:296.e1–8.
[16] Xing D, Martins JB. Myocardial ischemia-reperfusion damage impacts occurrence of ventricular fibrillation in dogs. Am J Physiol Heart Circ Physiol 2001;280:684–92.
[17] Demidova MM, Martín-Yebra A, van der Pals J, Koul S, Erlinge D, Laguna P, et al. Transient and rapid QRS-widening associated with a J-wave pattern predicts impending ventricular fibrillation in experimental myocardial infarction. Heart Rhythm 2014;11:1195–201.
[18] Janse MJ, Capucci A, Coronel R, Fabius MA. Variability of recovery of excitability in the normal canine and the ischaemic porcine heart. Eur Heart J 1985;6:41–52.
[19] Sridhar A, Nishijima Y, Terentyev D, Terentyeva R, Uelme R, Kukielka M, et al. Repolarization abnormalities and afterdepolarizations in a canine model of sudden cardiac death. Am J Physiol Regul Integr Comp Physiol 2008;295(5):1463–72.
[20] Wit AL, Janse JM. Reperfusion arrhythmias and sudden cardiac death: a century of progress toward an understanding of the mechanisms. Circ Res 2001;89(9):741–3.
[21] Weiss JN, Garfinkel A, Karagueuzian HS, Chen PS, Qu Z. Early afterdepolarizations and cardiac arrhythmias. Heart Rhythm 2010;7:1891–9.
[22] Brooks WW, Conrad CH, Morgan JP. Reperfusion induced arrhythmias following ischaemia in intact rat heart: role of intracellular calcium. Cardiovasc Res 1995;29(4):536–42.
[23] Panikkath R, Reinier K, Uy-Evanado A, Teodorescu C, Hattenhauer J, Mariani R, et al. Prolonged Tpeak-to-Tend interval on the resting ECG is associated with increased risk of sudden cardiac death. Circ Arrhythm Electrophysiol 2011;4:441–7.
[24] Hetland M, Haugaa KH, Sarvari SI, Erikssen G, Kongsgaard E, Edvardsen T. A novel ECG-index for prediction of ventricular arrhythmias in patients after myocardial infarction. Ann Noninvasive Electrocardiol 2014;19:330–7.

Please cite this article as: Bernikova OG, et al, Repolarization in perfused myocardium predicts reperfusion ventricular tachyarrhythmias, Journal of Electrocardiology (2017), https://doi.org/10.1016/j.jelectrocard.2017.12.003

Discussion

Alterations of repolarization heterogeneity in the heart has been established as an arrhythmogenic factor predisposing to malignant cardiac arrhythmias which can result in sudden cardiac death. Electrocardiogram represents the most convenient and cost-effective method of monitoring electrical activity of the heart, however, the relation between ECG morphology and repolarization heterogeneity is not clear. Therefore, the present study was designed to contribute to improvement of diagnostic power of the ECG methods in the prevention and treatment of malignant arrhythmias. The specific parameters of myocardial repolarization that could serve as predictors of ventricular tachyarrhythmias were determined and electrocardiographic manifestation of these parameters were suggested.

Dispersion of repolarization in the intact heart and Tpeak-Tend interval

The non-uniformity of action potential duration in different layers and areas of ventricles and the depolarization sequence are responsible for the heterogeneity of repolarization in the ventricles and for the genesis of T wave in body surface ECGs. Dispersion of repolarization being a quantitative index of repolarization heterogeneity is defined as the time difference between the earliest and the latest repolarization time (Burton, Cobbe, 2001). The Tpeak–Tend interval is considered as a marker of the repolarization dispersion, however, the electrophysiological basis for it is not clear. Specifically, the contribution of the transmural repolarization gradient to the T-wave development and remains controversial. The transmural repolarization gradient is considered as the key factor for the genesis of T-wave in ECG, as supported by the discovery of M cells in the isolated wedge preparation (Yan, Antzelevitch, 1998; Patel et al, 2009). However, originally, in the 19th century, the T-wave was established to result from the apicobasal heterogeneity of repolarization in the ventricles (Opthof et al, 2009). Recent studies confirm this original concept and consider the T-wave in the body surface ECGs as a result of apicobasal and anterior–posterior differences in repolarization times, rejecting significant repolarization gradients between endocardium and epicardium in the intact heart (Janse et al, 2012, Arteyeva, Azarov 2017). Experimental measurements in this study demonstrated the presence of the transmural gradient in the intact heart but the contribution of the transmural APD gradient to the Tpeak-Tend interval was minor to that of the apicobasal APD gradient and apicobasal AT difference.

Therefore, the Tpeak-Tend interval reflects the global dispersion of repolarization (dominant repolarization gradient), which can differ between intact heart with prevalent apicobasal and interventricular gradients and myocardial wedge preparation having the transmural gradient only. The prognostic value of the Tpeak-Tend interval for assessment of the global dispersion of repolarization was confirmed but there could be some technical issues concerning the T-wave end determination for pathologically changed T-wave morphology.

Assessment of repolarization heterogeneity alterations

Ischemia-related alterations of myocardial action potential (Carmeliet, 1999) provide the increase of the dispersion of repolarization due to local APD shortening in the ischemic area. In this study, the echinochrome was applied as antioxidant to minimize the extent of the above mentioned changes. Accordingly, the ischemia-induced increase of repolarization inhomogeneity was associated with the increase of the QTc and Tpeak-Tend intervals in the limb leads in controls but the attenuation of repolarization changes by echinochrome abolished the corresponding ECG alterations. The differences between controls and echinochrome given could be related to the apicobasal gradient of repolarization. The role of transmural gradient was not significant, due to uniform electrophysiological changes in epicardial, intramural and endocardial layers of the ischemic zone and, consequently, unchanged transmural repolarization gradient (Sedova et al, 2013). The effectiveness of the Tpeak-Tend interval to assess the ischemic-induced increase of repolarization dispersion was supported by our experimental model of diabetes mellitus **(Sedova et al, 2016, App. A)** and in the simulation study in the rabbit heart (Arteyeva, Azarov, 2017).

The clinical use of the QT and Tpeak-Tend intervals as a marker of repolarization heterogeneity for prediction of ventricular arrhythmias are not clear (Panikkath at al. 2011, Smetana et al. 2011, Porthan et al. 2013, Hetland et al. 2014). Clinically unsatisfactory predictive values of these indices could be due to the technical difficulty of the T wave end measurement. Thus, the T-wave voltage determinations could present an alternative approach for the evaluation of the repolarization dispersion. Present study demonstrated the relation between longitudinal T-wave amplitude dispersion and epicardial dispersion of repolarization during ischemic exposure. Therefore, the measurement of the differences between the T-wave voltages in the “basal” and “apical” precordial leads might present a useful tool for the evaluation of myocardial dispersion of repolarization (Sedova et al. 2015). This hypothesis was confirmed in our parallel research aimed to investigate the contribution of ventricular

repolarization dispersion and RT gradients to electrocardiographic T wave parameters in experimental rabbit diabetes mellitus model. It was found that the alterations in the myocardial RT gradients (apicobasal, interventricular, anteroposterior) could be assessed by corresponding T-wave amplitude dispersion (**Sedova et al. 2017, app. B**)

Reduction of the dispersion of repolarization and corresponding ECG changes after application of antioxidant agent did not influence the incidence of reentrant arrhythmias. Additional study of repolarization heterogeneity in diabetic rabbits demonstrated that either decreased or increased apicobasal repolarization gradient did not reflect the vulnerability of the heart to arrhythmias **(Ovechkin et al. 2015, app. C)**. This observation is consistent with the suggestion that the dispersion of repolarization could not solely predict reentrant arrhythmias (Coronel et al, 2009).

Thus, the findings suggest that longitudinal T-wave amplitude dispersion, Tpeak-Tend and QTc intervals could serve as indicators of the repolarization dispersion but cannot reflect myocardial vulnerability to tachyarrhythmias (Sedova et al, 2015).

Prediction of ventricular tachyarrhythmias in ischemia/reperfusion model

The prevention of life-threatening arrhythmias during the acute coronary syndrome requires reliable ECG markers that may be related either to the processes of ventricular depolarization or/and repolarization. The QRS prolongation and J wave pattern have been reported to be predictors of VF in acute ischemia (Demidova et al, 2014). In the present study, ventricular repolarization parameters involved in VT/VF development were revealed. The prolongation of the nonischemic RTs, due to corresponding alterations in the area adjacent to the ischemic zone (so-called “border” zone) was recognized as independent predictor for arrhythmic event. The increased nonischemic RTs could influence arrhythmogenesis in two ways. First, under conditions of local APD shortening in the ischemic area, the longer nonischemic (border) APD provided the greater dispersion of repolarization underlying the unidirectional conduction block and reentrant arrhythmias. This concept is supported by the fact that the experimentally measured border RT dispersion is larger in VT/VF group, however, dispersion of repolarization (either global, or transmural) did not serve as an independent predictor of arrhythmias. Second possible mechanism of arrhythmic susceptibility could be related to the local prolongation of repolarization and development of early afterdepolarizations in the border zone (Weiss et al. 2010). This triggering mechanism in combination with the increased dispersion of repolarization could result in the development of VT/VF. Thus, the treatment for prevention of

malignant arrhythmias during the ischemic attack could be targeted to the nonischemic areas, which could be treated much more easily during the ischemic episode.

Computer simulations were applied to found out the ECG index of the long nonischemic RTs recognized as independent predictors of the life-threatening ventricular arrhythmias. It was suggested that the APD prolongation in the border zone produced the negative terminal phase of the T wave in the precordial leads. This suggestion could not be tested directly in the experiment as the thorax was opened and recording of precordial ECG leads was impossible. However, similar myocardial electrograms were consistently recorded in the anterior wall leads in animals with VT/VF. Thus, the terminal T wave inversion reflecting the border APD prolongation could serve as a predictor of the fatal ventricular tachyarrhythmias. Our findings are in agreement with the recent study demonstrating an association between increase of the Tpeak-Tend interval and ischemia-induced ventricular fibrillation in a porcine myocardial infarction (Azarov et al. 2017). Likewise, the combination of the ST segment elevation and the T wave inversion was suggested as predictor of the spontaneous reperfusion arrhythmias in anterior STEMI patients (Hira et al. 2014).

Therefore, taking into account that among ECG parameters considered as predictors of ventricular arrhythmias, QT dispersion has been compromised (Zabel et al. 1998), and the clinical utility of the Tpeak-Tend interval remains ambiguous (Smetana et al. 2011, Porthan et al. 2013, Hetland et al. 2014), the prognostic criteria based on the morphological or amplitude ECG indices are much more promising. The presence of terminal T-wave inversion could be useful for the VT/VF prognosis during ischemic attack as it could be clearly seen in the ECG tracings.

Limitations

The interpretation of the findings in the present study should be made with account of some limitations. Results of the animal experiments have contributed to underfunding of the value of ECG repolarization indices in prediction reperfusion-induced ventricular tachyarrhythmias during acute coronary syndrome, but in clinical settings their value in diagnostic strategies remain unclear. Our experimental animal model included only the left anterior deseeding coronary artery occlusion, during uniform duration of ischemia. The issues regarding applicability of the predictors of fatal arrhythmias for different localization of ischemic injury or duration of ischemia require feather clinical studies.

Conclusions

The presence of transmural and apicobasal differences in repolarization durations was found in the ventricular myocardium *in vivo*. The simulations demonstrated that the global dispersion of repolarization resulting from the apicobasal and transmural repolarizations gradients is reflected in the Tpeak-Tend interval in body surface electrocardiogram (Arteyeva et al. 2013).

Under ischemic conditions the global, apicobasal, and borderline dispersions of repolarization increased, whereas the transmural gradients did not change (Sedova et al. 2013).

The increase of borderline, apicobasal and global dispersions of repolarization was associated with prolongation of the Tpeak-Tend and QTc interval as well as the longitudinal T wave amplitude dispersion in the precordial leads (Sedova et al. 2015, Sedova et al 2016).

The reperfusion VT/VFs were independently predicted by longer RTs in the nonischemic zone reflected in the terminal negative phase of the electrocardiographic T wave, which warrants further evaluation in clinical settings (Bernikova et al. 2017 In press: J Electrocardiol).

Relevant publications

The dissertation is based on the following articles:

I. BERNIKOVA OG, **SEDOVA KA**, ARTEYEVA NV, OVECHKIN AO, KHARIN SN, SHMAKOV DN, AZAROV JE. REPOLARIZATION IN PERFUSED MYOCARDIUM PREDICTS REPERFUSION VENTRICULAR TACHYARRHYTHMIAS. J ELECTROCARDIOL 2017. IN PRESS. **JCR IF 2016 - 1.514**

II. **SEDOVA K**, BERNIKOVA O, AZAROV J, SHMAKOV D, VITYAZEV V, KHARIN S. EFFECTS OF ECHINOCHROME ON VENTRICULAR REPOLARIZATION IN ACUTE ISCHEMIA. J ELECTROCARDIOL 2015. 48(2): 181-6. **JCR IF 2014 - 1.361**

III. **SEDOVA KA**, BERNIKOVA OG, GOSHKA SL, SHMAKOV DN, KHARIN SN. EFFECTS OF AN ANTIOXIDANT AGENT ON ALTERATIONS OF VENTRICULAR REPOLARIZATION IN A CORONARY ARTERY OCCLUSION-REPERFUSION EXPERIMENTAL MODEL. EXP CLIN CARDIOL 2013. 19(1): 1-6. **JCR IF 2012 - 1.100**

IV. ARTEYEVA NV, GOSHKA SL, **SEDOVA KA**, BERNIKOVA OG, AZAROV JE. WHAT DOES THE T PEAK-T END INTERVAL REFLECT? AN EXPERIMENTAL AND MODEL STUDY. J ELECTROCARDIOL 2013. 46(4): 296.E1–E8. **JCR IF 2012 - 1.093**

Other relevant publications in journals with Impact Factor:

1. **Sedova KA**, Azarov JE, Arteyeva NV, Ovechkin AO, Vaykshnorayte MA, Vityazev VA, Bernikova OG, Shmakov DN, Kneppo P. Mechanism of electrocardiographic T wave flattening in diabetes mellitus: experimental and simulation study. Physiol Res 2017, 66: 781-789. **JCR IF 2016 - 1.461**
2. **Sedova KA**, Vaykshnorayte MA, Ovechkin AO, Kneppo P, Bernikova OG, Vityazev VA, Azarov JE. Ventricular electrical heterogeneity in experimental diabetes mellitus: effect of myocardial ischemia. Physiol Res. 2016. 65(3):437-45. **JCR IF 2015 - 1.643**
3. Ovechkin A, Vaykshnorayte M, **Sedova K,** Shumikhin K, Arteyeva N, Azarov J. Functional role of myicardial electrical remodeling in diabetic rabbits. Can J Physiol Pharmacol 2015. 93(4): 245-52. **JCR IF 2014 - 1.770**
4. Ovechkin AO, Vaykshnorayte MA, **Sedova KA**, Shmakov DN, Shumikhin KV, Medvedeva S Yu, Danilova IG, Azarov JE. Esmolol abolishes repolarization gradients in diabetic rabbit hearts. Exp Clin Cardiol 2014. 20(8): 3780-93. **JCR IF 2013 - 0.758**

Proceedings and abstracts

5. Azarov I, Ovechkin A, Vaykshnorayte M, **Sedova K**, Bernikova O, Arteyeva N, Shmakov D. Ventricular repolarization pattern and ischemic arrhythmia susceptibility at different follow-ups of diabetes mellitus. FASEB JOURNAL 2015. 29(1): 958.1. **JCR IF 2014 - 5.043.**
6. **Sedova K**, Bernikova O, Kharin S, Shmakov D. Effects of Echinochrome on Ventricular Repolarization in Acute Ischemia. ELECTROCARDIOLOGY 2014. Proceedings of the 41st International Congress on Electrocardiology. P. 121-124.
7. Vaykshnorayte MA, **Sedova KA**, Bernikova OG, Ovechkin AO, Azarov JE.Body Surface T-wave Amplitude Dispersion in Diabetic Rabbits and Epicardial Repolarization Pattern.

ELECTROCARDIOLOGY 2014. Abstracts of the 41st International Congress on Electrocardiology. P. 39.

8. **Sedova K**, Bernikova O, Kharin S, Shmakov D. Effects of Echinochrome on Ventricular Repolarization in Acute Ischemia ELECTROCARDIOLOGY 2014. Abstracts of the 41st International Congress on Electrocardiology. P. 62.
9. Bernikova OG, Azarov JE, **Sedova KA**, Kharin SN, Shmakov DN. Ventricular repolarization indices as predictors of fatal arrhythmias in ischemia/reperfusion model. Abstract. J Electrocardiol 2013. 46: e25. **JCR IF 2012 - 1.093**
10. Vaykshnorayte MA, Ovechkin AO, **Sedova KA**, Azarov JE. Ventricular epicardial repolarization pattern in diabetic rabbits. Abstract. J Electrocardiol 2013. 46: e31. **JCR IF 2012 - 1.093**
11. Azarov JE, Ovechkin AO, Vaykshnorayte MA, **Sedova KA**, Shmakov DN. Ventricular epicardial repolarization pattern in diabetic rabbits. FASEB JOURNAL 2012. 26. **JCR IF 2011 - 5.712**

References

1. Antzelevitch C, Viskin S, Shimizu W, Yan GX, Kowey P, Zhang L, Sicouri S, Di Diego JM, Burashnikov A. Does Tpeak-Tend provide an index of transmural dispersion of repolarization? Heart Rhythm 2007. 4(8): 1114-1116.
2. Arteyeva NV, Azarov JE. Effect of action potential duration on Tpeak-Tend interval, T-wave area and T-wave amplitude as indices of dispersion of repolarization: Theoretical and simulation study in the rabbit heart. J Electrocardiol 2017. 50: 919-924.
3. Arteyeva NV, Goshka SL, Sedova KA, Bernikova OG, Azarov JE. What does the T(peak)-T(end) interval reflect? An experimental and model study. J Electrocardiol 2013. 46(4): 296.e1-8.
4. Azarov JE, Demidova MM, Koul S, van der Pals J, Erlinge D, Platonov PG. Progressive increase of the Tpeak-Tend interval is associated with ischaemia-induced ventricular fibrillation in a porcinemyocardial infarction model. Europace 2017. 00: 1-7.
5. Bernikova OG, Sedova KA, Arteyeva NV, Ovechkin AO, Kharin SN, Shmakov DN, Azarov JE. Repolarization in perfused myocardium predicts reperfusion ventricular tachyarrhythmias. J Electrocardiol 2017. In press.
6. Bernikova OG, Sedova KA, Azarov YE, Shmakov DN. Ventricular myocardial repolarization in acute coronary occlusion and reperfusion in cats. Dokl Biol Sci 2011. 437: 69-71.
7. Brendorp B, Elming H, Jun L, Kober L, Malik M, Jensen GB, Torp-Pedersen C. QT dispersion has no prognostic information for patients with advanced congestive heart failure and reduced left ventricular systolic function. Circulation 2001. 103(6): 831-835.
8. Burton FL, Cobbe SM. Dispersion of ventricular repolarization and refractory period. Cardiovasc Res 2001. 50(1): 10-23.

9. Carlsson L, Abrahamsson C, Andersson B, Duker G, Schiller-Linhardt G. Proarrhythmic effects of the class III agent almokalant: importance of infusion rate, QT dispersion, and early afterdepolarizations. Cardiovasc Res 1993. 27: 2186–2193.
10. Carmeliet E. Cardiac ionic currents and acute ischemia: from channels to arrhythmias. Physiological Reviews 1999. 79:917-1017.
11. Coronel R, de Bakker JM, Wilms-Schopman FJ, Opthof T, Linnenbank AC, Belterman CN, Janse MJ. Monophasic action potentials and activation recovery intervals as measures of ventricular action potential duration: experimental evidence to resolve some controversies. Heart Rhythm 2006. 3(9): 1043–1050.
12. Coronel R, Wilms-Schopman FJ, Opthof T, Janse MJ. Dispersion of repolarization and arrhythmogenesis. Heart Rhythm 2009. 6: 537-543.
13. Demidova MM, Martín-Yebra A, van der Pals J, Koul S, Erlinge D, Laguna P et al. Transient and rapid QRS-widening associated with a J-wave pattern predicts impending ventricular fibrillation in experimental myocardial infarction. Heart Rhythm 2014. 11: 1195-1201.
14. Guerard N, Jordaan P, Dumotier B. Analysis of unipolar electrograms in rabbit heart demonstrated the key role of ventricular apicobasal dispersion in arrhythmogenicity. Cardiovasc Toxicol 2014. 14: 316–328.
15. Hetland M, Haugaa KH, Sarvari SI, Erikssen G, Kongsgaard E, Edvardsen T: A novel ECG-index for prediction of ventricular arrhythmias in patients after myocardial infarction. Ann Noninvasive Electrocardiol 2014. 19: 330-337.
16. Hira, RS, Moore C, Huang HD, Wilson JM, Birnbaum Y: T wave inversions in leads with ST elevations in patients with acute anterior ST elevation myocardial infarction is associated with patency of the infarct related artery. J Electrocardiol 2014. 47: 472-477.

17. Janse MJ, Coronel R, Opthof T, Sosunov EA, Anyukhovsky EP, Rosen MR. Repolarization gradients in the intact heart: transmural or apico-basal? Prog Biophys Mol Biol 2012. 109: 6-15.
18. Kimura S, Bassett AL, Kohya T, Kozlovskis PL, Myerburg RJ. Simultaneous recording of action potentials from endocardium and epicardium during ischemia in the isolated cat ventricle: relation of temporal electrophysiologic heterogeneities to arrhythmias. Circulation 1986. 74: 401-409.
19. Lukas A, Antzelevitch C. Differences in the electrophysiological response of canine ventricular epicardium and endocardium to ischemia. Circulation 1993. 88: 2903-2915.
20. Malik M, Batcharov VN. Measurement, interpretation and clinical potential of QT dispersion. Journal of the American College of Cardiology 2000. 36(6): 1749-1766.
21. Mehta RH, Starr AZ, Lopes RD, Hochman JS, Widimsky P, Pieper KS, Armstrong PW, Granger CB. APEX AMI Investigators: Incidence of and outcomes associated with ventricular tachycardia or fibrillation in patients undergoing primary percutaneous coronary intervention. JAMA 2009. 301: 1779-1789.
22. Meijborg VM, Conrath CE, Opthof T, Belterman CN, de Bakker JM, Coronel R. Electrocardiographic T wave and its relation with ventricular repolarization along major anatomical axes. Circ Arrhythm Electrophysiol 2014. 7: 524-531.
23. Opthof T, Coronel R, Wilms-Schopman FJ, Plotnikov AN, Shlapakova IN, Danilo PJr, Rosen MR, Janse MJ. Dispersion of repolarization in canine ventricle and the electrocardiographic T wave: Tp-e interval does not reflect transmural dispersion. Heart Rhythm 2007. 4(3): 341-348.
24. Opthof T, Coronel R, Janse MJ. Is there a significant transmural gradient in repolarization time in the intact heart? Repolarization Gradients in the Intact Heart. Circ Arrhythm Electrophysiol 2009. 2: 89-96.

25. Pak HN, Hong SJ, Hwang GS, Lee HS, Park SW, Ahn JC, Moo Ro Y, Kim YH. Spatial dispersion of action potential duration restitution kinetics is associated with induction of ventricular tachycardia/fibrillation in humans. Journal of cardiovascular electrophysiology 2004. 15: 1357–1363.
26. Panikkath R, Reinier K, Uy-Evanado A, Teodorescu C, Hattenhauer J, Mariani R, Gunson K, Jui J, Chugh SS. Prolonged Tpeak-to-Tend interval on the resting ECG is associated with increased risk of sudden cardiac death. Circ Arrhythm Electrophysiol 2011. 4: 441-447.
27. Patel C, Burke JF, Patel H, Gupta P, Kowey PR, Antzelevitch C, Yan GX. Is there a significant transmural gradient in repolarization time in the intact heart? Cellular basis of the T wave: a century of controversy. Circ Arrhythm Electrophysiol 2009. 2: 80-88.
28. Porthan K, Viitasalo M, Toivonen L, Havulinna AS, Jula A, Tikkanen JT, Väänänen H, Nieminen MS, Huikuri HV, Newton-Cheh C, Salomaa V, Oikarinen L. Predictive value of electrocardiographic T-wave morphology parameters and T-wave peak to T-wave end interval for sudden cardiac death in the general population. Circ Arrhythm Electrophysiol 2013. 6: 690-696.
29. Priori SG, Napolitano C, Diehl L, Schwartz PJ. Dispersion of the QT interval. A marker of therapeutic efficacy in the idiopathic long QT syndrome. Circulation 1994. 89(4): 1681-1689.
30. Sedova K, Bernikova O, Azarov J, Shmakov D, Vityazev V, Kharin S. Effects of echinochrome on ventricular repolarization in acute ischemia. J Electrocardiol 2015. 48(2): 181-186.
31. Sedova KA, Bernikova OG, Goshka SL, Pokhilo ND, Atopkina LN, Shmakov DN, Kharin SN. Effects of an antioxidant agent on alterations of ventricular repolarization

in a coronary artery occlusion-reperfusion experimental model. Experimental&Clinical Cardiology 2013.

32. Smetana P, Schmidt A, Zabel M, Hnatkova K, Franz M, Huber K, Malik M. Assessment of repolarization heterogeneity for prediction of mortality in cardiovascular disease: peak to the end of the T wave interval and nondipolar repolarization components. J Electrocardiol 2011. 44: 301-308.
33. Taggart P, Sutton PM, Opthof T, Coronel R, Trimlett R, Pugsley W, Kallis P: Transmural repolarisation in the left ventricle in humans during normoxia and ischaemia. Cardiovasc Res 2001. 50: 454-462.
34. Tsang HG, Rashdan NA, Whitelaw CBA, Corcoran BM, Summers KM, Mac Rae VE. Large animal models of cardiovascular disease. Cell Biochem Funct 2016. 34: 113–132.
35. Vaykshnorayte MA, Azarov JE, Tsvetkova AS, Vityazev VA, Ovechkin AO, Shmakov DN. The contribution of ventricular apicobasal and transmural repolarization patterns to the development of the T wave body surface potentials in frogs (Rana temporaria) and pike (Esox lucius). Comp Biochem Physiol A Mol Integr Physiol 2011. 159(1): 39-45.
36. Voss F, Opthof T, Marker J, Bauer A, Katus HA, Becker R. There is no transmural heterogeneity in an index of action potential duration in the canine left ventricle. Heart Rhythm 2009. 6(7): 1028-1034.
37. Weiss JN, Garfinkel A, Karagueuzian HS, Chen PS, Qu Z: Early afterdepolarizations and cardiac arrhythmias. Heart Rhythm 2010. 7:1891-1899.
38. Wit AL, Janse MJ. Reperfusion arrhythmias and sudden cardiac death: a century of progress toward an understanding of the mechanisms Circ Res. 2001. 89: 741-743.
39. World health statistics 2017: monitoring health for the SDGs, Sustainable Development Goals. Geneva: World Health Organization, 2017.

40. Xia Y, Liang Y, Kongstad O, Holm M, Olsson B, Yuan S: Tpeak-Tend interval as an index of global dispersion of ventricular repolarization: evaluations using monophasic action potential mapping of the epi- and endocardium in swine. J Interv Card Electrophysiol 2005. 14: 79-87.
41. Xue J, Chen Y, Han X, Gao W. Electrocardiographic morphology changes with different type of repolarization dispersions. J Electrocardiol 2010. 43(6): 553-559.
42. Yan GX, Antzelevitch C. Cellular basis for the normal T wave and the electrocardiographic manifestations of the long-QT syndrome. Circulation 1998. 98(18): 1928-1936.
43. Zabel M, Klingenheben T, Franz MR, Hohnloser SH. Assessment of QT dispersion for prediction of mortality or arrhythmic events after myocardial infarction: results of a prospective, long-term follow-up study. Circulation 1998. 97: 2543-2550.

Appendices

Appendix A: *Sedova KA, Vaykshnorayte MA, Ovechkin AO, Kneppo P, Bernikova OG, Vityazev VA, Azarov JE. Ventricular electrical heterogeneity in experimental diabetes mellitus: effect of myocardial ischemia. Physiol Res. 2016. 65(3): 437-45. JCR IF 2016 - 1.461.*

Physiol. Res. 65: 437-445, 2016

Ventricular Electrical Heterogeneity in Experimental Diabetes Mellitus: Effect of Myocardial Ischemia

K. A. SEDOVA[1,2], M. A. VAYKSHNORAYTE[2], A. O. OVECHKIN[2,3], P. KNEPPO[1], O. G. BERNIKOVA[2,3], V. A. VITYAZEV[2,3], J. E. AZAROV[2,3]

[1]Department of Biomedical Technology, Faculty of Biomedical Engineering, Czech Technical University, Kladno, Czech Republic, [2]Laboratory of Cardiac Physiology, Institute of Physiology, Komi Science Center, Ural Branch, Russian Academy of Sciences, Syktyvkar, Russia, [3]Department of Physiology, Medical Institute of Pitirim Sorokin Syktyvkar State University, Syktyvkar, Russia

Received August 4, 2015
Accepted January 19, 2016
On-line April 12, 2016

Summary

Aims of the study were to compare the development of electrocardiographic responses of the ischemia-induced heterogeneities of activation and repolarization in the ventricular myocardium of normal and diabetic animals. Body surface ECGs and unipolar electrograms in 64 epicardial leads were recorded before and during 20 min after the ligation of the left anterior descending artery in diabetic (alloxan model, 4 weeks, n=8) and control (n=8) rabbits. Activation times (ATs), end of repolarization times (RTs) and repolarization durations (activation-recovery intervals, ARIs) were determined in ischemic and periischemic zones. In contrast to the controls, the diabetic rabbits demonstrated the significant prolongation of ATs and shortening of ARIs ($P<0.05$) during ischemia in the affected region resulting in the development and progressive increase of the ARI and RT gradients across the ischemic zone boundary. The alterations of global and local dispersions of the RTs in diabetics correlated with the T_{peak}-T_{end} interval changes in the limb leads ECGs. In the ischemic conditions, the diabetic animals differed from the controls by the activation delay, significant repolarization duration shortening, and the increase of local repolarization dispersion; the latter could be assessed by the T_{peak}-T_{end} interval measurements in the body surface ECGs.

Key words

Cardiac electrophysiology • Diabetes mellitus • Regional ischemia • Myocardium • Electrocardiography

Corresponding author

K. A. Sedova, Department of Biomedical Technology, Faculty of Biomedical Engineering, Czech Technical University in Prague, Sítná sq. 3105, 27201 Kladno, Czech Republic. E-mail: ksenia.sedova@fbmi.cvut.cz

Introduction

The excessive myocardial electrical heterogeneity dictates the level of electrical instability of the heart, whereas the myocardial ischemia is a major event exacerbating electrical inhomogeneities and leading to malignant ventricular arrhythmias. Clinical studies have found that diabetes mellitus (DM) enhances the risk of ventricular tachyarrhythmias and mortality in acute myocardial infarction even more (Cho *et al.* 2002, Dziewierz *et al.* 2010, Sanjuan *et al.* 2011). On the other hand, experimental studies of diabetic hearts demonstrated either the increased (Hekimian *et al.* 1985, Bakth *et al.* 1986, Wang *et al.* 2012) or decreased (Kusama *et al.* 1992, Ravingerová *et al.* 2000, Galagudza *et al.* 2007, Matejíková *et al.* 2008) susceptibility to ventricular arrhythmias in ischemic conditions. Spooner (2008) pointed out that DM while worsening the long-term prognosis does not affect the susceptibility to ventricular arrhythmias in acute settings in patients with cardiovascular diseases. Some clinical observations suggested that the susceptibility to ventricular arrhythmias could be related to concomitant factors such

as hypoglycemic episodes or medication (Chow *et al.* 2014, Curione *et al.* 2014, Pistrosch *et al.* 2015). These conflicting data on the electrical stability of the heart in diabetes mellitus under ischemia suggest that the diabetic myocardium may have a specific electrophysiological response to the ischemic insult.

The diabetic cardiomyopathy is associated with the electrophysiological alterations in the myocardium. The DM-related changes in the cardiac electrical properties, specifically the prolongation of action potential durations, have been well documented at the cellular level (Magyar *et al.* 1992, Zhang *et al.* 2007, Lengyel *et al.* 2008, Gallego *et al.* 2009). Equally important would be largely lacking thus far data on the distribution of the electrophysiological properties throughout the myocardium and its dynamical changes in ischemia. This spatiotemporal electrical pattern is quantitated as a dispersion of repolarization that is, in turn, attempted to be assessed by ECG. For this purpose, several ECG indices were considered, including T_{peak}-T_{end} interval, a promising index for the estimation of the dispersion of repolarization. Clinical investigations either supported (Panikkath *et al.* 2011, Hetland *et al.* 2014, Mozos 2015) or opposed (Smetana *et al.* 2011, Porthan *et al.* 2013) to its prognostic utility suggesting that electrophysiological information content of T_{peak}-T_{end} interval could vary in different conditions. T_{peak}-T_{end} interval has been also tested in diabetic patients (Clemente *et al.* 2012, Miki *et al.* 2014). However, the behavior of the T_{peak}-T_{end} and its relation to the dispersion of repolarization in an arrhythmogenic stress conditions, such as myocardial ischemia, is largely unknown in the setting of DM.

The objective of the present study was to compare the ischemia-induced changes of ventricular epicardial activation and repolarization patterns and their expressions in the parameters of the body surface ECGs in normal and diabetic rabbit hearts.

Methods

The experiments were carried out in adult Chinchilla rabbits (age from 7 to 9 months, body mass from 2.9 to 3.3 kg). The investigation conformed to the *Guide for the Care and Use of Laboratory Animals* (2011). Experimental type 1 DM was induced in 8 animals (5 females) by a single intravenous alloxan injection (120 mg/kg body mass, 4 weeks follow-up), and 8 healthy animals (4 females) served as controls. DM was confirmed by at least double determinations of fasting venous blood glucose level more than 7 mmol/l with OneTouch glucometer (LifeScan Inc, USA). The open-heart experiments were consistently done during the daytime hours (from 11-00 to 13-00) on the animals anesthetized with zoletil (15 mg/kg body mass, intramuscular injection), intubated and mechanically ventilated. The heart was exposed by a midsternal incision. The temperature of the heart was maintained at 37-38 ºC by the irrigation with warm saline and warming the room air. An electrode sock with 64 leads (3-5 mm interelectrode distance) was placed on the ventricular surface, and the unipolar electrograms were simultaneously recorded in reference to Wilson's terminal at spontaneous sinus rhythm. The data acquisition was done using a custom-designed mapping system (16 bits; bandwidth 0.05 to 1000 Hz; sampling rate 4000 Hz).

Electrograms were recorded in the baseline and in the course of 20-min ischemia, which was produced by the ligation of the left anterior descending coronary artery (LAD). Evans blue dye (Sigma-Aldrich GmbH, Germany, 0.5 %) was injected postmortemly into the aorta. The ischemic zone was determined by the absence of Evans blue perfusion, and its size was estimated as the area of the figure circumscribed by the leads on the border of the ischemic zone.

Limb lead ECGs were monitored in the course of the experiment, and the QRS and QT durations were measured in the limb lead II. The corrected QT interval was calculated by the equation QTc=QT-0.175×(RR-300) (Carlsson *et al.* 1993). The total duration of the T_{peak}-T_{end} interval was measured as a period between the earliest T_{peak} and the latest T_{end} in the limb leads. In each epicardial lead, the activation time (AT) and the end of repolarization time (RT) were determined as dV/dt_{min} during the QRS complex and dV/dt_{max} during the T wave, respectively (Coronel *et al.* 2006). The activation-recovery interval (ARI) serving as a measure of local repolarization duration was measured as the difference between the RT and AT. The averaged values of these variables were calculated for different myocardial regions and specifically for the ischemic zone and the adjacent 3 to 5 mm width band of perfused myocardium referred to as a periischemic zone. The differences in the ATs, ARIs, and RTs between the ventricular regions were referred to as gradients (e.g. boundary gradient) and the difference between the earliest and the latest RT values throughout the ventricular epicardium was referred to as

the dispersion of repolarization.

Statistical analysis was performed with the SPSS 11.5 software packages. The data are given as medians and interquartile intervals. Wilcoxon test and Fridman test with Dunnett *post-hoc* procedure were utilized for the single and multiple comparisons within the groups, respectively. Mann-Whitney U-test was used to compare different groups of animals. The correlation between epicardial mapping indices and ECG parameters was evaluated with Spearman rank correlation test as the evaluated parameters were not normally distributed. The differences were considered significant at $P<0.05$.

Results

The control and DM groups matched with each other for sex, age, body mass and heart to body mass ratio. As expected, the glycemia level was significantly higher in diabetic animals as compared to controls [15.3 (8.8; 20.0) mmol/l vs. 5.9 (5.7; 6.3) mmol/l, respectively, $P<0.01$]. RR, QT, QTc and T_{peak}-T_{end} intervals were longer in animals with DM, whereas the QRS duration was similar in both groups (Table 1). The epicardial AT sequences in normals and diabetics were similar and directed from the left ventricular (LV) apex to the LV base and from the right ventricular (RV) free wall to the LV free wall. The spatial distribution of RTs was relatively uniform in healthy animals and heterogeneous in diabetics. In the latter group, the RV RTs were longer than the LV RTs [DM: 134 (119; 142) ms vs. 106 (104; 114) ms, $P=0.012$; Control: 115 (106; 127) ms vs. 114 (99; 119) ms, $P>0.05$, respectively].

Table 1. ECG parameters in rabbits of control and DM groups [Median and interquartile intervals (25 %, 75 %)].

		RR, ms	QRS, ms	QT, ms	QTc, ms	T_{peak} - T_{end}, ms
Baseline	*control*	230 (220; 247)	33 (31; 36)	159 (147; 160)	163 (159; 171)	41.5 (39; 45)
	DM	269 (249; 282)	32 (30; 35)	182 (171; 186)	188 (180; 190)	49 (46; 68)
	P	0.03	ns	0.003	0.009	0.04
10` ischemia	*control*	229 (209; 247)	34 (30; 38)	147 (139; 171)	160 (153; 180)	49 (43; 60)
	DM	252 (239; 264)	32 (31; 36)	160* (151; 169)	170* (160; 175)	47 (43; 53)
	P	ns	ns	ns	ns	ns
20` ischemia	*control*	225 (205; 240)	33 (31; 39)	147 (134; 166)	160 (151; 177)	38.5 (31; 52)
	DM	252 (243; 267)	33 (30; 38)	155* (148; 168)	164* (157; 173)	50.5 (37; 54)
	P	ns	ns	ns	ns	ns

* $P<0.05$ vs. baseline; DM, diabetes mellitus; ns, nonsignificant.

The size of the ischemic area was similar in the diabetic and control animals [75.6 (56.5; 86.0) mm^2 vs. 55.3 (42.4; 63.5) mm^2, for control and DM animals, respectively, $P>0.05$]. Isolated premature ventricular beats were sporadically observed in both groups. During ischemia, the QT and QTc intervals shortened in the DM group (Table 1). Coronary occlusion induced changes in electrograms recorded from the ischemic zone (Fig. 1), but the alterations found in this area differed in the control and diabetic animals (Fig. 2). The statistically significant activation delay in the ischemic zone was found only in diabetics ($P<0.05$). At 20-min of coronary occlusion, there were no statistically significant effects on ARIs in the control group. At least in part, this could be ascribed to variable individual profiles of ARI changes in the control group, which demonstrated either ARI shortening or prolongation, while the consistent shortening was found in the DM group (Fig. 3).

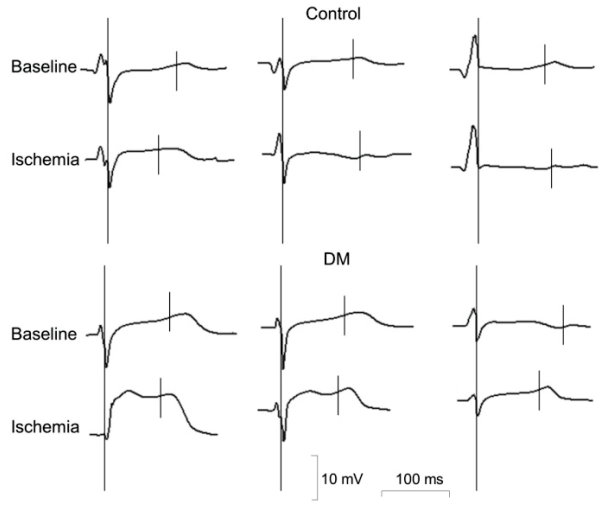

Fig. 1. Representative electrograms led across the ischemic zone in the apical third of the anterior left ventricle in the control and diabetic rabbits. Electrograms in baseline and ischemia are aligned by the activation times (AT, long vertical bars) and the end of repolarization times (RT) are indicated by the short vertical bars. See nonuniform changes of ARIs (RT-AT differences) in the control animals in ischemia.

Ischemia induced the development of specific epicardial activation and repolarization patterns (Fig. 4) characterized by the abrupt spatial differences in ATs and RTs corresponding to the area of ischemia (Fig. 4). Such differences were more pronounced in the DM group as compared to controls. The substantial ARI shortening in diabetics resulted in the development of a boundary ARI and RT gradients between the ischemic and adjacent periischemic zones, which progressively increased during the ischemic episode (Table 2). A significant correlation was found between the T_{peak}-T_{end} interval duration and the global RT dispersion in the diabetic rabbits under 20-min ischemia (r=0.86, P=0.007). In turn, the global RT dispersion was associated with the magnitude of the boundary RT gradient (r=0.857, P=0.007) which accordingly explains the correlation between the T_{peak}-T_{end} interval duration and the boundary RT gradient found only in the DM group (r=0.714, P=0.047).

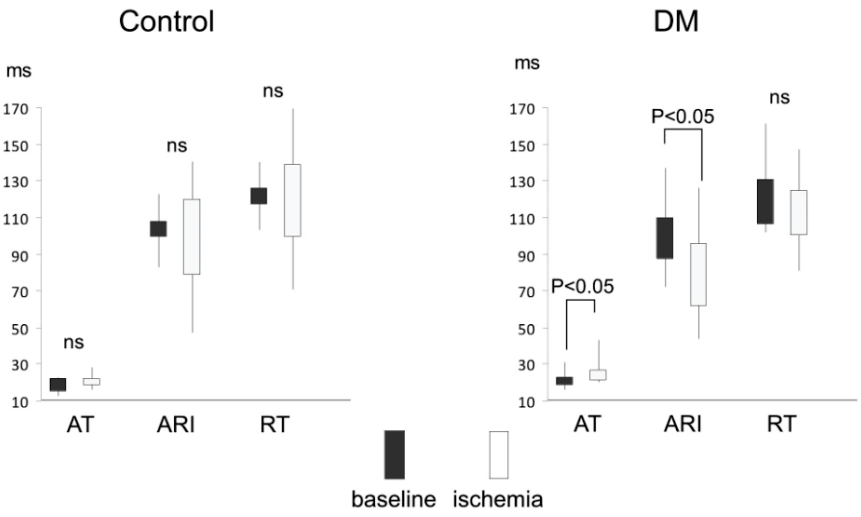

Fig. 2. The changes of the activation times (AT), activation-recovery intervals (ARI) and end of repolarization times (RT) in the ischemic zone in the control and DM groups. Boxes and bars identify the interquartile intervals and maximal and minimal values, respectively.

Table 2. The changes of activation time gradients, activation recovery interval gradients and end of repolarization time gradients between ischemic and periischemic (i/p) myocardium in control and DM groups [Median and interquartile intervals (25 %, 75 %)].

	Control			DM		
	AT i/p gradients	**ARI i/p gradients**	**RT i/p gradients**	**AT i/p gradients**	**ARI i/p gradients**	**RT i/p gradients**
Baseline (future ischemic zone)	0.24(-2.1;0.8)	5.1(0.1;13.2)	5.5(-1.2;12.1)	-0.3(-1.0;0.4)	0.45 (-3.0;2.4)	-0.98 (-3.6;0.9)
1` ischemia	-0.27(-1.1;1.8)	2.8(-2.2;7.6)	3.0(-2.8;13.1)	0.5(-0.3;0.6)	-14.8 (-21.3;-6.7)†	-15.3 (-22.4;-5.6) †
10` ischemia	0.4(-1.0;2.5)	0.6(-12.5;6.0)	0.02(-9.8;7.9)	1.7(0.4;2.9)	-20.0 (-29.6;-16.9)* †	-22.8 (-24.1;-11.2)*†
20` ischemia	0.4(-0.7;2.6)	-1.2(-12.2;4.3)	-0.7(-10.1;3.6)	1.7(0.5;2.7)	-25.3 (-32.4;-4.3)* †	-24.5 (-28.6;-4.5)

* p<0.05 for Dunnett *post-hoc* test (vs. baseline), † p<0.05 for Mann-Whitney (vs. control).

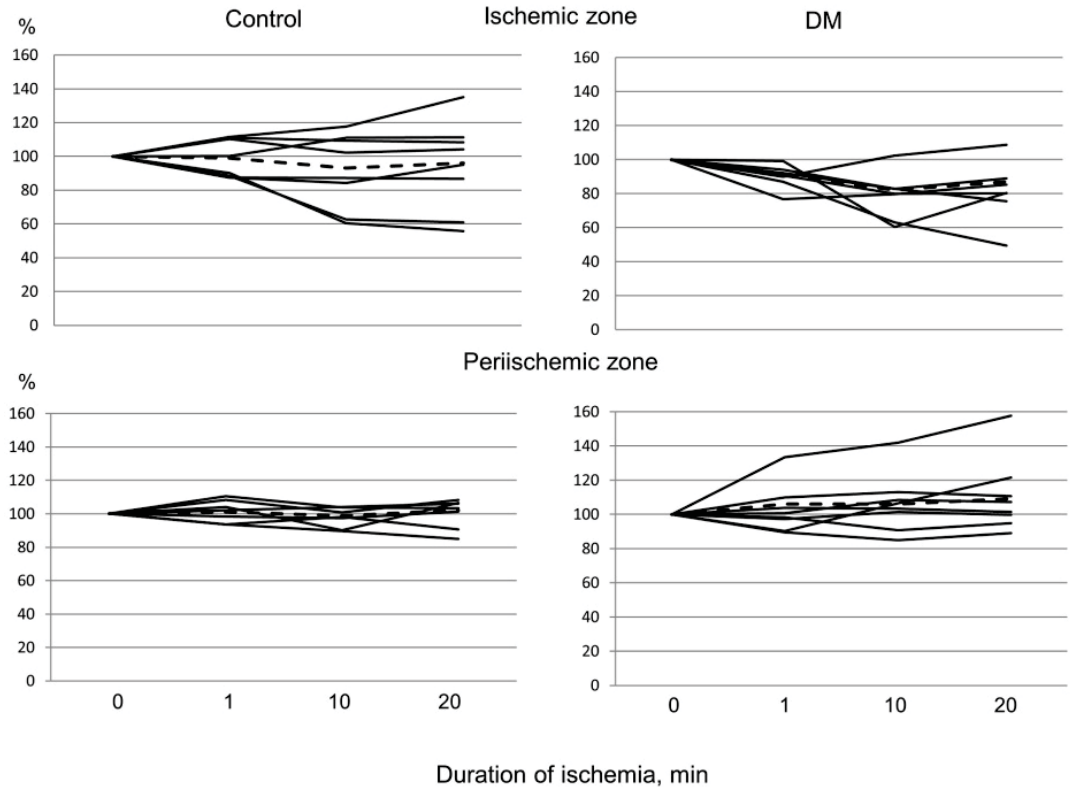

Fig. 3. Individual ARI changes (%) in the periischemic and ischemic zones during the ischemic episode in the control and diabetic animals. The baseline value is 100 %. Dashed lines identify for the means.

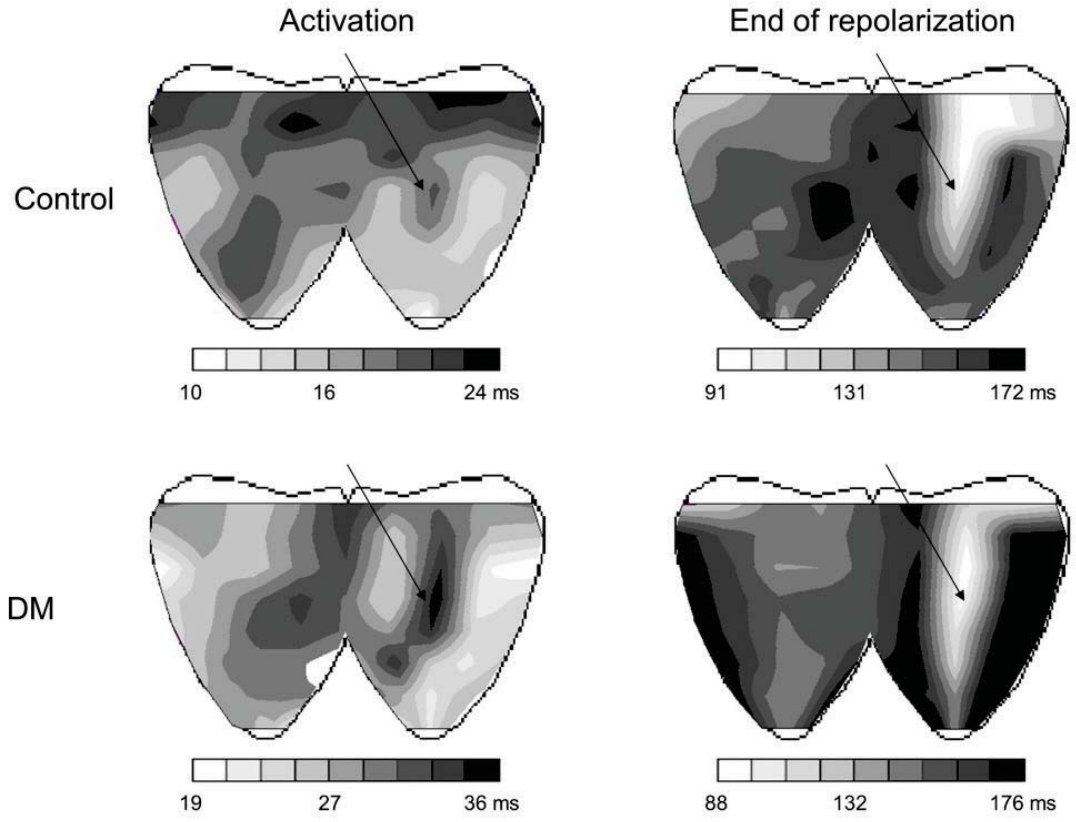

Fig. 4. Representative isochronal maps of activation and end of repolarization times in the control and diabetic animals at 20 min of coronary occlusion that produced the regional ischemia (arrows). Numbers on the scales indicate the time elapsed from the QRS onset. The left, and right sides of each map correspond to the anterior and posterior surfaces of the ventricles, respectively. The greater contrast and "denser" isochrones at the margins of ischemic area demonstrates the greater effects ischemia produced in the diabetic animals. DM, diabetes mellitus.

Discussion

The prolonged QTc found in the diabetic rabbits is consistent with our previous observations (Vaykshnorayte *et al.* 2012, Ovechkin *et al.* 2015) and data obtained in other animal species (Howarth *et al.* 2011) or humans (Žákovičová *et al.* 2014). This suggested that the average ventricular repolarization duration prolonged, presumably due to the downregulation of potassium repolarizing currents (Magyar *et al.* 1992, Zhang *et al.* 2007, Lengyel *et al.* 2008, Gallego *et al.* 2009). The observed interventricular RT difference implied that the action potential duration lengthening should be heterogeneous in ventricular myocardium and be predominantly expressed in the RV at least at 1-month follow-up from the DM induction. Likewise, the shortening of QT and QTc during the ischemic exposure was consistent with the repolarization duration shortening in the DM group.

During ischemia, ATs and ARIs did not change significantly in the control group, and the marked interindividual variations in the ischemia-induced ARI response were observed. It is noteworthy that several control animals demonstrated the prolongation of ARIs. Verkerk *et al.* (1996) showed that more than a half of rabbit cardiomyocytes demonstrated phasic prolongation of action potential duration in ischemic conditions due to I_{to} inhibition. This initial prolongation was followed by the shortening of repolarization presumably due to the increase of $I_{K(ATP)}$. The similar reaction was observed in human cells, which makes these observations clinically relevant. The above considerations could explain the varied ARI response to ischemia observed in the control group. As a result, the slight changes in activation and the variable alterations of repolarization caused the RT dispersion in the controls to be statistically unchanged. Therefore, the difference between diabetics and nondiabetics in the repolarization response to ischemia was possibly caused by the different relationships between I_{to}-dependent prolongation and $I_{K(ATP)}$-dependent shortening. This concept remains to be further evaluated.

On the other hand, the diabetics demonstrated a significant though small AT delay in the ischemic zone. This effect was not expressed in the QRS prolongation but could reflect the local changes of the depolarization process, for example, the reduced I_{Na} in the diabetic rabbit myocardium (Stables *et al.* 2014). In contrast to the control group, repolarization durations significantly shortened in the ischemic zone that was associated with the shortening of QT and QTc intervals on the body surface ECG. The difference between the controls and diabetics in the reaction of the repolarization duration to ischemia could be due to the down-regulation of I_{to} current in the diabetic animals (Gallego *et al.* 2009). The inhibition of this current was shown to be responsible for the transient action potential duration prolongation in ischemia (Verkerk *et al.* 1996). Accordingly, such an effect was not observed in the DM group. The effects of ATs and ARIs oppositely influenced the local RTs thus reducing their change. As the magnitude in milliseconds of the ARI decrease was greater than the AT increase, the boundary RT heterogeneities developed in the diabetic myocardium at ischemia.

Since the diabetic rabbits differed from the normals in their electrophysiological response to ischemia, the abovementioned alterations of ventricular repolarization were likely to be differently expressed in the ECG indices in the control and DM groups. Theoretically, a correlation between the global RT dispersion and the T_{peak}-T_{end} interval duration could be expected (Arteyeva *et al.* 2013) and such a correlation was indeed found, but only in diabetics during the ischemic exposure. This observation at least in part could be explained by the fact that the global RT dispersion in the ischemic diabetic myocardium was significantly correlated with the newly developed boundary RT gradient absent in the control group and the DM group before exposure. Our further observation of the correlation between the T_{peak}-T_{end} interval duration and the boundary RT gradient in diabetics under ischemia supports the above explanation. Furthermore, it suggests that the measurements of the T_{peak}-T_{end} interval could be more effective in the assessment of the local ischemic electrical heterogeneities in a subset of patients with DM as compared to the nondiabetics.

Limitations

The limitations of the present study concerned at least the short follow-up of DM and the short ischemia exposure. It is not excluded that the longer ones could lead to the more pronounced electrophysiological effects and possibly the spontaneous arrhythmia incidence. Repolarization parameters are often reported to be subject to sex differences. In the present study, we could not specify the effects in males and females. However, the diabetic and control groups did not differ significantly from each other in the male-to-female ratio, and therefore we believe that the observed results could not be

attributed to gender effects. Anesthesia could have affected the myocardial electrophysiological properties; however, we believe that these effects should be similar in controls and diabetics and should not significantly modify the major findings of the study.

Conclusion

Thus, the more pronounced ischemia-related prolongation of activation and shortening of repolarization in diabetic animals presumably due to the I_{Na} and I_{to}-down-regulation in DM led to the increase of local electrical inhomogeneities that in turn could be assessed by the T_{peak}-T_{end} interval. The findings of the present study suggest that the T_{peak}-T_{end} interval can be of different diagnostic utility in different pathological conditions.

Conflict of Interest

There is no conflict of interest.

Acknowledgements

The study was supported by the Ural Branch of the Russian Academy of Sciences (Project 13-4-032-KSC) and the Russian Foundation for Basic Research (Grant 14-04-31070, young_a).

References

ARTEYEVA NV, GOSHKA SL, SEDOVA KA, BERNIKOVA OG, AZAROV JE: What does the T(peak)-T(end) interval reflect? An experimental and model study. *J Electrocardiol* **46**: 296.e1-8, 2013.

BAKTH S, ARENA J, LEE W, TORRES R, HAIDER B, PATEL BC, LYONS MM, REGAN TJ: Arrhythmia susceptibility and myocardial composition in diabetes. Influence of physical conditioning. *J Clin Invest* **77**: 382-395, 1986.

CARLSSON L, ABRAHAMSSON C, ANDERSSON B, DUKER G, SCHILLER-LINHARDT G: Proarrhythmic effects of the class III agent almokalant: importance of infusion rate, QT dispersion, and early afterdepolarizations. *Cardiovasc Res* **27**: 2186-2193, 1993.

CHO E, RIMM EB, STAMPFER MJ, WILLETT WC, HU FB: The impact of diabetes mellitus and prior myocardial infarction on mortality from all causes and from coronary heart disease in men. *J Am Coll Cardiol* **40**: 954-960, 2002.

CHOW E, BERNJAK A, WILLIAMS S, FAWDRY RA, HIBBERT S, FREEMAN J, SHERIDAN PJ, HELLER SR: Risk of cardiac arrhythmias during hypoglycemia in patients with type 2 diabetes and cardiovascular risk. *Diabetes* **63**: 1738-1747, 2014.

CLEMENTE D, PEREIRA T, RIBEIRO S: Ventricular repolarization in diabetic patients: characterization and clinical implications. *Arq Bras Cardiol* **99**: 1015-1022, 2012.

CORONEL R, DE BAKKER JM, WILMS-SCHOPMAN FJ, OPTHOF T, LINNENBANK AC, BELTERMAN CN, JANSE MJ: Monophasic action potentials and activation recovery intervals as measures of ventricular action potential duration: experimental evidence to resolve some controversies. *Heart Rhythm* **3**: 1043-1050, 2006.

CURIONE M, DI BONA S, AMATO S, TURINESE I, TARQUINI G, GATTI A, MANDOSI E, ROSSETTI M, VARRENTI M, SALVATORE S, BAIOCCO E, MORANO S: Lack of the QTc physiologic decrease during cardiac stress test in patients with type 2 diabetes treated with secretagogues. *Acta Diabetol* **51**: 31-33, 2014.

DZIEWIERZ A, GISZTEROWICZ D, SIUDAK Z, RAKOWSKI T, DUBIEL JS, DUDEK D: Admission glucose level and in-hospital outcomes in diabetic and non-diabetic patients with acute myocardial infarction. *Clin Res Cardiol* **99**: 715-721, 2010.

GALAGUDZA MM, NEKRASOVA MK, SYRENSKII AV, NIFONTOV EM: Resistance of the myocardium to ischemia and the efficacy of ischemic preconditioning in experimental diabetes mellitus. *Neurosci Behav Physiol* **37**: 489-493, 2007.

GALLEGO M, ALDAY A, URRUTIA J, CASIS O: Transient outward potassium channel regulation in healthy and diabetic hearts. *Can J Physiol Pharmacol* **87**: 77-83, 2009.

HEKIMIAN G, KHANDORIDI N, FEUVRAY D, BEIGELMAN PM: Abnormal cardiac rhythm in diabetic rats. *Life Sci* **37**: 547-551, 1985.

HETLAND M, HAUGAA KH, SARVARI SI, ERIKSSEN G, KONGSGAARD E, EDVARDSEN T: A novel ECG-index for prediction of ventricular arrhythmias in patients after myocardial infarction. *Ann Noninvasive Electrocardiol* **19**: 330-337, 2014.

HOWARTH FC, JACOBSON M, SHAFIULLAH M, LJUBISAVLJEVIC M, ADEGHATE E: Heart rate, body temperature and physical activity are variously affected during insulin treatment in alloxan-induced type 1 diabetic rat. *Physiol Res* **60**: 65-73, 2011.

KUSAMA Y, HEARSE DJ, AVKIRAN M: Diabetes and susceptibility to reperfusion-induced ventricular arrhythmias. *J Mol Cell Cardiol* **24**: 411-421, 1992.

LENGYEL C, VIRÁG L, KOVÁCS PP, KRISTÓF A, PACHER P, KOCSIS E, KOLTAY ZM, NÁNÁSI PP, TÓTH M, KECSKEMÉTI V, PAPP JG, VARRÓ A, JOST N: Role of slow delayed rectifier K^+-current in QT prolongation in the alloxan-induced diabetic rabbit heart. *Acta Physiol (Oxf)* **192**: 359-368, 2008.

MAGYAR J, RUSZNÁK Z, SZENTESI P, SZÛCS G, KOVÁCS L: Action potentials and potassium currents in rat ventricular muscle during experimental diabetes. *J Mol Cell Cardiol* **24**: 841-853, 1992.

MATEJÍKOVÁ J, KUCHARSKÁ J, PANCZA D, RAVINGEROVÁ T: The effect of antioxidant treatment and NOS inhibition on the incidence of ischemia-induced arrhythmias in the diabetic rat heart. *Physiol Res* **57** (Suppl 2): S55-S60, 2008.

MIKI T, TOBISAWA T, SATO T, TANNO M, YANO T, AKASAKA H, KUNO A, OGASAWARA M, MURASE H, SAITOH S, MIURA T: Does glycemic control reverse dispersion of ventricular repolarization in type 2 diabetes? *Cardiovasc Diabetol* **13**: 125, 2014.

MOZOS I: Arrhythmia risk in liver cirrhosis. *World J Hepatol* **7**: 662-672, 2015.

OVECHKIN AO, VAYKSHNORAYTE MA, SEDOVA K, SHUMIKHIN KV, ARTEYEVA NV, AZAROV JE: Functional role of myocardial electrical remodeling in diabetic rabbits. *Can J Physiol Pharmacol* **93**: 245-252, 2015.

PANIKKATH R, REINIER K, UY-EVANADO A, TEODORESCU C, HATTENHAUER J, MARIANI R, GUNSON K, JUI J, CHUGH SS: Prolonged Tpeak-to-Tend interval on the resting ECG is associated with increased risk of sudden cardiac death. *Circ Arrhythm Electrophysiol* **4**: 441-447, 2011.

PISTROSCH F, GANZ X, BORNSTEIN SR, BIRKENFELD AL, HENKEL E, HANEFELD M: Risk of and risk factors for hypoglycemia and associated arrhythmias in patients with type 2 diabetes and cardiovascular disease: a cohort study under real-world conditions. *Acta Diabetol* **52**: 889-895, 2015.

PORTHAN K, VIITASALO M, TOIVONEN L, HAVULINNA AS, JULA A, TIKKANEN JT, VÄÄNÄNEN H, NIEMINEN MS, HUIKURI HV, NEWTON-CHEH C, SALOMAA V, OIKARINEN L: Predictive value of electrocardiographic T-wave morphology parameters and T-wave peak to T-wave end interval for sudden cardiac death in the general population. *Circ Arrhythm Electrophysiol* **6**: 690-696, 2013.

RAVINGEROVÁ T, STETKA R, PANCZA D, ULICNÁ O, ZIEGELHÖFFER A, STYK J: Susceptibility to ischemia-induced arrhythmias and the effect of preconditioning in the diabetic rat heart. *Physiol Res* **49**: 607-616, 2000.

SANJUAN R, BLASCO ML, MARTINEZ-MAICAS H, CARBONELL N, MIÑANA G, NUÑEZ J, BODÍ V, SANCHIS J: Acute myocardial infarction: high risk ventricular tachyarrhythmias and admission glucose level in patients with and without diabetes mellitus. *Curr Diabetes Rev* **7**: 126-134, 2011.

SMETANA P, SCHMIDT A, ZABEL M, HNATKOVA K, FRANZ M, HUBER K, MALIK M: Assessment of repolarization heterogeneity for prediction of mortality in cardiovascular disease: peak to the end of the T wave interval and nondipolar repolarization components. *J Electrocardiol* **44**: 301-308, 2011.

SPOONER PM: Sudden cardiac death: influence of diabetes. *Diabetes Obes Metab* **10**: 523-532, 2008.

STABLES CL, MUSA H, MITRA A, BHUSHAL S, DEO M, GUERRERO-SERNA G, MIRONOV S, ZARZOSO M, VIKSTROM KL, CAWTHORN W, PANDIT SV: Reduced Na^+ current density underlies impaired propagation in the diabetic rabbit ventricle. *J Mol Cell Cardiol* **69**: 24-31, 2014.

VAYKSHNORAYTE MA, OVECHKIN AO, AZAROV JE: The effect of diabetes mellitus on the ventricular epicardial activation and repolarization in mice. *Physiol Res* **61**: 363-370, 2012.

VERKERK AO, VELDKAMP MW, VAN GINNEKEN AC, BOUMAN LN: Biphasic response of action potential duration to metabolic inhibition in rabbit and human ventricular myocytes: role of transient outward current and ATP-regulated potassium current. *J Mol Cell Cardiol* **28**: 2443-2456, 1996.

WANG Y, XUAN YL, HU HS, LI XL, XUE M, CHENG WJ, SUO F, YAN SH: Risk of ventricular arrhythmias after myocardial infarction with diabetes associated with sympathetic neural remodeling in rabbits. *Cardiology* **121**: 1-9, 2012.

ZHANG Y, XIAO J, LIN H, LUO X, WANG H, BAI Y, WANG J, ZHANG H, YANG B, WANG Z: Ionic mechanisms underlying abnormal QT prolongation and the associated arrhythmias in diabetic rabbits: a role of rapid delayed rectifier K^+ current. *Cell Physiol Biochem* **19**: 225-238, 2007.

ŽÁKOVIČOVÁ E, KITTNAR O, SLAVÍČEK J, MEDOVÁ E, ŠVÁB P, CHARVÁT J: ECG body surface mapping in patients with gestational diabetes mellitus and optimal metabolic compensation. *Physiol Res* **63** (Suppl 4): S479-S487, 2014.

Appendix B: *Sedova KA, Azarov JE, Arteyeva NV, Ovechkin AO, Vaykshnorayte MA, Vityazev VA, Bernikova OG, Shmakov DN, Kneppo P. Mechanism of electrocardiographic T wave flattening in diabetes mellitus: experimental and simulation study. Physiol Res 2017. 66(5): 781-789. JCR IF 2016 - 1.461*

Physiol. Res. 66: 781-789, 2017

Mechanism of Electrocardiographic T-Wave Flattening in Diabetes Mellitus: Experimental and Simulation Study

K. A. SEDOVA[1,2], J. E. AZAROV[2,3], N. V. ARTEYEVA[2], A. O. OVECHKIN[2,5], M. A. VAYKSHNORAYTE[2], V. A. VITYAZEV[2,4], O. G. BERNIKOVA[2,5], D. N. SHMAKOV[2], P. KNEPPO[1]

[1]Department of Biomedical Technology, Faculty of Biomedical Engineering, Czech Technical University in Prague, Kladno, Czech Republic, [2]Laboratory of Cardiac Physiology, Institute of Physiology, Komi Science Center, Ural Branch, Russian Academy of Sciences, Syktyvkar, Russia, [3]Department of Cardiology, Lund University, Lund, Sweden, [4]Department of Physiology, Medical Institute of Pitirim Sorokin Syktyvkar State University, Syktyvkar, Russia, [5]Department of Internal Diseases, Medical Institute of Pitirim Sorokin, Syktyvkar State University, Syktyvkar, Russia

Received September 26, 2016
Accepted March 31, 2017
On-line July 18, 2017

Summary

In the present study we investigated the contribution of ventricular repolarization time (RT) dispersion (the maximal difference in RT) and RT gradients (the differences in RT in apicobasal, anteroposterior and interventricular directions) to T-wave flattening in a setting of experimental diabetes mellitus. In 9 healthy and 11 diabetic (alloxan model) open-chest rabbits, we measured RT in ventricular epicardial electrograms. To specify the contributions of apicobasal, interventricular and anteroposterior RT gradients and RT dispersion to the body surface potentials we determined T-wave voltage differences between modified upper- and lower-chest precordial leads (T-wave amplitude dispersions, TWAD). Expression of RT gradients and RT dispersion in the correspondent TWAD parameters was studied by computer simulations. Diabetic rabbits demonstrated flattened T-waves in precordial leads associated with increased anteroposterior and decreased apicobasal RT gradients ($P<0.05$) due to RT prolongation at the apex. For diabetics, simulations predicted the preserved T-vector length and altered sagittal and longitudinal TWAD proven by experimental measurements. T-wave flattening in the diabetic rabbits was not due to changes in RT dispersion, but reflected the redistributed ventricular repolarization pattern with prolonged apical repolarization resulting in increased anteroposterior and decreased apicobasal RT gradients.

Key words

Diabetes • Dispersion of repolarization • Repolarization gradients • T-vector • T-wave

Corresponding author

K. A. Sedova, Department of Biomedical Technology, Faculty of Biomedical Engineering, Czech Technical University in Prague, Sítná sq. 3105, 272 01 Kladno, Czech Republic. E-mail: ksenia.sedova@fbmi.cvut.cz

Introduction

Diabetes mellitus (DM) is a recognized public health burden, characterized, among other complications, by increased risk of life-threatening ventricular arrhythmias and sudden cardiac death (Spooner 2008). An underlying functional arrhythmic substrate requires the presence of several conditions, including an increased dispersion of repolarization (DOR) defined as a maximal difference between repolarization times (RT) irrespective of lead sites within the ventricular myocardium. Relationship between RT differences and T-wave generation on the body surface ECG provides a rationale for using electrocardiographic T-wave indices to estimate heterogeneities of repolarization as well as arrhythmia susceptibility.

Diabetic patients demonstrate changes in both QT interval duration and T-wave amplitude (Kittnar 2016). However, the electrophysiological basis for these alterations is not fully established. The mechanism of prolongation of rate-corrected QT intervals is relatively clear and is attributed to lengthening of action potential durations (Magyar *et al.* 1992). However, the mechanism of T-wave voltage changes in DM has not been directly studied. As T-wave genesis is usually attributed to ventricular repolarization gradients (RT differences on definite axes, such as apicobasal, interventricular, anteroposterior and transmural) (Meijborg *et al.* 2014), it is reasonable to suggest that flattening of the T-wave in diabetics results from RT redistribution within heart ventricles. However, such repolarization pattern could correspond to two conditions: either 1) DOR decreases but the proportion between RT gradients is the same; or 2) a predominant repolarization gradient changes but the DOR magnitude preserves. Distinguishing between these two alternatives is important, as the former is expected to affect the reentrant arrhythmogenesis, while the latter could reflect involvement of specific myocardial regions. Therefore, elaborating on how the different ventricular repolarization gradients and DOR contribute to the DM-related T-wave changes is needed for a comprehensive ECG interpretation.

T-wave amplitude parameters have been studied less extensively than temporal markers; however, evaluating T-wave amplitude could be a promising approach for assessing repolarization heterogeneity. Our previous study (Sedova *et al.* 2015) demonstrated that DOR changes were associated with T-wave amplitude dispersion (TWAD), defined as the difference in the T-wave peak voltages between upper- and lower-chest precordial leads. However, a concept of T-wave generation in a given condition is required for clearly interpretating its amplitude changes.

An objective of the present study was to determine the contribution of apicobasal, interventricular and anteroposterior repolarization gradients and DOR to body surface T-wave parameters in an experimental rabbit DM model. Previous investigations (Arteyeva *et al.* 2013, Meijborg *et al.* 2014, Arteyeva *et al.* 2015) suggested that transmural gradient contribution to generating T-waves was much less pronounced, if at all present, as compared to the contribution of other gradients. Therefore, here we did not address the transmural gradient, instead focusing studying the epicardial repolarization pattern.

Methods

Overview

We (i) experimentally recorded cardiac potentials on body and epicardial surfaces in control and diabetic rabbits; (ii) described differences between the two groups in apicobasal, interventricular and anteroposterior RT gradients; (iii) constructed x-, y-, and z- components of T-vector for the diabetics and controls on the basis of experimentally-measured RT gradients; (iv) simulated body surface potential distributions using these constructed T-vector components; (v) compared computed and measured body surface potentials in both groups; (vi) compared T-vector components derived from *measured* body surface potentials between control and diabetic groups; and (vii) tested if a relationship between these measured T-vector components is similar to the relationship between experimentally-determined RT gradients.

Experimental study

The experiments were performed on Chinchilla breed rabbits of either sex, age of 6-8 months and body mass of 2.5-4.0 kg. The procedures conformed to the *Guide for the Care and Use of Laboratory Animals, 8th Edition* published by the National Academies Press (US) 2011 and to the *Declaration of Helsinki* and were approved by the ethical committee of the Institute of Physiology of the Komi Science Centre, Ural Branch of the Russian Academy of Sciences. Type 1 DM was induced in 11 animals (7 males) by a single dose of alloxan (120 mg/kg body weight, i.v.) and 9 (6 males) animals served as controls.

After one month, DM and control rabbits were anesthetized with Zoletil (15 mg/kg body weight, i.m.) and put on mechanical ventilation. ECGs were recorded with subcutaneous needle electrodes from conventional limb leads and six modified precordial leads described elsewhere (Sedova *et al.* 2015). In short, there were three upper-chest leads (J1-J3) shifted to the jugular notch level, and three lower-chest leads (J4-J6) positioned at the inferior costal margin level. J1 and J6 leads and J3 and J4 leads were placed in the right and left anterior axillary lines, respectively; while J2 and J5 leads were in the midline. After ECG recording, the heart was exposed *via* midline incision, and heart temperature was maintained at 37-38 °C by irrigation with warm saline and warmed indoor air. At spontaneous sinus rhythm, unipolar ventricular electrograms were registered from a 64-lead

epicardial sock array (3-5 mm interelectrode distance) in reference to Wilson's central terminal with a custom-designed mapping system (16 bits; bandwidth 0.05 to 1,000 Hz; sampling rate 4,000 Hz).

In each epicardial unipolar electrogram, activation time (AT) and repolarization time (RT) were measured as the instants of the minimum of first time derivative of potential (dV/dt min) during QRS complex and the maximum of the first time derivative of potential (dV/dt max) during T-wave, respectively, in relation to QRS complex onset in the II limb lead (Coronel *et al.* 2006). The activation-recovery interval (ARI) serving as a measure of local repolarization duration was taken as the difference between RT and AT. Apicobasal, interventricular and anteroposterior RT gradients were calculated using average RT values in the appropriate epicardial leads (for example, apicobasal RT gradient equaled to the difference between the average basal RT and the average apical RT, etc, is in Fig. 1). Total DOR was determined as the difference between maximal and minimal RT values on the ventricular epicardium (Fig. 1). T-wave amplitude dispersion (TWAD) parameters were measured as the difference between T-wave voltages in body surface ECG leads (J1-J6) using formulas suggested for calculating T-vector components (see below).

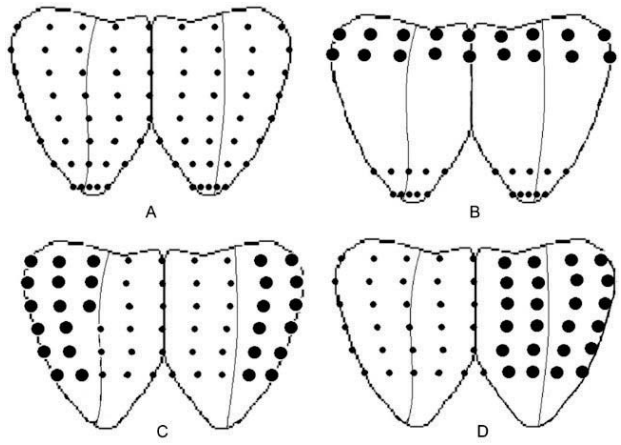

Fig. 1. Schematic presentation of determining epicardial repolarization parameters. Each map displays anterior (left part) and posterior (right part) aspects of the heart. The margins between left and right ventricles (anterior and posterior interventricular grooves) are depicted by thin solid lines. (**A**) Lead distribution on epicardial surface. Dispersion of repolarization is calculated as the difference between the earliest and the latest repolarization times on the overall surface. Apicobasal (**B**), interventricular (**C**) and anteroposterior (**D**) repolarization gradients are determined as differences between the average RT values obtained from areas designated by small and large lead points.

Statistical analysis was performed using SPSS 11.5. Data are given as medians and interquartile intervals. The Mann-Whitney U-test was used to compare control and diabetic groups of animals. Student's paired and unpaired t-tests were used to assess intra- and inter-observer variabilities, and agreement between measurements was evaluated with the Bland-Altman plot. Differences were considered significant at $P<0.05$.

T-vector components

Direct determination. In order to relate ventricular repolarization gradients to body surface ECG, we simulated the electrical vector of ventricular repolarization (T-vector) as a single dipole located in the center of the heart ventricles. T-vector direction was based on experimentally measured ventricular repolarization gradients: the component Tx was proportional to the interventricular gradient, the component Ty was proportional to the apicobasal gradient, and the component Tz was proportional to the anteroposterior gradient (in vectorcardiographic coordinate system X, Y, Z). A potential distribution produced by this T-vector was calculated for an elliptical cylinder imitating the torso of a rabbit, taking into account the heart's realistic position within the rabbit torso, using the following formula:

$$\varphi = (R \cdot T) / R^3 \qquad (1),$$

where φ is a potential value in an observation point, T is T-vector, R is a vector directed from the observation point to the T-vector origin, R is the length of R. The computed potentials were compared with measured body surface ECGs.

Inverse determination. T-vector components were then also inversely calculated from body surface potentials. Since there is no generally accepted method of calculating VCG from ECG for the rabbit, we used the following empirical formulas based on differences in potential magnitude in modified precordial leads J1-J6 taking into account their mutual positions on the torso.

$$\text{Longitudinal:} \quad Ty = ((J6\text{-}J1) + (J4\text{-}J3)) / 2 \qquad (2),$$

$$\text{Left-to-Right:} \quad Tx = ((J3\text{-}J1) + (J4\text{-}J6)) / 2 \qquad (3),$$

$$\text{Sagittal:} \quad Tz = 10 \times ((J2\text{-}J1) + (J2\text{-}J3) + (J5\text{-}J4) + 2 \times (J5\text{-}J6)) / 4 \qquad (4).$$

Results

Fasting plasma glucose concentration was significantly higher in the diabetic animals than in

controls [26.6 (17.8; 27.5) mmol/l and 5.7 (4.9; 6.0) mmol/l, P<0.05, respectively], although both groups were of the same sex, age, body mass and heart mass.

Body surface ECGs

The diabetic rabbits demonstrated flattened T-waves in modified upper-chest and lower-chest precordial leads (Fig. 2). T-wave amplitudes in individual precordial leads were lower in the DM group than in the control group (Table 1). Longitudinal, left-to-right and sagittal TWAD indices calculated using formulas (2-4) (suggested for the corresponding T-vector components) differed between the control group and the DM group. The diabetic rabbits had greater $TWAD_{sagittal}$ and lower $TWAD_{longitudinal}$ than controls (Table 1).

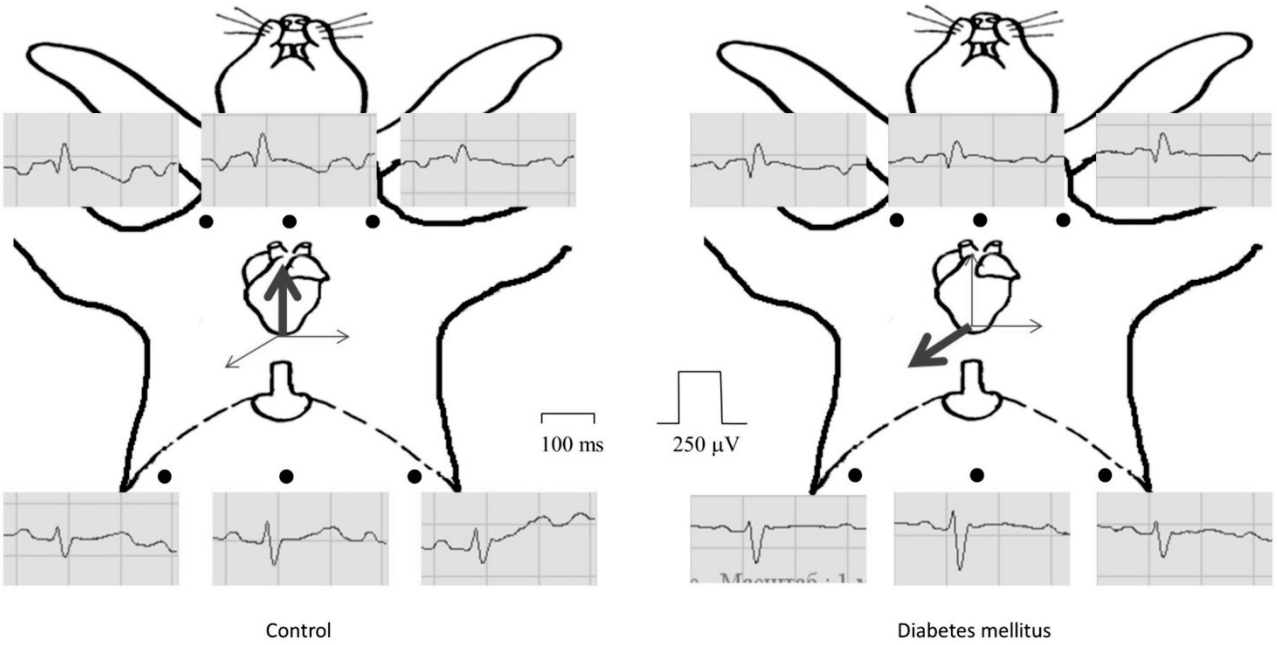

Fig. 2. Representative ECG tracings in modified precordial leads J1-J6 (solid black points) in control and diabetic rabbits. The heart position is indicated by thick arrows depicting predominant apicobasal and anteroposterior RT gradients for non-diabetic and diabetic animals, respectively.

Table 1. Cardiac and body surface ECG indices of ventricular repolarization in healthy and diabetic rabbits [Median and interquartile intervals (25 %, 75 %)].

Parameter	Control, n=9	DM, n=11	P
Apicobasal RT gradient (ms)	17 (10; 18)	2 (-7; 4)	**0.002**
Interventricular RT gradient (ms)	-6 (-12; 0.2)	7 (-0.3; 10)	0.087
Anteroposterior RT gradient (ms)	-7 (-12; 9)	11 (6; 17)	**0.016**
DOR (ms)	51 (43; 57)	56 (41; 75)	0.351
Maximal lower-chest T-wave voltage (μV)	162 (144; 226)	119 (0; 143)	**0.020**
Minimal upper-chest T-wave voltage (μV)	-242 (-266; -212)	-170 (-218; -121)	0.052
$TWAD_{Longitudinal}$ *(μV)*	197 (120; 236)	105 (88; 158)	**0.023**
$TWAD_{Left\text{-}to\text{-}Right}$ *(μV)*	64 (53; 84)	45 (18; 66)	0.119
$TWAD_{Sagittal}$ *(μV)*	58 (-144; 355)	-210 (-303; -95)	**0.045**
$TWAD_{Sum}$ *(μV)*	338 (234; 471)	282 (178; 428)	0.340

DM – diabetes mellitus; RT – repolarization time; DOR – dispersion of repolarization; TWAD – T-wave amplitude dispersion.

Epicardial potential mapping

AT measurements were done automatically, while determining RTs included inspection by experienced observers (AOO, MAV). Therefore, the data were tested for inter- and intraobserver reproducibility. Sample measurements (n=83) done by the same observer on different days demonstrated no significant differences in RT interval (values are given for the combined group of healthy and diabetic animals): 186.6±32.1 vs. 185.42±32.9 ms, p=0.91 and S.D. of the difference was 18.6 ms or 9.9 % of the mean. The difference between the first and the second observer's data was also insignificant: 186.1±38.8 vs. 187.0±40.6 ms, p=0.44 and S.D. of the difference 10.8 ms or 5.8 % of the mean.

At one-month follow-up, rabbits with DM and controls had similar sequences and durations of ventricular epicardial activation, but the epicardial repolarization pattern differed between the two groups (Fig. 3). In control animals, repolarization durations (measured as ARIs) were shorter at the apex and longer at the base manifesting in a dominant apicobasal RT gradient in respect to interventricular and anteroposterior gradients (Table 1). In diabetic animals, repolarization durations were redistributed with an area of prolonged ARIs development mainly on the anterior apical portion (mainly, the heart apex and the adjacent right ventricular area). This effect resulted in a pattern with decreased apicobasal and increased anteroposterior RT gradients in the diabetic hearts (Table 1). Despite the differences in ventricular repolarization gradients, there was no difference in total DOR between the control and DM groups.

Computer simulations

We simulated body surface potential distributions for both non-diabetic and diabetic rabbits (Fig. 4) according to experimentally-measured epicardial RT gradients. For the control rabbit, the T-vector was oriented forward, downward and to the left, with a dominant longitudinal component. For the diabetic rabbit, T-vector was oriented backward, downward and to the left, the longitudinal component was decreased, and the anteroposterior component was dominant. T-vector length was the same because total RT dispersion in DM was found to be close to that of non-diabetic rabbits.

The different T-vector directions in non-diabetic and diabetic animal models resulted in different simulated body surface potential distributions (Fig. 4). In the points corresponding to leads J1-J6, potential magnitudes decreased, but their polarity remained unchanged. These changes were similar to the changes observed in leads J1-J6 in diabetic rabbits (Fig. 2). T-vector directions calculated from the differences in measured potential magnitude in leads J1-J6 were similar to T-vector directions set in the model on the basis of measured RT gradients (Fig. 4).

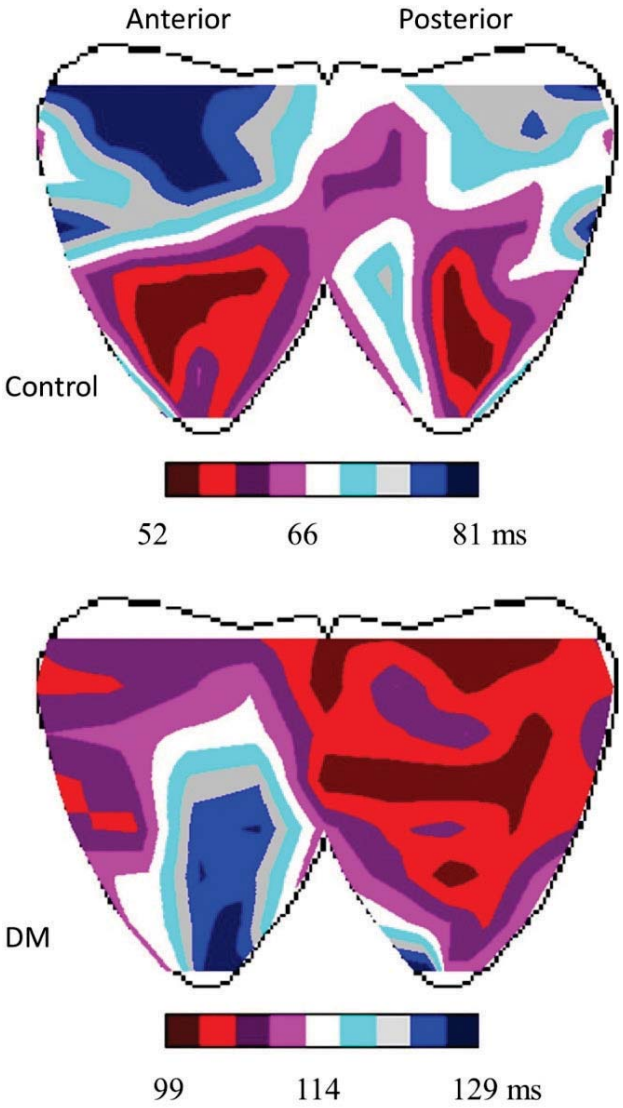

Fig. 3. Representative maps of epicardial ventricular distribution of ARIs in control and diabetic (DM) rabbits. See the prolonged repolarization area on the anterior apical portion in the diabetic rabbit heart.

Discussion

In order to explain the T-wave changes in DM, we first studied the spatial patterns of ventricular repolarization, and then reconstructed the expression of

these cardiac repolarization patterns in body surface potentials using computer simulations. Finally, we tested the predictions of simulations by comparing measured body surface potential distributions in non-diabetic and diabetic animals.

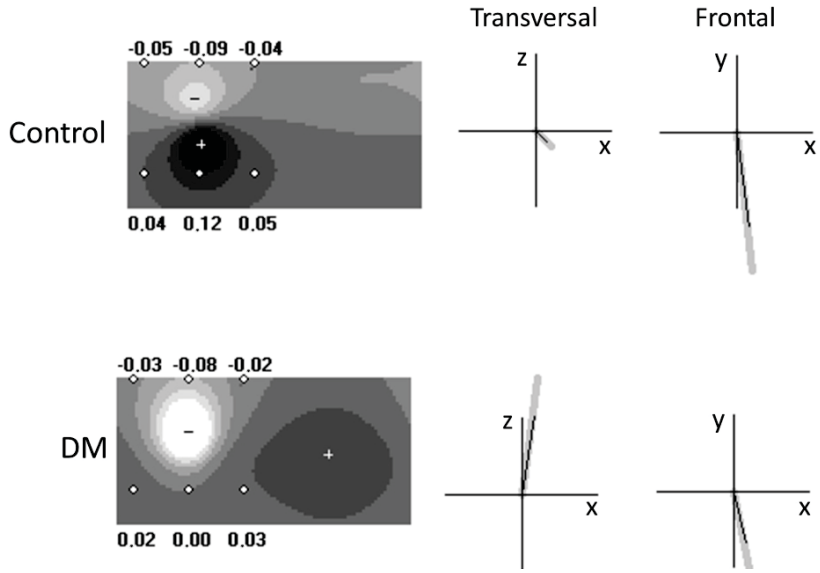

Fig. 4. Simulated body surface potential maps during T-wave peak for the control and diabetic rabbits. Simulated voltages in J1-J6 leads are shown. The transversal and frontal projections of the T-vectors set directly (bold gray) and calculated from the TWAD (black) are displayed to the right of each map.

Our primary objective was to find out the DM-related T-wave flattening mechanisms as they relate to changing ventricular gradients of repolarization. We found that the decrease in T-wave amplitudes in modified precordial leads was associated with altering two repolarization gradients, namely: 1) increase in the anteroposterior gradient with early posterior and late anterior RTs, and 2) decrease in the apicobasal gradient. These two differences between non-diabetic and diabetic rabbits were accounted for by repolarization duration prolongation at the RV apex, located mostly anteriorly. The specific involvement of RV in diabetic cardiomyopathy was reported earlier (Karamitsos *et al.* 2007, van den Brom *et al.* 2010, Vaykshnorayte *et al.* 2012, Olsen *et al.* 2013, Axelsen *et al.* 2015). Our study suggests that T-wave flattening was the electrocardiographic expression of the RV electrophysiological alteration, at least in the present DM model. The repolarization prolongation in DM is usually ascribed to the down-regulation of potassium currents (Zhang *et al.* 2007, Lengyel *et al.* 2008, Gallego *et al.* 2009); however, the exact mechanism of such spatially specific electrophysiological effect is largely unknown. Previous studies (Palova *et al.* 2010, Ovechkin *et al.* 2014) showed that an abnormal sympathetic tone possibly plays a role.

Thus, a redistributed spatiotemporal ventricular repolarization pattern in diabetic rabbits was associated with flattened body surface T-waves. Theoretically, the observed changes in body surface T-wave voltages associated with DM could be ascribed to three different myocardial alterations, namely: 1) decrease of the apicobasal RT gradient; 2) increase of the anteroposterior RT gradient; and 3) replacement of the apicobasal RT gradient by the anteroposterior RT gradient as a dominant RT gradient. In the context of arrhythmogenesis, it is important to note that these scenarios implied decreased, increased or unchanged DOR, respectively. Thus, further specification of the contribution of the different repolarization gradients to body surface potentials is required. As the next step of the present study, we performed computer simulations in order to test if T-wave voltage parameters could distinguish between the different variants of ventricular repolarization changes in DM.

Despite the *de facto* disappearance of vectorcardiography from routine clinical practice, vectorial characteristics of the repolarization cardiac electric field derived from ECG records are considered useful for diagnosis and prognosis (Man *et al.* 2015). Such indices could be obtained by reconstructing a vectorcardiogram from ECGs (Schreurs *et al.* 2010, Engels *et al.* 2015). The resultant T-vector is a characteristic related to the vectorcardiographic loop, and is considered to be a simple and useful representation of the ventricular repolarization process (Waks *et al.* 2015, Cortez *et al.* 2016), where its direction reflects the

gross repolarization sequence, its length (magnitude) is proportional to the resultant intensity of electric generators in the heart ventricles (indirectly total DOR), and its apicobasal, interventricular and anteroposterior components are related to the apicobasal, interventricular and anteroposterior RT gradients, respectively. The modified precordial leads J1-J6 were positioned on the body surface so that the heart was the center of symmetry, which allowed us to easily obtain the relationship between the apicobasal and interventricular T-vector components and the correspondent longitudinal and left-to-right TWAD indices. Since the heart is located within the thorax anteriorly, and the distance between the medial and lateral leads on the sagittal projection axis is small, scaling coefficients were required for estimating the sagittal T-vector component.

As the diabetic rabbits had the redistributed ventricular repolarization pattern with the increased anteroposterior and decreased apicobasal RT gradients, and, consequently altered T-vector components, we were able to test our approach to estimating the T-vector components. We found that the longitudinal TWAD was lower and the sagittal TWAD was higher in the DM group than in the control group, suggesting that TWADs reflected the RT gradients in the correspondent directions, and could therefore be used for assessing the electrophysiological properties in specific myocardial regions. Our data suggest that T-wave changes in DM rabbits reflected RV involvement. However, our epicardial measurements showed similar total DOR in non-diabetic and diabetic animals; accordingly, the $TWAD_{sum}$, which was suggested as an estimate for T-vector length, and indirectly for total DOR, was no different for the DM and control groups.

Our findings demonstrated that precordial T-wave voltage decrease could be associated with unchanged DOR and oppositely changed different RT gradients. Measuring temporal ECG indices of ventricular repolarization, such as QT and T_{peak}-T_{end} intervals or their dispersions for assessing DOR and predicting arrhythmic events often give unsatisfactory results (Zabel *et al.* 1998, Porthan *et al.* 2013), due at least in part to technical problems with determining T-wave end. In our study, we could not measure QT and T_{peak}-T_{end} intervals in a number of animals because of overlapped P and T-waves. However, T-vector components specifically express the corresponding repolarization gradients, contain useful information on DOR, and may thus be tested as predictors of ventricular arrhythmias.

Limitations

We intended to establish the relationship between diabetic electrical myocardial remodeling and T-wave changes in body surface ECGs quantified as magnitudes of T-vector components to be further used as a noninvasive predictor of functional disturbances. From this point of view, several issues should be taken into account. Where there is attenuation of T-wave signals due to subcutaneous fat, a correction procedure may be required. It is also expected that $TWAD_{sum}$ (T-vector magnitude) may differ somewhat, with DOR remaining unchanged, in settings where action potential durations uniformly prolong or shorten, such as in electrolyte disturbances. We demonstrated that TWAD reflected the magnitude of the RT gradients being the differences in RTs between the definite ventricular regions, such as the apex and the base, etc. However, we did not test local electrophysiological heterogeneities, which may affect the DOR, but perhaps not affect the RT gradients.

Conclusions

Our study suggests that T-wave flattening in modified precordial leads in diabetic rabbits was associated with repolarization prolongation in the apical portion of the RV myocardium, resulting in decreased apicobasal gradient and increased anteroposterior gradient of RTs. These findings provide the basis for assessing RV functional changes in DM. The contribution of apicobasal, interventricular and anteroposterior repolarization gradients could be estimated by calculating the correspondent TWAD parameters. In diabetic rabbits, we found two associations: 1) the augmented anteroposterior RT gradient and the increased sagittal TWAD; 2) the diminished apicobasal RT gradient and the decreased longitudinal TWAD. The obtained results show that T-wave flattening does not necessarily imply changes in DOR, which in turn could be assessed by T-vector length and $TWAD_{sum}$.

Conflict of Interest

There is no conflict of interest.

Acknowledgements

The study was supported by a scholarship awarded to Dr. Azarov by The Swedish Institute's Visby Programme (No. 00073/2015, Sweden) and the RFBR grant (14-04-31070, young a). Funding agencies were not involved in designing, conducting or submitting the study.

References

ARTEYEVA NV, AZAROV JE, VITYAZEV VA, SHMAKOV DN: Action potential duration gradients in the heart ventricles and the cardiac electric field during ventricular repolarization (a model study). *J Electrocardiol* **48**: 678-685, 2015.

ARTEYEVA NV, GOSHKA SL, SEDOVA KA, BERNIKOVA OG, AZAROV JE: What does the T(peak)-T(end) interval reflect? An experimental and model study. *J Electrocardiol* **46**: 296.e1-e8, 2013.

AXELSEN LN, CALLOE K, BRAUNSTEIN TH, RIEMANN M, HOFGAARD JP, LIANG B, JENSEN CF, OLSEN KB, BARTELS ED, BAANDRUP U, ET AL.: Diet-induced pre-diabetes slows cardiac conductance and promotes arrhythmogenesis. *Cardiovasc Diabetol* **14**: 87, 2015.

CORONEL R, DE BAKKER JMT, WILMS-SCHOPMAN FJG, OPTHOF T, LINNENBANK AC, BELTERMAN CN, JANSE MJ: Monophasic action potentials and activation recovery intervals as measures of ventricular action potential duration: experimental evidence to resolve some controversies. *Heart Rhythm* **3**: 1043-1050, 2006.

CORTEZ D, PATEL SS, SHARMA N, LANDECK BF, MCCANTA AC, JONE PN: Repolarization vector magnitude differentiates kawasaki disease from normal children. *Ann Noninvasive Electrocardiol* **21**: 493-499, 2016.

ENGELS EB, ALSHEHRI S, VAN DEURSEN CJM, WECKE L, BERGFELDT L, VERNOOY K, PRINZEN FW: The synthesized vectorcardiogram resembles the measured vectorcardiogram in patients with dyssynchronous heart failure. *J Electrocardiol* **48**: 586-592, 2015.

GALLEGO M, ALDAY A, URRUTIA J, CASIS O: Transient outward potassium channel regulation in healthy and diabetic hearts. *Can J Physiol Pharmacol* **87**: 77-83, 2009.

KARAMITSOS TD, KARVOUNIS HI, DALAMANGA EG, PAPADOPOULOS CE, DIDANGELLOS TP, KARAMITSOS DT, PARHARIDIS GE, LOURIDAS GE: Early diastolic impairment of diabetic heart: The significance of right ventricle. *Int J Cardiol* **114**: 218-223, 2007.

KITTNAR O: Electrocardiographic changes in diabetes mellitus. *Physiol Res* **64** (Suppl 5): S559-S566, 2016.

LENGYEL C, VIRÁG L, KOVÁCS PP, KRISTÓF A, PACHER P, KOCSIS E, KOLTAY ZM, NÁNÁSI PP, TÓTH M, KECSKEMÉTI V, PAPP JG, VARRÓ A, JOST N: Role of slow delayed rectifier K+-current in QT prolongation in the alloxan-induced diabetic rabbit heart. *Acta Physiol (Oxf)* **192**: 359-368, 2008.

MAGYAR J, RUSZNÁK Z, SZENTESI P, SZÛCS G, KOVÁCS L: Action potentials and potassium currents in rat ventricular muscle during experimental diabetes. *J Mol Cell Cardiol* **24**: 841-853, 1992.

MAN S, MAAN AC, SCHALIJ MJ, SWENNE CA: Vectorcardiographic diagnostic & prognostic information derived from the 12-lead electrocardiogram: historical review and clinical perspective. *J Electrocardiol* **48**: 463-475, 2015.

MEIJBORG VM, CONRATH CE, OPTHOF T, BELTERMAN CN, DE BAKKER JM, CORONEL R: Electrocardiographic T wave and its relation with ventricular repolarization along major anatomical axes. *Circ Arrhythm Electrophysiol* **7**: 524-531, 2014.

OLSEN KB, AXELSEN LN, BRAUNSTEIN TH, SORENSEN CM, ANDERSEN CB, PLOUG T, HOLSTEIN-RATHLOU NH, NIELSEN MS: Myocardial impulse propagation is impaired in right ventricular tissue of Zucker diabetic fatty (ZDF) rats. *Cardiovasc Diabetol* **12**: 19, 2013.

OVECHKIN AO, VAYKSHNORAYTE MA, SEDOVA KA, SHMAKOV DN, SHUMIKHIN KV, MEDVEDEVA SY, DANILOVA IG, AZAROV JE: Esmolol abolishes repolarization gradients in diabetic rabbit hearts. *Exp Clin Cardiol* **20**: 3780-3793, 2014.

PALOVÁ S, SZABO K, CHARVÁT J, SLAVÍCEK J, MEDOVÁ E, MLCEK M, KITTNAR O: ECG body surface mapping changes in type 1 diabetic patients with and without autonomic neuropathy. *Physiol Res* **59**: 203-209, 2010.

PORTHAN K, VIITASALO M, TOIVONEN L, HAVULINNA AS, JULA A, TIKKANEN JT, VÄÄNÄNEN H, NIEMINEN MS, HUIKURI HV, NEWTON-CHEH C, ET AL.: Predictive value of electrocardiographic T-wave morphology parameters and T-wave peak to T-wave end interval for sudden cardiac death in the general population. *Circ Arrhythm Electrophysiol* **6**: 690-696, 2013.

SCHREURS CA, ALGRA AM, MAN SC, CANNEGIETER SC, VAN DER WALL EE, SCHALIJ MJ, KORS JA, SWENNE CA: The spatial QRS-T angle in the Frank vectorcardiogram: accuracy of estimates derived from the 12-lead electrocardiogram. *J Electrocardiol* **43**: 294-301, 2010.

SEDOVA K, BERNIKOVA O, AZAROV J, SHMAKOV D, VITYAZEV V, KHARIN S: Effects of echinochrome on ventricular repolarization in acute ischemia. *J Electrocardiol* **48**: 181-186, 2015.

SPOONER PM: Sudden cardiac death: influence of diabetes. *Diabetes Obes Metab* **10**: 523-532, 2008.

VAN DEN BROM CE, BOSMANS JW, VLASBLOM R, HANDOKO LM, HUISMAN MC, LUBBERINK M, MOLTHOFF CF, LAMMERTSMA AA, OUWENS MD, DIAMANT M, BOER C: Diabetic cardiomyopathy in Zucker diabetic fatty rats: the forgotten right ventricle. *Cardiovasc Diabetol* **9**: 25, 2010.

VAYKSHNORAYTE MA, OVECHKIN AO, AZAROV JE: The effect of diabetes mellitus on the ventricular epicardial activation and repolarization in mice. *Physiol Res* **61**: 363-370, 2012.

WAKS JW, SOLIMAN EZ, HENRIKSON CA, SOTOODEHNIA N, HAN L, AGARWAL SK, ARKING DE, SISCOVICK DS, SOLOMON SD, POST WS, JOSEPHSON ME, CORESH J, TERESHCHENKO LG: Beat-to-beat spatiotemporal variability in the T vector is associated with sudden cardiac death in participants without left ventricular hypertrophy: the Atherosclerosis Risk in Communities (ARIC) Study. *J Am Heart Assoc* **4**: e001357, 2015.

ZABEL M, KLINGENHEBEN T, FRANZ MR, HOHNLOSER SH: Assessment of QT dispersion for prediction of mortality or arrhythmic events after myocardial infarction: results of a prospective, long-term follow-up study. *Circulation* **97**: 2543-2550, 1998.

ZHANG Y, XIAO J, LIN H, LUO X, WANG H, BAI Y, WANG J, ZHANG H, YANG B, WANG Z: Ionic mechanisms underlying abnormal QT prolongation and the associated arrhythmias in diabetic rabbits: a role of rapid delayed rectifier K+ current. *Cell Physiol Biochem* **19**: 225-238, 2007.

Appendix C: *Ovechkin A, Vaykshnorayte M, Sedova K, Shumikhin K, Arteyeva N, Azarov J. Functional role of myicardial electrical remodeling in diabetic rabbits. Can J Physiol Pharmacol. 2015. 93(4): 245-252. JCR IF 2015 - 1.704*

NRC Research Press

ARTICLE

Functional role of myocardial electrical remodeling in diabetic rabbits

Alexey O. Ovechkin, Marina A. Vaykshnorayte, Ksenia Sedova, Konstantin V. Shumikhin, Natalia V. Arteyeva, and Jan E. Azarov

Abstract: The objective of the study was to investigate the role of electrical remodeling of the ventricular myocardium in hemodynamic impairment and the development of arrhythmogenic substrate. Experiments were conducted with 11 healthy and 12 diabetic (alloxan model, 4 weeks) rabbits. Left ventricular pressure was monitored and unipolar electrograms were recorded from 64 epicardial leads. Aortic banding was used to provoke arrhythmia. The diabetic rabbits had prolonged QTc, with activation–recovery intervals (surrogates for repolarization durations) being relatively short on the left ventricular base and long on the anterior apical portions of both ventricles ($P < 0.05$). In the diabetic rabbits, a negative correlation (−0.726 to −0.817) was observed between dP/dt_{max}, dP/dt_{min}, and repolarization dispersions. Under conditions of systolic overload (5 min), tachyarrhythmias were equally rare and the QTc and activation–recovery intervals were shortened in both groups ($P < 0.05$), whereas QRS was prolonged in the diabetic rabbits only. The repolarization shortening was more pronounced on the apex, which led to the development of apicobasal and interventricular end of repolarization gradients in the healthy animals, and to the flattening of the repolarization profile in the diabetic group. Thus, the diabetes-related pattern of ventricular repolarization was associated with inotropic and lusitropic impairment of the cardiac pump function.

Key words: activation–recovery intervals, arrhythmias, inotropy, lusitropy, repolarization.

Résumé : L'objectif de cette étude était d'estimer le rôle que le remodelage myocardique électrique pourrait jouer dans les déficiences hémodynamiques et le développement d'un substrat arythmogène ventriculaire. Des expériences ont été réalisées sur 11 lapins sains et 12 lapins diabétiques (modèle induit par l'alloxane, 4 semaines). La pression ventriculaire gauche a été suivie et des électrocardiogrammes unipolaires ont été enregistrés de 64 sondes épicardiques. Le cerclage aortique a été utilisé comme manœuvre pro-arythmique provocatrice. Les lapins diabétiques présentaient un QTc prolongé, avec des intervalles d'activation–récupération (substitut des durées de repolarisation) relativement courts à la base ventriculaire gauche et longue dans les portions apicales antérieures des deux ventricules ($P < 0,05$). Chez les animaux diabétiques, une corrélation négative (−0,726 à −0,817) a été observée entre le dP/dt_{max}, le dP/dt_{min} et les dispersions de repolarisation. Lors d'une surcharge systolique (5 min), les tachyarythmies étaient rares chez les deux groupes, le QRS était prolongé chez les diabétiques, alors que le QTc et les intervalles d'activation–récupération étaient raccourcis chez les deux groupes ($P < 0,05$). Le raccourcissement de la repolarisation était plus prononcé à l'apex, ce qui menait au développement de gradients de repolarisation des extrémités apico-basale et inter-ventriculaire chez les animaux sains, et à l'aplatissement du profile de repolarisation chez les diabétiques. Ainsi, le patron de repolarisation ventriculaire lié au diabète était associé à des déficiences inotropes et lusitropes de la fonction de la pompe cardiaque. [Traduit par la Rédaction]

Mots-clés : intervalles d'activation–récupération, arythmie, inotropie, lusitropie, repolarisation.

Introduction

Diabetes mellitus (DM) leads to electrical myocardial remodeling, which manifests as prolonged action potential duration due to the down-regulation of potassium currents (Magyar et al. 1992; Zhang et al. 2006, 2007; Lengyel et al. 2008, Gallego et al. 2009), and (or) slowed conduction, possibly due to a reduction in the sodium current density (Stables et al. 2014). The electrical remodeling attends the well-known diabetes-induced dysfunction of the heart known as diabetic cardiomyopathy (Miki et al. 2013). The mechanical and electrophysiological changes associated with DM are often considered separately; however, the cause–effect relationship between them should not be excluded. For example, the

Received 30 July 2014. Accepted 8 December 2014.

A.O. Ovechkin. Laboratory of Cardiac Physiology, Institute of Physiology, Komi Science Center, Ural Branch, Russian Academy of Sciences, 50 Pervomayskaya Street, 167982 Syktyvkar, Russia; First Department of Internal Diseases of Komi Branch of Kirov State Medical Academy, 11 Babushkin Street, Syktyvkar 167000, Russia; Department of Physiology, Medical Institute of Syktyvkar State University, 11 Babushkin Street, Syktyvkar 167000, Russia.
M.A. Vaykshnorayte and N.V. Arteyeva. Laboratory of Cardiac Physiology, Institute of Physiology, Komi Science Center, Ural Branch, Russian Academy of Sciences, 50 Pervomayskaya Street, 167982 Syktyvkar, Russia.
K. Sedova. Laboratory of Cardiac Physiology, Institute of Physiology, Komi Science Center, Ural Branch, Russian Academy of Sciences, 50 Pervomayskaya Street, 167982 Syktyvkar, Russia; Faculty of Biomedical Engineering, Czech Technical University, Nám Sítná 3105, Kladno, Czech Republic.
K.V. Shumikhin. Department of Physiology of Komi Branch of Kirov State Medical Academy, 11 Babushkin Street, Syktyvkar 167000, Russia.
J.E. Azarov. Laboratory of Cardiac Physiology, Institute of Physiology, Komi Science Center, Ural Branch, Russian Academy of Sciences, 50 Pervomayskaya Street, 167982 Syktyvkar, Russia; Department of Physiology, Medical Institute of Syktyvkar State University, 11 Babushkin Street, Syktyvkar 167000, Russia; Department of Physiology of Komi Branch of Kirov State Medical Academy, 11 Babushkin Street, Syktyvkar 167000, Russia.
Corresponding author: Jan E. Azarov (e-mail: j.azarov@gmail.com).

Table 1. Fasting venous plasma glucose level and mass indices in the healthy and diabetic rabbits [median and interquartile intervals (25%; 75%)].

	Glucose, (mmol/L)	Body mass (kg)	Heart mass (g)	Heart:body mass ratio (g/kg)
Control group (n = 11)	5.8 (5.3; 6.3)	3.2 (2.8; 3.5)	8.6 (8.3; 9.9)	2.7 (2.5; 3.0)
"To be DM" group (prior to alloxan injection; n = 12)	6.1 (5.7; 6.4)	2.8 (2.5; 2.9)	—	—
DM group (4 weeks after alloxan injection; n = 12)	20.5 (18.2; 27.5)	2.9 (2.7; 3.0)	7.8 (6.6; 9.3)	2.7 (2.4; 3.1)
P value (DM vs. control)	$P < 0.02$	$P > 0.05$	$P > 0.05$	$P > 0.05$

Note: DM, diabetes mellitus.

lengthening of repolarization due to down-regulation of potassium currents could maintain calcium transients, and thereby affect inotropic and lusitropic properties in a manner similar to that demonstrated in the heart failure model (Michael et al. 2009). The experimental and simulation studies have demonstrated that the optimal contraction of interacting myocardial elements requires a definite extent of the spatiotemporal asynchrony of activation and the heterogeneity of electrical properties (Markhasin et al. 2012); consequently, the changes in activation times and the redistribution of action potential duration are expected to result in changes to cardiac contractile function. Furthermore, the transmural repolarization sequence is known to be related to the relaxation pattern of a ventricular wall segment (Ashikaga et al. 2007; Zhu et al. 2009). However, studies of the relationship between global ventricular repolarization patterns and the pump function in normal and diseased hearts are generally lacking, and specifically from those with DM.

Another functional consequence of the DM-induced electrical remodeling could be a change in the risk for arrhythmia. DM increases the risk of ventricular arrhythmia and sudden cardiac death in patients with coronary artery disease as well as those with no signs of heart problems (Balkau et al. 1999; Jouven et al. 2005). The specific mechanism for increased vulnerability to arrhythmia is largely unknown, although there are recent data pointing to oxidative stress as a significant contributing factor (Xie et al. 2013). On the other hand, a set of experimental data has suggested that DM could produce a paradoxical antiarrhythmic effect (Beatch and McNeill 1988; Kusama et al. 1992; Ravingerová et al. 2000; Ravingerova et al. 2001; Matejíková et al. 2008). The discrepancy between the clinical and experimental findings could be related to the myocardial electrophysiological properties of the experimental animals (e.g., small rat heart having an extremely fast I_{to}-based ventricular repolarization), short follow-up of DM in experimental studies, concomitant pathologies in patients observed in clinical investigations, etc. However, the eventual electrophysiological basis for this "protective" action of DM is unclear. Likewise, in the clinical setting it was found that whereas DM predisposes to sudden cardiac death in the long-term, acute susceptibility to ventricular arrhythmias did not differ among diabetics and nondiabetics (Spooner 2008).

The objective of this investigation was to elucidate the functional role of the changes in spatiotemporal patterns of activation and repolarization related to changes in pump function and the development of arrhythmogenic substrate in an experimental model of type 1 DM. Taking into account that the paradoxical "protective" effect of DM observed in the previous studies cited above may have been caused by some specific experimental conditions, we attempted to test the arrhythmic risk in a different experimental setting. First, a systolic overload was applied as a provocative proarrhythmic maneuver, instead of the widely utilized ishchemia–reperfusion model. Second, we studied the hearts in situ to have realistic hemodynamics and autonomic innervation, which is subject to diabetic autonomic neuropathy, and which in turn may cause functional impairment. Third, we used rabbits instead of the commonly investigated rat to have model animals with a set of cardiac ionic currents that are similar (although not identical) to humans.

Fig. 1. Microphotographs of the Van Gieson stained cross-sections of the left ventricular myocardium from healthy (A) and diabetic (B) Chinchilla rabbits. Note the significant collagen deposits in the diabetic heart (black arrows). Original magnification ×200. Scale bar = 100 μm.

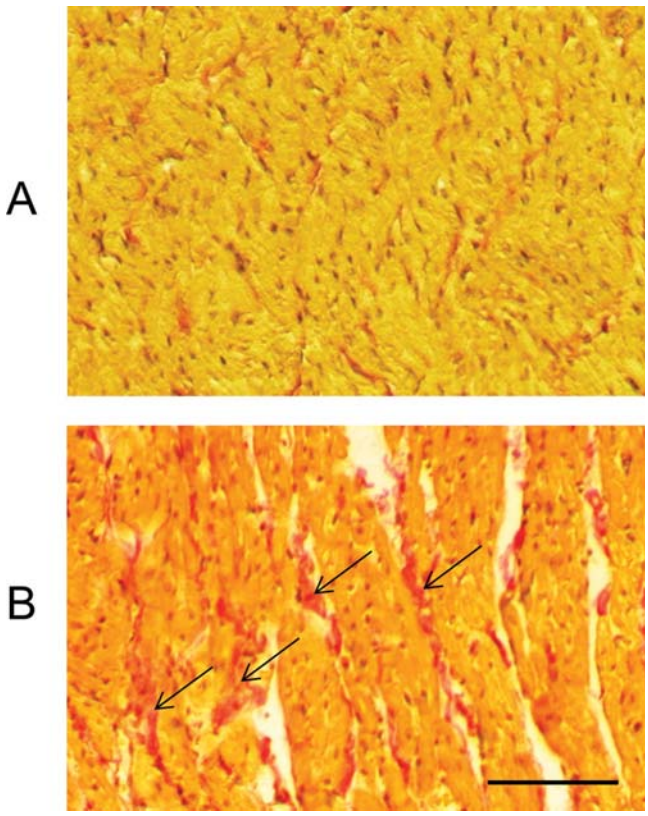

Materials and methods

Experimental preparation and protocol

The investigation conformed to the *Guide for the Care and Use of Laboratory Animals* (NAC 2011). The experiments were done on Chinchilla rabbits of either sex, aged 6–8 months. To induce the type 1 DM, 24 rabbits were given a single dose of alloxan (120 mg/kg body mass, by intravenous injection). The glucose concentration was measured from the venous blood once a week with a OneTouch glucometer (LifeScan). Subsequently, 7 animals died before the follow-up, 12 animals became diabetic, and DM did not develop in 5 animals (fasting venous plasma glucose level being <7.0 mmol/L). As a result, the open-chest electrophysiological

Table 2. The QRS, QT, QTc, and activation–recovery intervals [median and interquartile intervals (25%; 75%)] of the healthy and diabetic rabbits in the baseline state and under the LV overload.

	Baseline		*P*	Overload		*P*
Duration, ms	Control (n = 11)	DM (n = 12)	DM vs. control	Control (n = 11)	DM (n = 12)	DM vs. control
QRS	30 (25; 35)	28 (22; 30)	>0.05	32 (26; 36)	36 (31; 45)	>0.05
QT	139 (131; 149)	160 (143; 170)	0.023	118 (114; 126)	128 (122; 135)	>0.05
QTc	148 (143; 157)	168 (152; 175)	0.034	134 (113; 139)	139 (133; 149)	>0.05
ARI LV apex	100 (84; 118)	91 (79; 113)	>0.05	75 (67; 100)	71 (65; 85)	>0.05
ARI LV base	90 (82; 96)	85 (73; 103)	>0.05	77 (69; 97)	70 (67; 78)	>0.05
ARI LV lateral	93 (86; 104)	86 (72; 105)	>0.05	73 (71; 89)	70 (65; 79)	>0.05
ARI RV lateral	102 (96; 108)	94 (85; 107)	>0.05	78 (68; 87)	78 (65; 89)	>0.05
RT LV apex	119 (100; 135)	110 (91; 132)	>0.05	99 (90; 107)	91 (81; 107)	>0.05
RT LV base	117 (109; 127)	110 (93; 126)	>0.05	108 (101; 120)	92 (89; 102)	>0.05
RT LV lateral	118 (108; 130)	108 (95; 127)	>0.05	108 (94; 112)	94 (88; 103)	>0.05
RT RV lateral	121 (114; 127)	114 (99; 126)	>0.05	98 (83; 105)	92 (82; 113)	>0.05

Note: ARI, activation–recovery interval; DM, diabetes mellitus; LV, left ventricular; RT, end of repolarization time; RV, right ventricular.

measurements were carried out in 12 rabbits (7 females) with DM, with a 4 week follow-up, and 11 control animals (8 females).

The rabbits were anesthetized with zoletil (15 mg/kg body mass, by intramuscular injection), intubated, and mechanically ventilated. After exposure of the heart, the animal's temperature was maintained at 37–38 °C by irrigation with warm saline and increasing the room temperature. At spontaneous sinus rhythm, unipolar electrograms were registered from 64 ventricular epicardial leads organized in a sock array (3.0–5.0 mm inter-electrode distance) with reference to Wilson's central terminal. The recording was done by means of a custom-designed mapping system (16 bits; bandwidth 0.05–1000.0 Hz; sampling rate 4000 Hz). In each epicardial lead, the activation time (AT) and the end of repolarization time (RT) were determined from dV/dt_{min} during the QRS complex and dV/dt_{max} during the T wave, respectively (Coronel et al. 2006), and the activation–recovery interval (ARI), serving as a measure of the local repolarization duration, was measured as the difference between RT and AT.

A catheter (internal diameter 0.6 mm) was introduced into the left ventricle via the left carotid artery and attached to a pressure transducer SP844 (50 $\mu V \cdot V^{-1} \cdot (cm\ Hg)^{-1}$; MEMSCAP). The left intraventricular pressure was monitored and measured with the Prucka Mac-Lab 2000 system (GE Medical Systems) for the course of experiment. The highest velocity for the left ventricular (LV) pressure increase (dP/dt_{max}) and decrease (dP/dt_{min}) measured during the isovolumic contraction and relaxation served as indices of the LV inotropic and lusitropic properties, respectively. To test for arrhythmogenic substrate in the myocardium, the LV systolic overload was produced with 5 min aortic stenosis, which was produced by banding between the origins of the brachiocephalic and left subclavicular arteries.

The limb lead ECGs were recorded in the course of experiment. The QT interval was measured in the II limb lead and the corrected QT interval (QTc) was calculated using the equation QTc = QT – 0.175 × (RR – 300) (Carlsson et al. 1993), where RR represents the value for the RR interval. An occurrence of life-threatening ventricular arrhythmias, namely ventricular fibrillation (VF) and ventricular tachycardia (VT), was monitored during the overload period.

At the end of the experiment, the animal was sacrificed with deep anesthesia, then the heart was excised and the myocardial mass was measured. Examination of the Van Gieson stained sections of the left ventricular myocardium was performed using light microscopy to estimate the collagen deposits. The morphological characteristics were determined and interpreted by an investigator following a blind protocol.

Statistical analysis

BioStat 4.03 was used for the statistical analysis. The data presented are the median and interquartile intervals (25%; 75%), and nonparametric criteria were used according to the non-Gaussian distribution of variables. Wilcoxon tests were used for the comparisons between the baseline and overload values, and the Mann–Whitney U test was used to compare the DM group with the control group. The occurrence of arrhythmias in different settings was assessed using χ^2 criteria. The differences were considered statistically significant at values for $P \leq 0.05$.

Results

As expected, the rabbits from the control and DM groups differed from each other in their venous plasma glucose levels (Table 1). Microscopic examination of the postmortem samples showed the presence of significant collagen deposits in the diabetic hearts (Fig. 1), whereas the myocardial mass indices were similar for both groups (Table 1). Before the heart of the anaesthetized animals was exposed, the heart rate and QRS duration were similar in both groups; however, the measured and corrected QT intervals were longer in the DM group (Table 2).

The hemodynamic measurements documented the impairment of cardiac pump function in the DM group. Table 3 shows the indices obtained at the time when the thorax was opened and the epicardial leads were placed on the ventricular surface. These values were lower compared with those taken just after the induction of anesthesia but before exposure of the heart (e.g., dP/dt_{max} differed 1.07- and 1.3-fold in the control and diabetic animals, respectively); however, the relationships between these values for the control and DM groups were similar before and after the opening of the thorax. Subsequently, the hemodynamic data summarized in Table 3 was analyzed in relation to the electrophysiological data recorded in the same conditions from the ventricular surface.

The ventricular epicardial activation patterns were the same in the DM and control groups. Briefly, the activation wave originally emerged at 2 independent breakthroughs in the RV and LV, and then spread from the apex to the base and from the RV to the LV (Fig. 2A). The duration of epicardial activation (AT dispersions), which was measured as the difference between the earliest and latest epicardial ATs, were similar in control and DM groups (Table 4). In the control group, we did not observe any significant gradients of ARIs on the apicobasal and interventricular axes, whereas the rabbits with DM had an ARI pattern with the shortest durations on the LV base and the longest ones on the apical portions of the LV and RV (Fig. 2B). The ARI dispersions, which were determined as the difference between the longest and shortest ARIs regardless of the region, did not distinguish between the DM

Table 3. The cardiac and systemic hemodynamic variables in the open-chest normal and diabetic Chinchilla rabbits [median and interquartile intervals (25%; 75%)].

	Heart rate (bpm)	Sysolic pressure (mm Hg)	Diastolic pressure (mm Hg)	dP/dt_{max} (mm Hg/s)	dP/dt_{min} (mm Hg/s)	LVEDP, (mm Hg)
Control (n = 11)	285 (249; 303)	84 (75; 95)	0 (–1; 1)	3095 (2439; 3340)	2250 (1666; 3333)	2 (2; 5)
DM (n = 12)	249 (217; 275)	71 (59; 74)	–2 (–5; 0)	1824 (1250; 2256)	1248 (990; 2000)	5 (0; 5)
P (DM vs. control)	0.118	0.036	0.171	0.004	0.019	0.744

Note: bpm, beats per minute; 1 mm Hg = 133.322 Pa; DM, diabetes mellitus; LVEDP, left ventricular end diastolic pressure.

Fig. 2. The representative ventricular epicardial isochronal maps of the activation times (A), ARI distribution (B), and RTs (C) in the healthy and diabetic Chinchilla rabbits. The left and right parts of each map represent the anterior and posterior aspects of the ventricular epicardium, respectively. The scales demonstrate the time points with respect to the onset of the QRS complex (A and C) or durations (B). The difference bars and P values show the statistically significant interventricular and left ventricular apicobasal differences in ARI duration found in the diabetic, but not in the control group (B, right). ARI, activation–recovery interval; AT, activation time; RT, end of repolarization time.

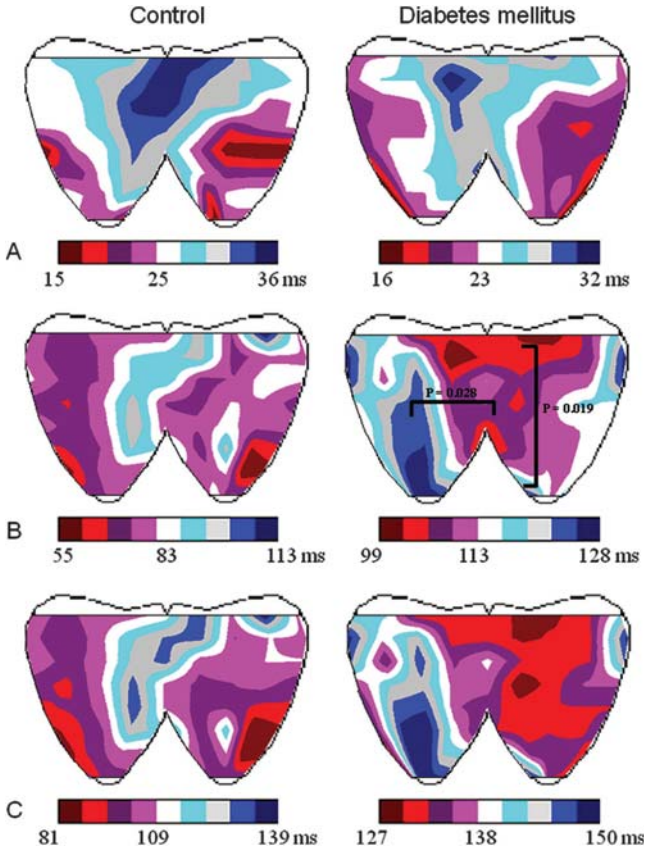

Table 4. The ventricular epicardial dispersions of activation times, activation–recovery intervals and end of repolarization times [median and interquartile intervals (25%; 75%)] from Chinchilla rabbits.

	AT dispersion (ms)	ARI dispersion (ms)	RT dispersion (ms)
Control (n = 11)	17 (15; 24)	17 (11; 29)	24 (14; 27)
DM (n = 12)	19 (17; 22)	17 (8; 25)	16 (10; 22)

Note: ARI, activation–recovery interval; AT, activation time; DM, diabetes mellitus; RT, end of repolarization time.

and the control group (Table 4). Likewise, the RT dispersions in both groups were similar (Table 4), and the epicardial sequences for the RTs (Fig. 2C) corresponded to the ARI distributions.

To determine the relationship between the electrophysiological variables on one hand, and the inotropic and lusitropic properties on the other, we calculated Spearman's correlation coefficients between dP/dt_{max}, dP/dt_{min}, and the indices characterizing the activation and repolarization patterns of ventricular epicardium in the control and DM groups. It was found that neither dP/dt_{max} nor dP/dt_{min} correlated with the duration of repolarization (estimated as the QT, maximal ARI, minimal ARI, and averaged ARI); the heart rate and the duration of epicardial activation (AT dispersion) in the control as well as in the DM groups. However, only in the DM group was a significant negative correlation observed between dP/dt_{max} and dP/dt_{min} on one hand, and the dispersions of ARIs on the other. Similar negative correlations were found between dP/dt_{max} and dP/dt_{min}, and the dispersions of RTs. The corresponding values from the healthy control rabbits were not significantly different (Table 5).

Aortic banding was applied to induce a systolic LV overload, which led to the systolic LV pressure increase from 73 (61; 82) to 116 (101; 120) mm Hg in the control group, and from 67 (59; 75) to 111 (101; 127) mm Hg in the DM group (1 mm Hg = 133.322 Pa). As a result, the epicardial ATs did not change significantly, whereas the QRS widened in the DM group, and the QTc decreased in both groups (Fig. 3; Table 2). The ARIs and RTs were generally shortened in both the control and DM groups, with a more pronounced effect in the apical area (Fig. 4; Table 2). Specifically in the healthy control group, the LV apical shortening of ARIs, combined with the earlier apical activation, produced significant apicobasal (Fig. 5) and interventricular (Fig. 6) RT gradients that were absent in the baseline state. On the other hand, in the DM group, significant ARI shortening within the LV was observed only in the LV apex, and it was relatively prolonged in the baseline state. As a consequence, the ARI distribution in the DM group became less heterogeneous, the RT gradients did not develop in the ventricles of the DM group, and the overall RT distribution remained relatively uniform (Figs. 4–6). By the 5th min of aortic banding, the ventricular tachyarrhythmias were rarely observed in either the control (2 VTs) or the DM groups (1 VT and 1 VF), suggesting that the myocardial vulnerability to tachyarrhythmias was not increased in the DM group under the conditions of 5 min systolic overload.

Discussion

This study demonstrated a negative correlation between the magnitude of the dispersion of repolarization and the velocity of the LV pressure increase and decrease (dP/dt_{max} and dP/dt_{min}, respectively) only in the DM group. Generally speaking, this finding could be explained by considering that the extent of the electrical heterogeneity in the DM group was higher than in the controls, which could impose an additional limitation in pump function in DM that was absent from the healthy myocardium. On the other hand, the increase in the dispersion of repolarization could result from primary mechanical impairment, and the greater the pump function deterioration, the greater the repolarization nonuniformity. However, the specific mechanisms for these relationships have yet to be determined.

Table 5. The correlation coefficients between the indices of pump function and the variables for dispersion of repolarization from Chinchilla rabbits.

ARI dispersion		RT dispersion	
dP/dt_{max}	dP/dt_{min}	dP/dt_{max}	dP/dt_{min}
Control (n = 11)			
–0.085, P = 0.815	–0.376, P = 0.284	–0.049, P = 0.894	0.019, P = 0.957
DM (n = 12)			
–0.817, P = 0.002	–0.726, P = 0.011	–0.776, P = 0.005	–0.795, P = 0.003

Note: ARI, activation–recovery interval; DM, diabetes mellitus; RT, end of repolarization time. P values identify for the significance of correlation.

Fig. 3. The changes in the limb lead ECG parameters in the healthy and diabetic rabbits at 5 min of systolic overload. (A and B) Changes in the median for QRS and QTc durations, respectively. (C) Representative II limb lead ECGs in the control and DM Chinchilla rabbits in the baseline (solid lines) and overload (broken lines) states. QRS, QRS complex; QTc, corrected QT interval; DM, diabetes mellitus.

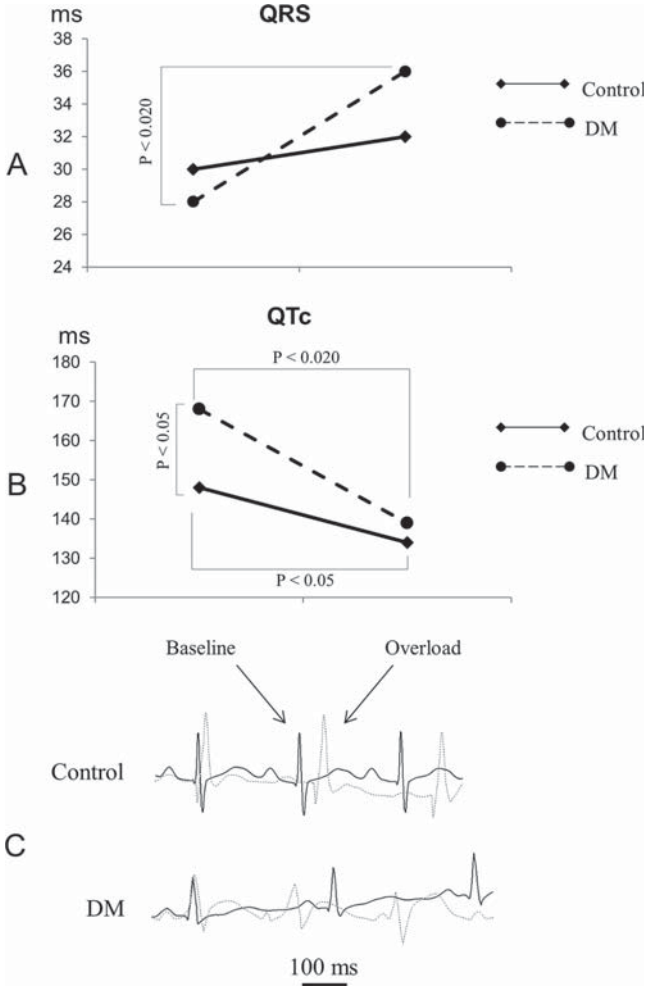

Fig. 4. The representative ventricular epicardial isochronal maps of the ATs (A), ARI distribution (B), and RTs (C) in healthy and diabetic Chinchilla rabbits at 5 min of aortic banding. The presentation of the data is the same as in Fig. 2. The difference bars and P values show the statistically significant interventricular and left ventricular apicobasal differences in RTs found in the control, but not in the diabetic group (C, left). ARI, activation–recovery interval; AT, activation time; RT, end of repolarization time.

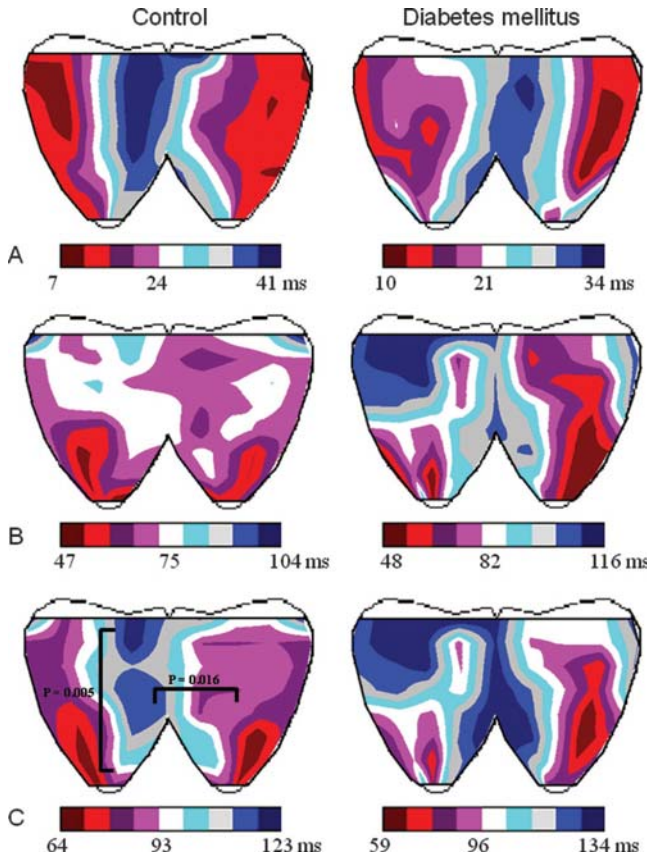

The association between the relaxation velocity, estimated as dP/dt_{min}, and the RT dispersion is relatively clear. As the local end of electrical excitation (i.e., RT) corresponds to the local end of the contraction process, the more synchronous the electrical repolarization (i.e., the lower the RT dispersion), the faster the relaxation, and the greater dP/dt_{min}. Ashikaga et al. (2007) and Zhu et al. (2009) have shown that the relaxation process on the transmural axis of the ventricular wall is associated with the transmural repolarization sequence, and the present study demonstrated the negative correlation between the RT dispersion and the relaxation velocity on the whole-heart scale. The similar correlation between dP/dt_{min} and the ARI dispersion possibly indirectly reflects the close relationship between the global ARI distribution and RT pattern (Vaykshnorayte et al. 2011).

In contrast, the reason for the negative correlation between the dispersion of repolarization and dP/dt_{max} is unclear. On the one hand, the dispersion of ARIs could correspond to the extent of the synchronicity/dys-synchronicity of the contractile process, and dys-synchronous contraction could hamper pressure generation by the LV. On the other hand, dP/dt_{max} is observed during the isovolumic contraction phase, which is largely dependent on the activation sequence and not the repolarization duration pattern.

Fig. 5. The overload-induced changes in ARIs and RTs (medians) in the apical and basal regions of the ventricular epicardium of the control and diabetic Chinchilla rabbits. ARI, activation–recovery interval; DM, diabetes mellitus; RT, end of repolarization time.

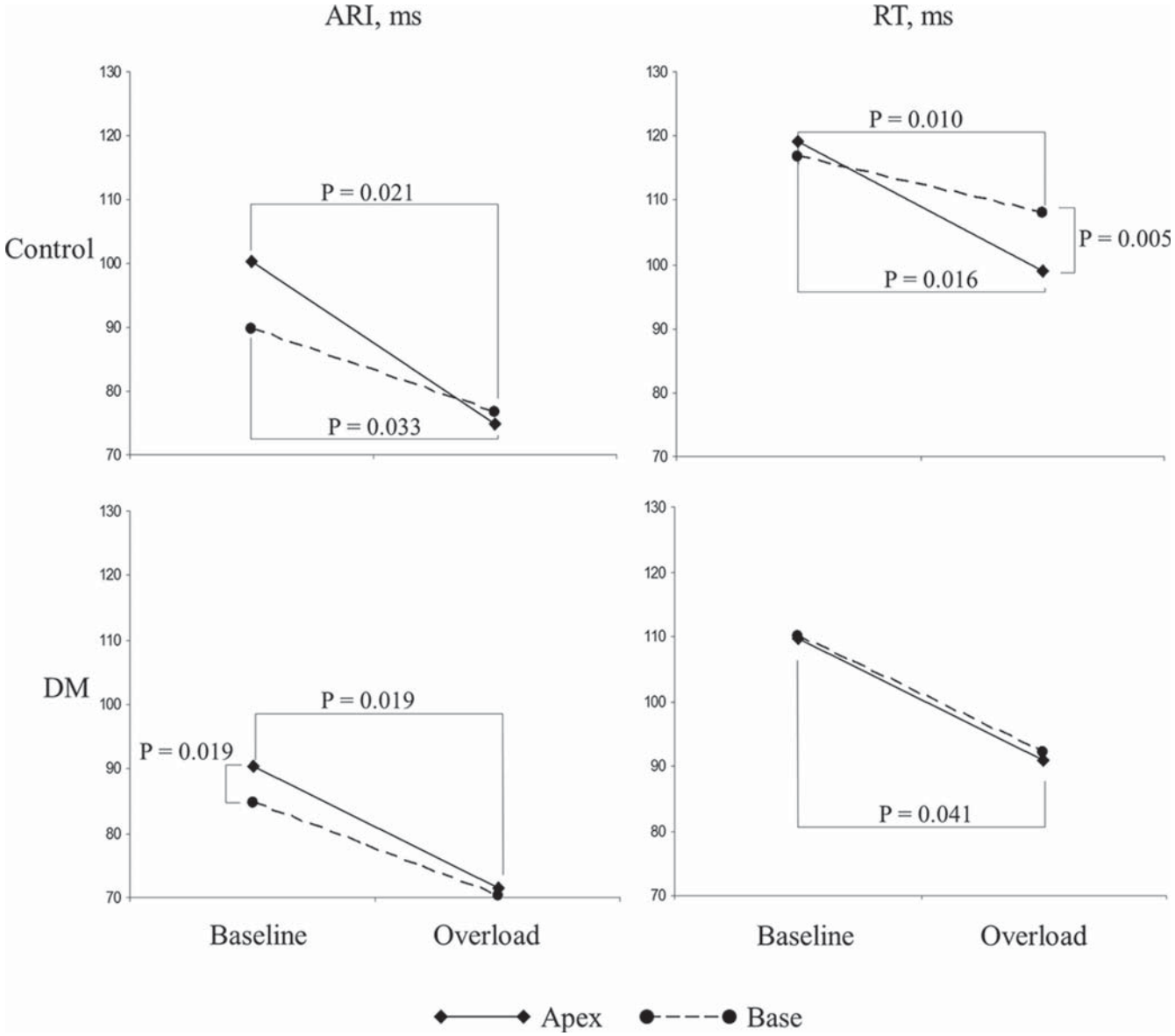

However, we did not observe any DM-induced alterations in the activation process one month after alloxan treatment, which could have been expected at the prolonged follow-up (Stables et al. 2014). Additionally, a definite extent of the activation asynchrony and the heterogeneity of electrical and mechanical properties is required for the optimal contractile function of the heart (Markhasin et al. 2012).

A relationship between the contractile properties (dP/dt_{max}) and the repolarization duration might have been expected (Chen et al. 2014). However, no such correlations were found between dP/dt and ARI duration (mean, maximal, and minimal) or with QT duration and heart rate, but only between dP/dt and repolarization dispersions. These findings could be ascribed to the relatively early stage of DM, which did not result in the statistically significant overall prolongation of ARIs in the diabetic animals, but only caused the development of new ventricular repolarization gradients and, hence, the specific spatiotemporal organization of the repolarization patterns.

The negative correlation between dP/dt and the dispersion of repolarization may be explained as follows. The primary myocardial DM-related inotropic deterioration induced the prolongation of action potential duration (Zhang et al. 2006, 2007; Lengyel et al. 2008) in an attempt to maintain calcium balance and contractile properties, which is an effect similar to that in heart failure (Michael et al. 2009). The worse the pump function and the lower the dP/dt_{max}, the greater the degree of electrical remodeling that is manifested in a heterogeneous manner, predominantly in the apical portions of the ventricles. Such a pattern of electrical remodeling resulted in the development of the specific diabetic pattern of repolarization timing, primarily ARIs and secondarily RTs, with the latter, in turn, affecting the relaxation process estimated using dP/dt_{min}.

Mechanical stimulation is known to induce malignant ventricular arrhythmias, with reentry serving as a major arrhythmogenic mechanism leading to VT/VF (Reiter et al. 1988; Quinn 2014), and the nonuniform repolarization may lead to the increased suscep-

Fig. 6. The overload-induced changes in ARIs and RTs (medians) in the left (LV) and right (RV) ventricular lateral free walls of the control and diabetic Chinchilla rabbits. ARI, activation–recovery interval; DM, diabetes mellitus; RT, end of repolarization time.

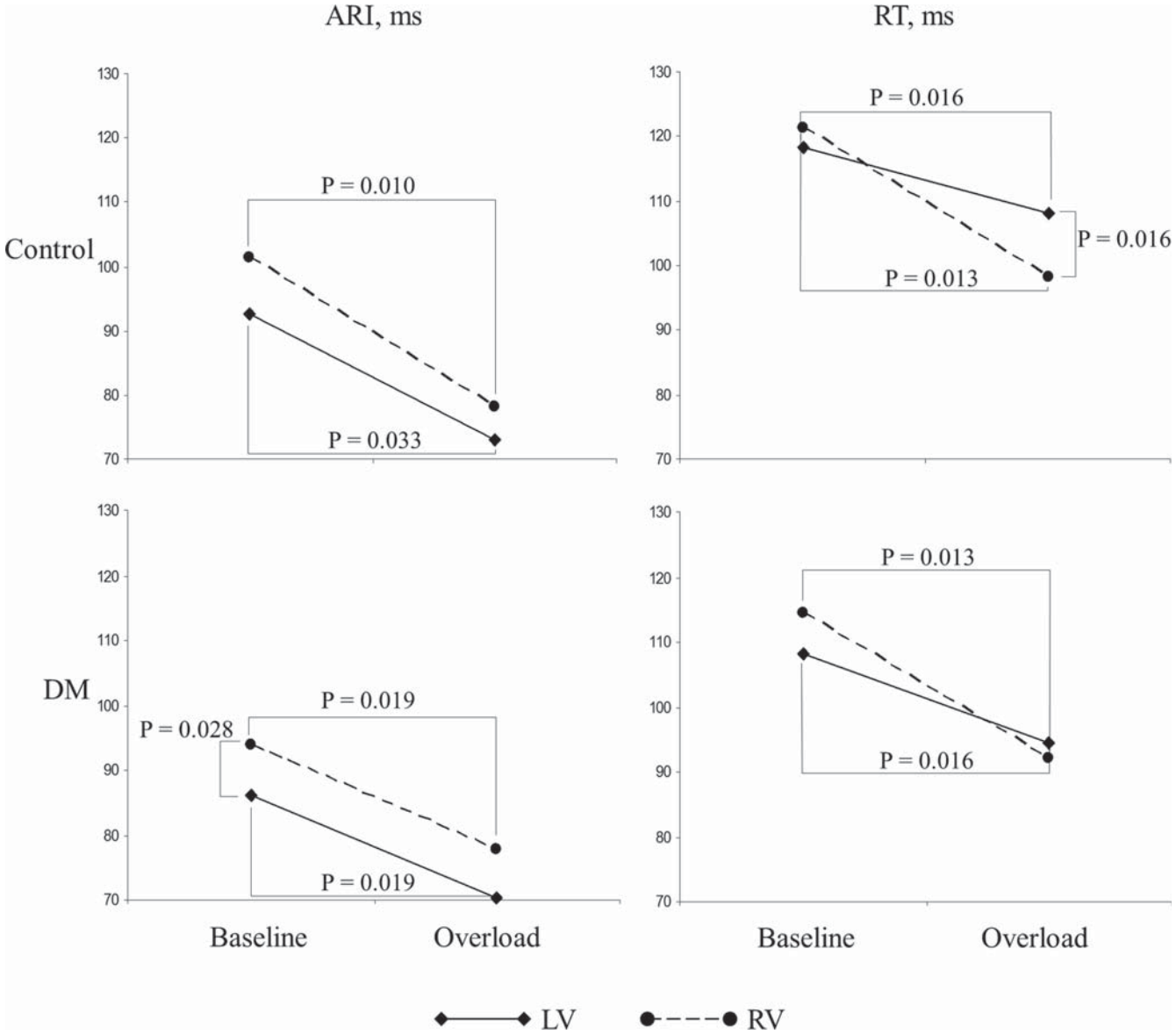

tibility to ventricular arrhythmias (Osadchii 2012) through the development of a unidirectional conduction block. Here, we could not directly estimate the mechanically induced after-depolarizations; however, this factor is considered mainly as a triggering event for VT or VF (Quinn 2014), which still requires an appropriate anatomical and functional substrate to ensure the sustained reentrant arrhythmias. In our pressure overload test, the diabetic hearts did not demonstrate increased susceptibility to VF, possibly due to the fact that during the aortic banding the diabetic hearts underwent proarrhythmic activation changes and antiarrhythmic repolarization changes in comparison with the controls.

Indeed, in the diabetic hearts the essential collagen deposits and QRS prolongation implied the development of the conditions for the activation wave slowing and circle spread. On the other hand, the pressure overload led to the shortening of repolarization duration, predominantly in the apical area. This response has been previously shown to be more pronounced under conditions of autonomic blockade (Sedova et al. 2011). Autonomic neuropathy is typical with DM and, moreover, is responsible for the relative prolongation of repolarization at the apex in the baseline conditions (Ovechkin et al. 2014). Therefore, it is expected that the overload-induced shortening of repolarization in the apical area would be more expressed in the diabetic animals and would compensate for the relative prolongation of repolarization in the very apical area in baseline. This effect could possibly render antiarrhythmic properties for the diabetic hearts, whereas the predominant repolarization shortening in the apical area of the healthy myocardium resulted in the development of the apicobasal and interventricular RT gradients, thereby increasing the heterogeneity of repolarization.

Limitations of the study

In this study, we found a functional association between the repolarization dispersion and the pump function in the rabbits with DM. However, the direct mechanism of this association and its consequences were not addressed directly. Some factors potentially contributing to this relation were not quantitated, such as the extent of fibrotic changes or tissue metabolic derangements

in the diabetic myocardium. Presuming that the autonomic dysfunction plays a significant role in electrophysiological remodeling, the present experiments were conducted in situ in the open-chest rabbits to preserve the contribution of innervation affected under DM. However, the conditions of the autonomic system in the setting of this study were definitely modified by the anesthesia, which should be taken into account. Similarly, the cardiac electrophysiological parameters are also subject to the influences from the anesthetic agents. In spite of the fact that the mechanical stress has long been recognized as a proarrhythmic factor (Babuty and Lab 2001), the present model did not provide us with a significant number of VT/VFs, suggesting that the arrhythmogenic impact was rather weak, and that the estimate for proarrhythmic/antiarrhythmic properties may be different in the more severe interventions.

Conclusions

This study demonstrated that the DM-related spatiotemporal pattern of ventricular repolarization, specifically basoapical and interventricular repolarization duration gradients, is associated with inotropic and lusitropic impairment.

Acknowledgements

The study was supported by the Ural Branch of the Russian Academy of Sciences (Projects No. 12-I-4-2059, 13-4-032-KSC, 14-4-SP-43) and by RFBR (Research project 14-04-31070 мол_а). Conflict of interest: The authors declare that there is no conflict of interest associated with this work.

References

Ashikaga, H., Coppola, B.A., Hopenfeld, B., Leifer, E.S., McVeigh, E.R., and Omens, J.H. 2007. Transmural dispersion of myofiber mechanics: implications for electrical heterogeneity in vivo. J. Am. Coll. Cardiol. **49**: 909–916. doi:10.1016/j.jacc.2006.07.074. PMID:17320750.

Babuty, D., and Lab, M.J. 2001. Mechanoelectric contributions to sudden cardiac death. Cardiovasc. Res. **50**: 270–279. doi:10.1016/S0008-6363(01)00255-3. PMID:11334831.

Balkau, B., Jouven, X., Ducimetiere, P., and Eschwege, E. 1999. Diabetes as a risk factor for sudden death. Lancet, **354**: 1968–1969. doi:10.1016/S0140-6736(99)04383-4. PMID:10622302.

Beatch, G.N., and McNeill, J.H. 1988. Ventricular arrhythmias following coronary artery occlusion in the streptozotocin diabetic rat. Can. J. Physiol. Pharmacol. **66**: 312–317. doi:10.1139/y88-053. PMID:3167669.

Carlsson, L., Abrahamsson, C., Andersson, B., Duker, G., and Schiller-Linhardt, G. 1993. Proarrhythmic effects of the class III agent almokalant: importance of infusion rate, QT dispersion, and early afterdepolarizations. Cardiovasc. Res. **27**: 2186–2193. doi:10.1093/cvr/27.12.2186. PMID:8313427.

Chen, Z., Hanson, B., Sohal, M., Sammut, E., Child, N., Shetty, A., et al. 2014. Left ventricular epicardial electrograms show divergent changes in action potential duration in responders and nonresponders to cardiac resynchronization therapy. Circ. Arrhythm. Electrophysiol. **6**: 265–271. doi:10.1161/CIRCEP.112.000148. PMID:23476036.

Coronel, R., de Bakker, J.M., Wilms-Schopman, F.J., Opthof, T., Linnenbank, A.C., Belterman, C.N., and Janse, M.J. 2006. Monophasic action potentials and activation recovery intervals as measures of ventricular action potential duration: experimental evidence to resolve some controversies. Heart Rhythm, **3**: 1043–1050. doi:10.1016/j.hrthm.2006.05.027. PMID:16945799.

Gallego, M., Alday, A., Urrutia, J., and Casis, O. 2009. Transient outward potassium channel regulation in healthy and diabetic hearts. Can. J. Physiol. Pharmacol. **87**(2): 77–83. doi:10.1139/Y08-106. PMID:19234570.

Jouven, X., Lemaitre, R.N., Rea, T.D., Sotoodehnia, N., Empana, J.P., and Siscovick, D.S. 2005. Diabetes, glucose level, and risk of sudden cardiac death. Eur. Heart J. **26**: 2142–2147. doi:10.1093/eurheartj/ehi376. PMID:15980034.

Kusama, Y., Hearse, D.J., and Avkiran, M. 1992. Diabetes and susceptibility to reperfusion-induced ventricular arrhythmias. J. Mol. Cell. Cardiol. **24**: 411–421. doi:10.1016/0022-2828(92)93195-P. PMID:1619670.

Lengyel, C., Virág, L., Kovács, P.P., Kristóf, A., Pacher, P., Kocsis, E., et al. 2008. Role of slow delayed rectifier K+-current in QT prolongation in the alloxan-induced diabetic rabbit heart. Acta Physiol. (Oxf.), **192**: 359–368. doi:10.1111/j.1748-1716.2007.01753.x.

Magyar, J., Rusznák, Z., Szentesi, P., Szûcs, G., and Kovács, L. 1992. Action potentials and potassium currents in rat ventricular muscle during experimental diabetes. J. Mol. Cell. Cardiol. **24**: 841–853. doi:10.1016/0022-2828(92)91098-P. PMID:1433314.

Markhasin, V.S., Balakin, A.A., Katsnelson, L.B., Konovalov, P., Lookin, O.N., Protsenko, Y., and Solovyova, O. 2012. Slow force response and auto-regulation of contractility in heterogeneous myocardium. Prog. Biophys. Mol. Biol. **110**: 305–318. doi:10.1016/j.pbiomolbio.2012.08.011. PMID:22929956.

Matejíková, J., Kucharská, J., Pancza, D., and Ravingerová, T. 2008. The effect of antioxidant treatment and NOS inhibition on the incidence of ischemia-induced arrhythmias in the diabetic rat heart. Physiol. Res. **57**(Suppl. 2): S55–S60. PMID:18373392.

Michael, G., Xiao, L., Qi, X.Y., Dobrev, D., and Nattel, S. 2009. Remodelling of cardiac repolarization: how homeostatic responses can lead to arrhythmogenesis. Cardiovasc. Res. **81**: 491–499. doi:10.1093/cvr/cvn266. PMID:18826964.

Miki, T., Yuda, S., Kouzu, H., and Miura, T. 2013. Diabetic cardiomyopathy: pathophysiology and clinical features. Heart Fail. Rev. **18**: 149–166. doi:10.1007/s10741-012-9313-3. PMID:22453289.

NAC (National Academy of Sciences). 2011. Guide for the care and use of laboratory animals. 8th Ed. National Academy Press, Washington, D.C. [Available from www.nap.edu/catalog.php?record_id=12910].

Osadchii, O.E. 2012. Impact of Na+ channel blockers on transmural dispersion of refractoriness and arrhythmic susceptibility in guinea-pig left ventricle. Eur. J. Pharmacol. **691**: 173–181. doi:10.1016/j.ejphar.2012.07.015. PMID:22800935.

Ovechkin, A.O., Vaykshnorayte, M.A., Sedova, K.A., Shmakov, D.N., Shumikhin, K.V., Medvedeva, S.Y., et al. 2014. Esmolol abolishes repolarization gradients in diabetic rabbit hearts. Exp. Clin. Cardiol. **20**: 3780–3793.

Quinn, T.A. 2014. The importance of non-uniformities in mechano-electric coupling for ventricular arrhythmias. J. Interv. Card. Electrophysiol. **39**: 25–35. doi:10.1007/s10840-013-9852-0. PMID:24338157.

Ravingerová, T., Stetka, R., Pancza, D., Ulicná, O., Ziegelhöffer, A., and Styk, J. 2000. Susceptibility to ischemia-induced arrhythmias and the effect of preconditioning in the diabetic rat heart. Physiol. Res. **49**: 607–616. PMID:11191365.

Ravingerova, T., Neckar, J., Kolar, F., Stetka, R., Volkovova, K., Ziegelhöffer, A., and Styk, J. 2001. Ventricular arrhythmias following coronary artery occlusion in rats: is the diabetic heart less or more sensitive to ischaemia? Basic Res. Cardiol. **96**: 160–168. doi:10.1007/s003950170066. PMID:11327334.

Reiter, M.J., Synhorst, D.P., and Mann, D.E. 1988. Electrophysiological effects of acute ventricular dilatation in the isolated rabbit heart. Circ. Res. **62**: 554–562. doi:10.1161/01.RES.62.3.554. PMID:3342478.

Sedova, K.A., Goshka, S.L., Vityazev, V.A., Shmakov, D.N., and Azarov, J.E. 2011. Load-induced changes in ventricular repolarization: evidence of autonomic modulation. Can. J. Physiol. Pharmacol. **89**: 935–944. doi:10.1139/y11-098. PMID:22114768.

Spooner, P.M. 2008. Sudden cardiac death: influence of diabetes. Diabetes Obes. Metab. **10**: 523–532. doi:10.1111/j.1463-1326.2007.00723.x. PMID:17451424.

Stables, C.L., Musa, H., Mitra, A., Bhushal, S., Deo, M., Guerrero-Serna, G., et al. 2014. Reduced Na^+ current density underlies impaired propagation in the diabetic rabbit ventricle. J. Mol. Cell. Cardiol. **69**: 24–31. doi:10.1016/j.yjmcc.2013.12.031. PMID:24412579.

Vaykshnorayte, M.A., Tsvetkova, A.S., and Azarov, J.E. 2011. Epicardial activation-to-repolarization coupling differs in the local areas and on the entire ventricular surface. J. Electrocardiol. **44**: 131–137. doi:10.1016/j.jelectrocard.2010.11.007. PMID:21216413.

Xie, C., Biary, N., Tocchetti, C.G., Aon, M.A., Paolocci, N., Kauffman, J., and Akar, F.G. 2013. Glutathione oxidation unmasks proarrhythmic vulnerability of chronically hyperglycemic guinea pigs. Am. J. Physiol. Heart Circ. Physiol. **304**: H916–H926. doi:10.1152/ajpheart.00026.2012. PMID:23376824.

Zhang, Y., Xiao, J., Wang, H., Luo, X., Wang, J., Villeneuve, L.R., et al. 2006. Restoring depressed HERG K+ channel function as a mechanism for insulin treatment of abnormal QT prolongation and associated arrhythmias in diabetic rabbits. Am. J. Physiol. Heart Circ. Physiol. **291**: H1446–H1455. doi:10.1152/ajpheart.01356.2005. PMID:16617123.

Zhang, Y., Xiao, J., Lin, H., Luo, X., Wang, H., Bai, Y., et al. 2007. Ionic mechanisms underlying abnormal QT prolongation and the associated arrhythmias in diabetic rabbits: a role of rapid delayed rectifier K+ current. Cell. Physiol. Biochem. **19**: 225–238. PMID:17495463.

Zhu, T.G., Patel, C., Martin, S., Quan, X., Wu, Y., Burke, J.F., et al. 2009. Ventricular transmural repolarization sequence: its relationship with ventricular relaxation and role in ventricular diastolic function. Eur. Heart. J. **30**: 372–380. doi:10.1093/eurheartj/ehn585. PMID:19147608.